ACCELERATED VISCOELASTIC CHARACTERIZATION OF T300/5208 GRAPHITE-EPOXY LAMINATES

by

Mark E. Tuttle

Dissertation submitted to the Faculty of the
Virginia Polytechnic Institute and State University
in partial fulfillment of the requirements for the degree of

DOCTOR OF PHILOSOPHY

in

ENGINEERING MECHANICS

APPROVED

H.F. Brinson, Chairman

E.G. Henneke II

D.H. Morris

Robert M. Jones

J.P. Wightman

March 1984
Blacksburg, Virginia

ACCELERATED VISCOELASTIC CHARACTERIZATION OF T300/5208 GRAPHITE-EPOXY LAMINATES

by

Mark E. Tuttle

(ABSTRACT)

The viscoelastic response of polymer-based composite laminates, which may take years to develop in service, must be anticipated and accomodated at the design stage. Accelerated testing is therefore required to allow long-term compliance predictions for composite laminates of arbitrary layup, based solely upon short-term tests.

In this study, an accelerated viscoelastic characterization scheme is applied to T300/5208 graphite-epoxy laminates. The viscoelastic response of unidirectional specimens is modeled using the theory developed by Schapery. The transient component of the viscoelastic creep compliance is assumed to follow a power law approximation. A recursive relationship is developed, based upon the Schapery single-integral equation, which allows approximation of a continuous time-varying uniaxial load using discrete steps in stress.

The viscoelastic response of T300/5208 graphite-epoxy at 149C to transverse normal and shear stresses is determined

using 90-deg and 10-deg off-axis tensile specimens, respectively. In each case the seven viscoelastic material parameters required in the analysis are determined experimentally, using a short-term creep/creep recovery testing cycle. A sensitivity analysis is used to select the appropriate short-term test cycle. It is shown that an accurate measure of the power law exponent is crucial for accurate long-term predictions, and that the calculated value of the power law exponent is very sensitive to slight experimental error in recovery data. Based upon this analysis, a 480/120 minute creep/creep recovery test cycle is selected, and the power law exponent is calculated using creep data. A short-term test cycle selection procedure is proposed, which should provide useful guidelines when other viscoelastic materials are being evaluated.

Results from the short-term tests on unidirectional specimens are combined using classical lamination theory to provide long-term predictions for symmetric composite laminates. Experimental measurement of the long-term creep compliance at 149C of two distinct T300/5208 laminates is obtained. A reasonable comparison between theory and experiment is observed at time up to 10^5 minutes. Discrepancies which do exist are believed to be due to an insufficient modeling of biaxial stress interactions, to the accumulation of damage in the form of matrix cracks or

voids, and/or to interlaminar shear deformations which may occur due to viscoelastic effects or damage accumulation.

Acknowledgements

The author is indebted to many individuals whose contributions have helped make this work possible. Special acknowledgement is appropriate for the financial support of the National Aeronautics and Space Administration through Grant NASA-NSG 2038, monitored by Dr. H.G. Nelson. The author is deeply grateful to his major advisor, Dr. H.F. Brinson, for his guidance and support throughout this study. Special thanks is also given to the other committee members, Drs. D.H. Morris, E.G. Henneke II, R.M. Jones, J.P. Wightman, and D.W. Dwight, for reading the manuscript and for their many helpful suggestions.

The author would like to acknowledge the many discussions with Dr. C. Hiel, Mr. M. Rochefort, Dr. S.C. Yen, Mr. B.M. Barthelemy, and Mr. M. Zhang. The assistance of laboratory assistants Mr. D. Fitzgerald, Mr. M. DiBerardino, and Ms. R. Smith is gratefully acknowledged.

The author is indebted to Mr. R. Davis, Mr. K. McCauley, and Mr. A. Montgomery of the ESM Machine Shop for their assistance throughout the program. Special thanks is given to Mrs. Peggy Epperly for typing the equations and Ms. Catherine Brinson for inking the figures.

Finally, the author would especially like to thank his parents, James A. and Rita C. Tuttle, for their unfailing moral support and encouragement.

TABLE OF CONTENTS

LIST OF FIGURES

I. INTRODUCTION

In recent years, the use of advanced continuous fiber composite materials has expanded into a wide variety of market places. Products that have been fabricated at least in part from composite materials include military and commercial aircraft, space vehicles, rocket motor cases, turbine blades, automobile components, pressure vessels, and a variety of sporting goods. All indications are that advanced composites will become an increasingly important material system, competing favorably with the more conventional structural materials such as steel or aluminum. Perhaps the most attractive aspect of advanced composite materials is their very high strength-to-weight and stiffness-to-weight ratios. A modern design engineer must be concerned with total system weight in order to remain energy-efficient, and therefore composites are often ideal material systems due to the potential weight savings alone. However, composites offer other potential advantages over conventional structural materials as well. As examples, composites exhibit an improved resistance to fatigue failure, an improved resistance to corrosion, and composite laminates can be tailored to meet the strength, stiffness,

and thermal expansion characteristics required for a specific design application.

The mechanical behaviour of polymer-based composites differs from the behaviour of conventional structural materials in a variety of ways, and a great deal of research involving polymer-based composites is currently being conducted. For the purposes of the present discussion, these programs can be loosely grouped as those involving:

Orthotropic Effects. Composite lamina are highly orthotropic in both stiffness and strength. As a result, composite laminates may be quasi-isotropic, orthotropic, or anisotropic, depending on layup. Conversely, most conventional structural materials can be considered isotropic in both stiffness and strength.

Environmental Effects. The mechanical behaviour of composites can be dramatically affected by exposure to a variety of environmental conditions. Conventional structural materials can also be affected by environmental conditions, but they are less sensitive to many environmental conditions which are detrimental to composites, e.g., moderately elevated temperatures or ultraviolet radiation.

Viscoelastic Effects. Epoxy-matrix composites exhibit significant viscoelastic or time-dependent effects,

again depending upon laminate layup and also upon applied loading. This viscoelastic behaviour is often closely related to the environmental effects mentioned above. Conventional structural materials exhibit significant viscoelastic behaviour only at very high temperatures.

An important distinction to be made between these research programs is that those which involve orthotropic effects usually consist of a study of some time-independent phenomenon, whereas those involving environmental effects or viscoelastic effects consist of a study of a time-dependent phenomenon.

The orthotropic behaviour of composites has received the most attention in the literature, and methods to describe such behaviour have been proposed. As examples, the orthotropic stiffness properties of a composite laminate of arbitrary layup can be predicted through the use of classical lamination theory (CLT). Strength predictions of an arbitrary laminate can be obtained through the use of CLT coupled with an orthotropic failure law such as the Tsai-Hill failure criterion. Research in these areas is continuing. Some additional topics of current interest are interlaminar and free edge effects [1-5], buckling of composite structures [6-8], and the dynamic response of composite beams and plates [9,10].

The effect of environment on composite materials is also a very active area of current research. Some environmental factors of concern are temperature, moisture, occasional exposure to jet fuel or lubricants, and ultraviolet radiation. Of particular interest at present are the effects of moisture [11,12] and thermal spikes [13,14] on the stiffness and strength of composite materials. These studies are ultimately concerned with the long-term integrity of composite structures subjected to typical in-service environments.

The viscoelastic nature of composites is closely related to the environmental considerations described above, since many environmental conditions such as temperature or humidity serve to accelerate the viscoelastic process. This viscoelastic phenomenon can result in both a gradual decrease in effective overall structural stiffness (perhaps resulting in unacceptably large structural deformations) and also in delayed failures, which might well occur weeks, months, or years after initial introduction of a composite structure into service. Thus, possible viscoelastic effects must be considered over the entire life of a composite structure.

The present study is the continuation of a combined research effort by the Materials Science and Applications Office of the NASA-Ames Research Center and the Engineering

Science and Mechanics Department at Virginia Polytechnic Institute and State University. The research program has focused on the last two areas of composite research described above; environmental effects and viscoelastic effects in laminated epoxy-matrix composite materials. The work at NASA-Ames has been directed towards the effects of moisture on the fatigue life of composites [15-17], while the VPI&SU studies have been directed towards the viscoelastic effects [18-22].

The present study will build on much of the previous work conducted at VPI&SU involving the viscoelastic characterization of composite materials. Therefore, a brief review of the VPI&SU studies in this area will be presented in the next section. This is followed by a section describing the goals of the present study and the integration of these goals with previous efforts at VPI&SU.

Previous Research at VPI&SU

The viscoelastic nature of composite materials provides a unique challenge to the design engineer interested in using these materials in load-bearing structural applications. Namely, the long-term viscoelastic response of the composite structure (which may take years to develop in service) must be anticipated and accomodated at the

design stage. Obviously, it is impractical and prohibitively expensive to perform prototype testing over the total service times which might be involved, or even for all of the laminate layups which might be considered. Some form of accelerated testing/characterization is therefore required which would allow long-term stiffness and strength predictions for a composite laminate of arbitrary layup, subjected to an arbitrary stress and temperature loading history.

An accelerated characterization scheme was proposed by Brinson, Morris, and Yeow in 1978 [23]. As originally envisioned, the characterization procedure would utilize a minimal amount of short-term testing, coupled with the time-temperature superposition principle (TTSP) and CLT, to predict long-term laminate behaviour. The procedure as originally proposed is summarized in Figure 1.1. The first step in this proposed characterization process was to determine the elastic constants of the unidirectional composite lamina (E_1,E_2,G_{12}, and ν_{12}) and the lamina failure strengths (σ_{1f}, σ_{2f}, and τ_{12f}) (A). The standard transformation equations [24] were then used to obtain the lamina modulii corresponding to any arbitrary fiber angle (B), while a time independent failure theory was used to obtain the failure strengths at these arbitrary fiber angles (C). Creep tests were then performed to obtain the master

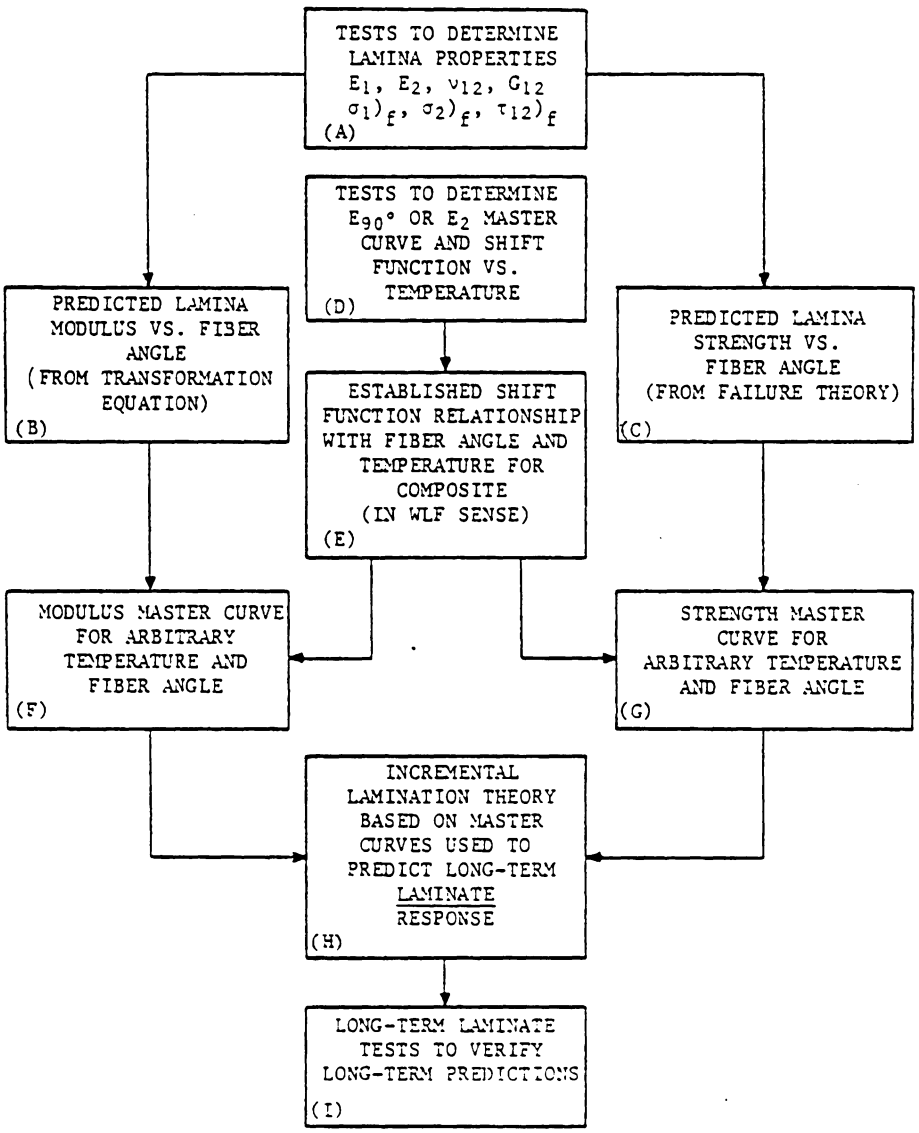

Figure 1.1: Flow Chart of the Proposed Procedure for Laminate Accelerated Characterization and Failure Prediction [23]

curves and shift functions vs. temperature associated with the TTSP (D). These results were used to establish the functional relationship between fiber angle and shift function (E). Once the shift function and modulii for any arbitrary fiber angle were determined, a modulus master curve for arbitrary temperature and fiber angle was generated, again using TTSP (F). A strength master curve was obtained for arbitrary temperature and fiber angle by using the same shift functions obtained from the modulus tests, with the implicit assumption that lamina strength varied in a manner similar to the modulii (G). Finally, the modulus and strength master curves at arbitrary temperature and fiber angles were merged in incremental fashion using CLT (H), which allows prediction of long-term laminate response. The accuracy of the above analysis was checked by actual long-term tests of a few selected composite laminates (I).

A great deal of research involving the accelerated characterization of composites has been performed since 1978. Extensive creep and creep rupture studies have been conducted using the graphite-epoxy composite material system T300/934. These tests were conducted at a variety of stress levels ranging from a few hundred psi to ultimate strength levels, and at a variety of temperatures ranging from room temperature to temperatures near the glass transition

temperature (T_g) of the epoxy matrix. Creep tests for 0-deg, 90-deg and 10-deg off-axis T300/934 specimens have been performed, as well as tests involving a variety of symmetric laminate layups. Perhaps the most important conclusions reached during these studies on T300/934 are:

* The fiber-dominated modulus E_1 is essentially time-independent [25]. Step (D) therefore requires creep tests to obtain master curves for E_2 and G_{12} only.

* The principal compliance matrix used in the modulus transformation equations remains symmetric even after viscoelastic deformation with time [25]. Step (B) is therefore valid.

* The shift function associated with the WLF equation[1] (step E) is independent of fiber angle [25]. This same conclusion has also been reported elsewhere [26].

The assumption that lamina strength varies in a manner similar to the modulii (step G) remains a reasonable but unproven assumption for T300/934 graphite-epoxy. A major difficulty encountered in assessing this concept has been

---

1. The WLF equation will be defined in Chapter II.

the collection of consistent creep rupture data. Considerable data have been collected, but excessive scatter prevents any conclusive interpretations. However, evidence supporting this assumption has been reported in reference [27], where experimental data are presented indicating that the fracture shift factors obtained for both a neat resin matrix and a graphite-epoxy composite were nearly identical to the compliance shift factors obtained using the same two materials.

The overall conclusion reached during the VPI&SU studies is that the accelerated characterization plan depicted in Figure 1.1 can be used to provide reasonably accurate predictions of long-term laminate response, at least for the T300/934 material system studied.

During the course of these studies, it became desirable to modify the proposed characterization plan by replacing the TTSP with some other viscoelastic modeling technique, for two reasons. First, Ferry reports [28] that the TTSP was proposed by Leaderman in 1943 as an empirical curve-fitting procedure. Since that time a theoretical basis for the TTSP has been developed, but only for linear viscoelastic behaviour, and only for temperatures at or above the T_g of the material. Composites are used for structural applications at temperatures well below their T_g to preserve structural rigidity. Additionally, nonlinear

viscoelastic behaviour has been observed for composites, particularily in shear [18,22,29]. Therefore, even though the TTSP appears to provide reasonably accurate predictions for composites, the use of the TTSP under the present conditions is not rigorously justified. Secondly, the conventional TTSP is a graphical procedure, requiring horizontal and vertical shifts of the experimental data to provide smooth uniform master curves. Producing these master curves is a tedious, time-consuming process which is subject to graphical error. Also, the amount and type of vertical shifting required depends upon the specific material system being studied, and no general rule exists for all materials which might be considered [19]. Hence, the TTSP is unwieldy when compared to other available viscoelastic models which are readily adapted to computer automation.

Two viscoelastic models were considered as replacements for the TTSP. These models were the theory proposed by Findley [30-32] and the theory proposed by Schapery [33-35]. The Findley theory is essentially empirical, whereas the Schapery theory can be derived using the concepts of irreversible thermodynamics. It has recently been pointed out that the Schapery theory can be considered to be an analytic form of the Time-Stress Superposition Principle (TSSP) [22]. Both the Findley and Schapery theories are

relatively simple to apply and have been successfully used to model a variety of materials. The model selected was eventually determined by the available data base. That is, the Findley theory requires only creep data to obtain the various material parameters involved, whereas the Schapery theory requires both creep and creep recovery data. Since the existing data base contained only creep data, the Findley theory was chosen to replace the TTSP, with the recommendation that the Schapery theory be included in future research endeavors.

An automated accelerated characterization scheme was developed [21], and a computer program called VISLAP was written which incorporates the accelerated characterization scheme described above. The program provides long-term predictions of the creep compliance and creep rupture times for composite laminates of arbitrary layup. VISLAP was modified for use during the present study, and details of the program structure will be given in Chapter III.

Typical predictions of long-term creep compliance which were obtained during previous efforts [21] are presented in Figure 1.2 for a $[30/-60]_{4s}$ T300/934 laminate at 160C (320F). Note that while the predictions are for several decades of time, actual experimental data exist for only about 30 minutes. The Findley parameters used to produce these curves are shown in Figure 1.3. As can be seen, the

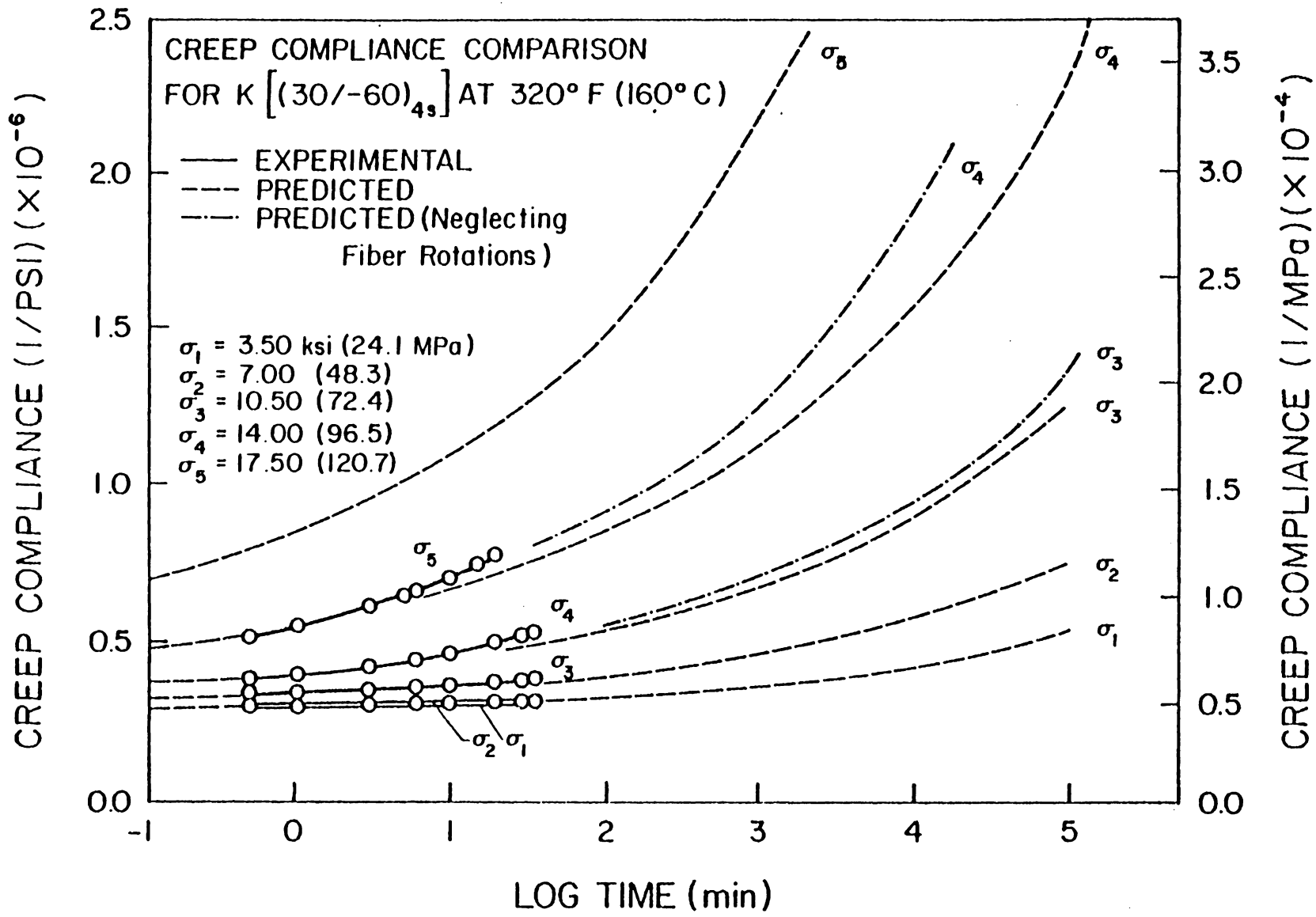

Figure 1.2: Comparison of predicted and experimental creep compliance for laminate K ($[30/-60]_{4s}$) at 320°F (160°C). [21]

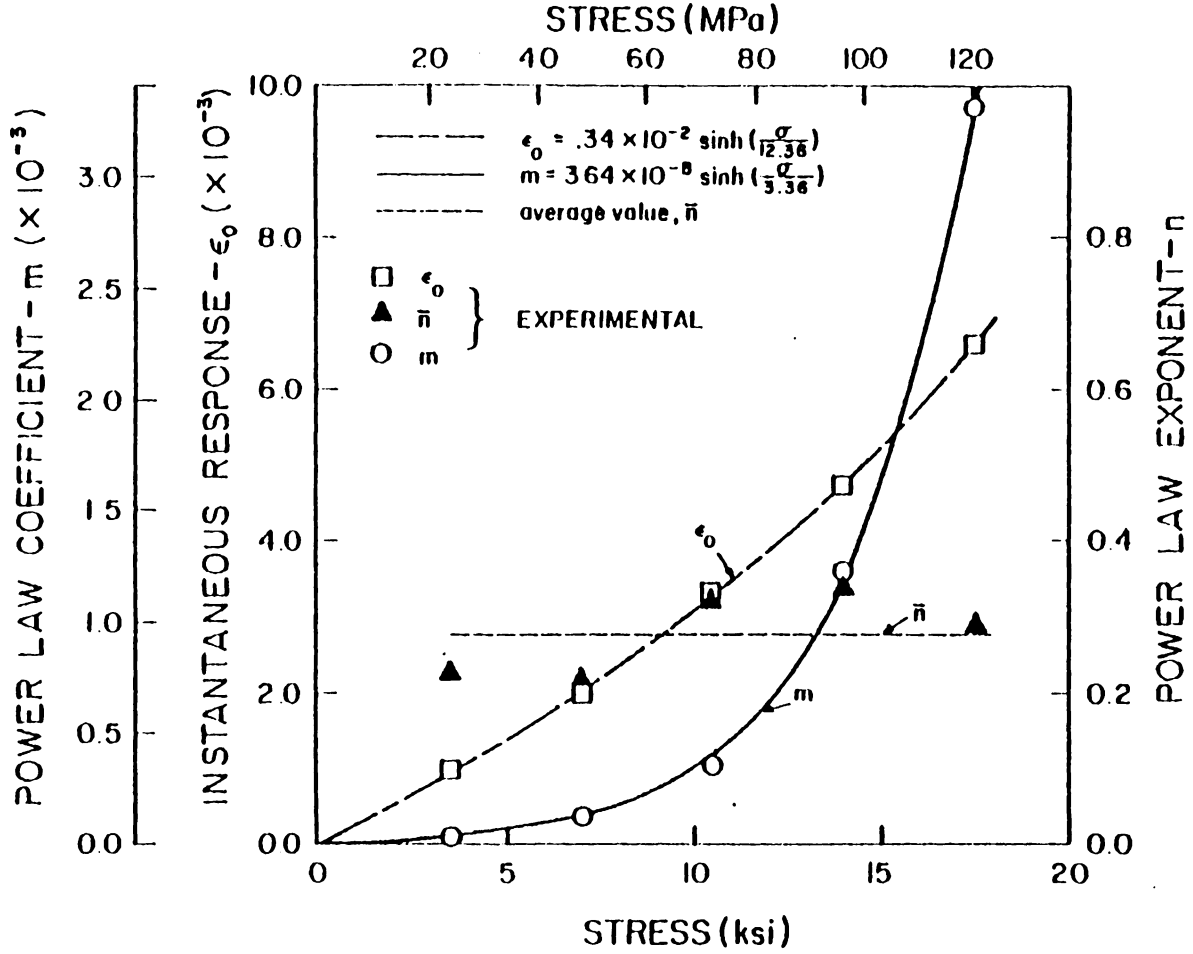

Figure 1.3: Power Law Parameters for Laminate K ($[30/-60]_{4s}$) at 320F (160C) [21]

instantaneous response, ε_o, and the power law coefficient, m, vary in a smooth and uniform manner. The power law exponent, n, was expected to remain constant with stress but experimental values show a significant scatter. An average value for n was eventually used in the study. An analysis of the power law showed that this instability was due to a singularity in n [21]. The experimental data fell near this singularity, and hence the evaluation of the power law exponent was very sensitive to small errors in the experimental data.

Predictions for creep rupture times are shown in Figure 1.4, again for a $[30/-60]_{4s}$ T300/934 laminate at 160C [21]. In general, the creep rupture data were characterized by significant scatter, which was mainly attributed to differences in the material properties of the composite panels used in the study. A major contributor may have been that the same postcure thermal treatment was not used for all specimens, which would have caused considerable differences in the viscoelastic response from specimen to specimen. In most cases, the predicted rupture times were conservative, although in some cases overly so.

Although the Schapery theory was not used in the computer program VISLAP, it has since been successfully used at VPI&SU to characterize the viscoelastic behaviour of polycarbonate [36], bulk samples of FM-73 structural

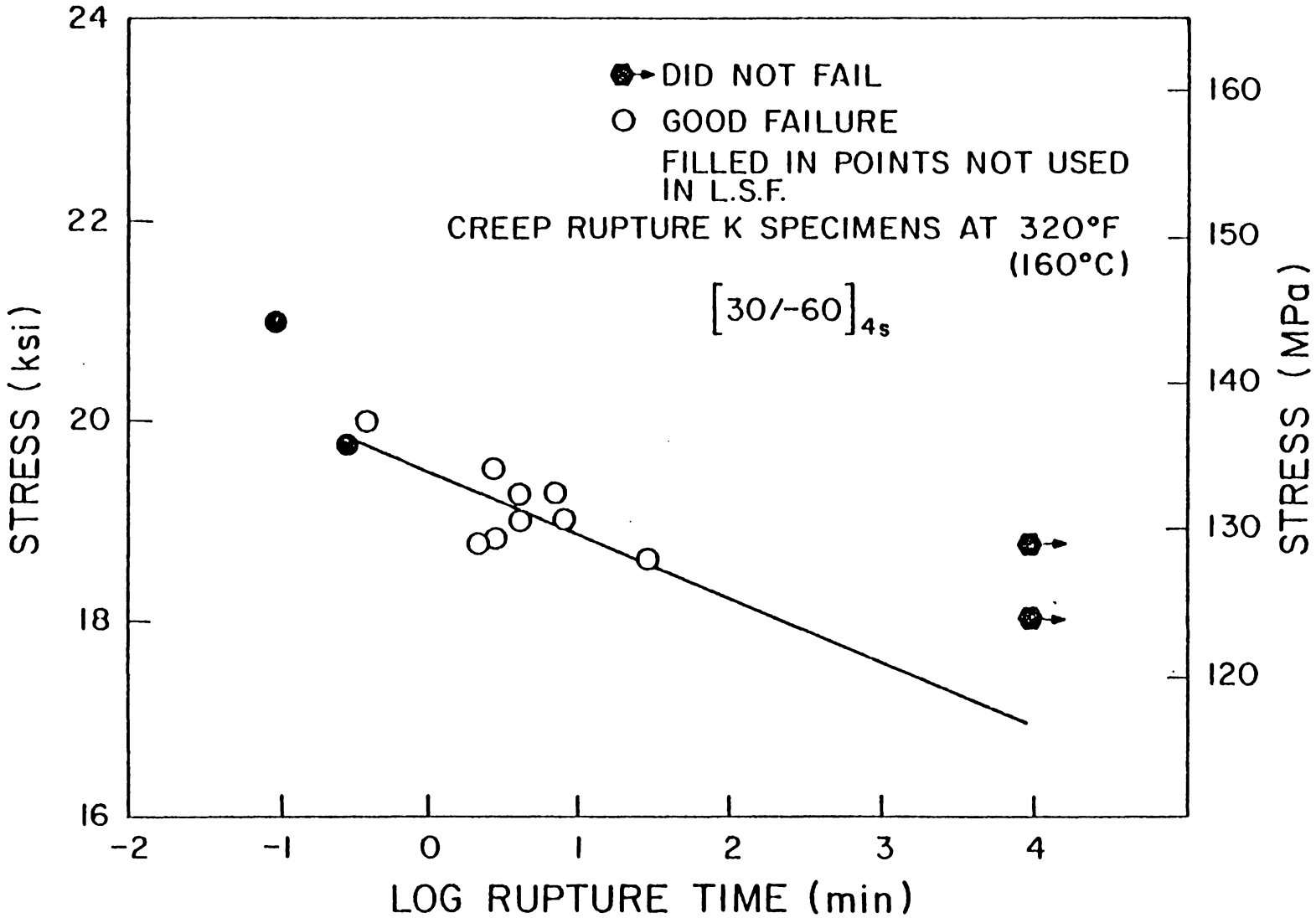

Figure 1.4: Creep ruptures of K specimens ($[-30/60]_{4s}$) at 320°F (160°C)[21]

adhesive [37], and unidirectional laminates of T300/934 [22]. Since the Schapery theory is derived directly from the principles of irreversible thermodynamics, it is somewhat more appealing than the purely empirical Findley equations. In addition, it accounts for some aspects of nonlinear viscoelastic behaviour which the Findley equations cannot model. Therefore, one of the objectives of the present study was to integrate the Schapery theory with the accelerated characterization scheme, and in particular to insert the Schapery equations into the computer program VISLAP.

It is evident from the above discussion that the process of accelerated characterization as applied at VPI&SU has been refined considerably since initiation of the program. The original accelerated characterization scheme previously illustrated in Figure 1.1 was based almost exclusively on the TTSP; subsequently several other viscoelastic and delayed failure models have been utilized. As a result, the procedure depicted in Figure 1.1 no longer accurately reflects the accelerated characterization procedure used at VPI&SU. The more general approach which has evolved has been discussed in Reference 38. An updated diagram illustrating the accelerated characterization procedure is given in Figure 1.5. As indicated, the fundamental concept remains; to use short-term data obtained from unidirectional

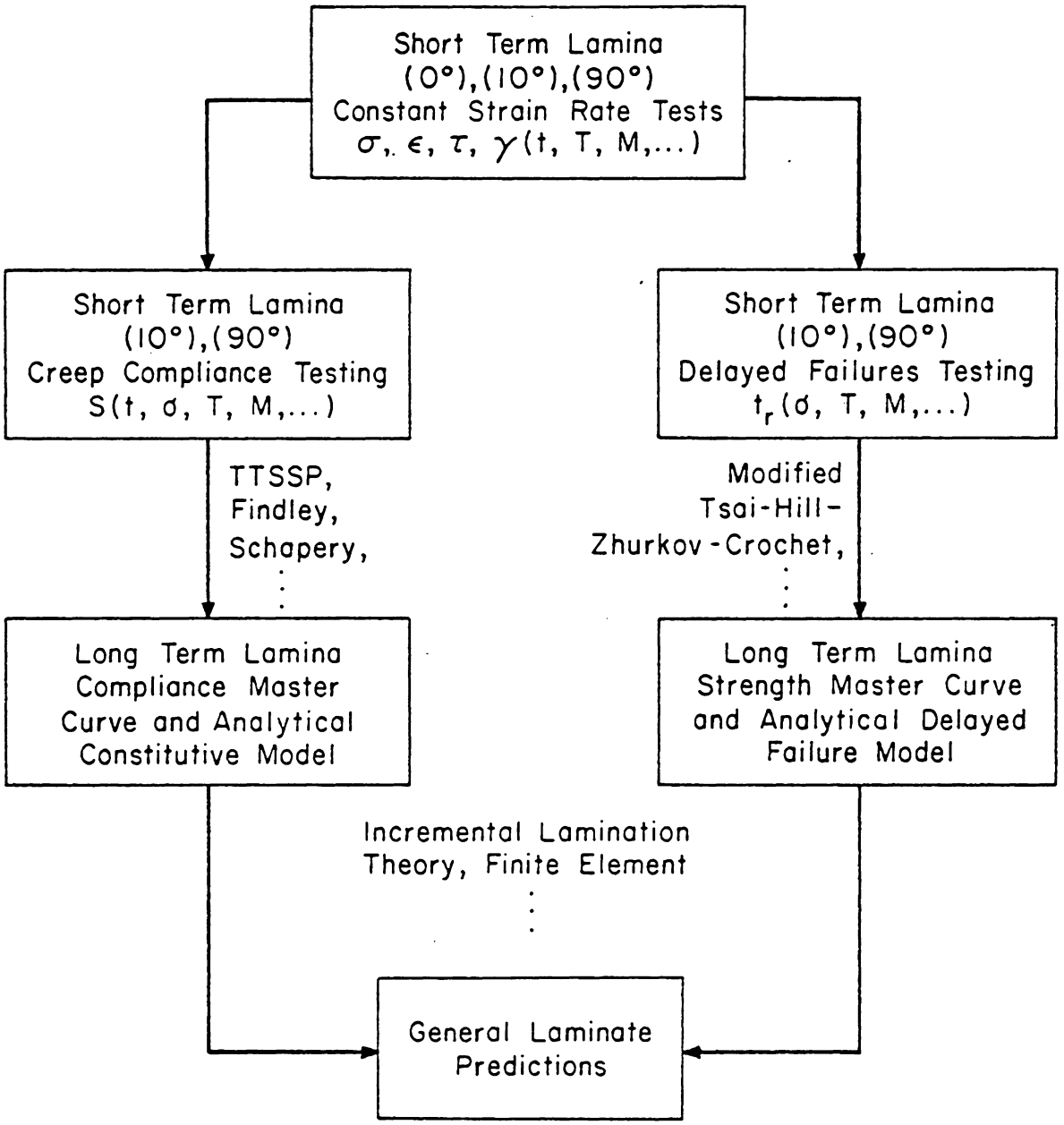

Figure 1.5: Current Accelerated Characterization Procedure Used at VPI&SU

composite specimens to predict the long-term behaviour of composite laminates of arbitrary layup.

Objectives of Present Study

The present research project is essentially a continuation of the accelerated characterization study described above. It was felt that previous studies had validated the concept of accelerated characterization, but a further refinement of the technique in terms of a more accurate compliance model and improved testing procedures was required. In addition, previous efforts focused exclusively on T300/934 graphite-epoxy. A different material system was selected for use in the present study; T300/5208 graphite-epoxy. This system was used because its viscoelastic behaviour had not been studied previously at VPI&SU. The intent was to validate the accelerated characterization method by ascertaining if it would be applicable to a new material system. Successful application would serve to indicate whether the method could be confidently applied to arbitrary reinforced plastics in general as well as T300/934 in particular.

Based upon these general guidelines, the following six program objectives were identified:

(1) The integration of the Schapery nonlinear viscoelastic theory with the accelerated characterization procedure. This principally involved modification of the computer program VISLAP, including additions and improvements to two subroutines, called INPUT and VISCO, and the creation of a new subroutine containing the Schapery equations, called SCHAP.

(2) To perform a numerical study of the sensitivity of the Findley/Schapery viscoelastic parameters to slight experimental error in strain measurement. As indicated in Figure 1.3, the experimentally determined values for the power law exponent n have been subject to significant scatter. Similar scatter has also been reported for the Schapery parameters determined using similar experimental procedures [37]. While a percentage of this scatter was undoubtedly due to actual differences in mechanical behaviour from specimen-to-specimen, there was some indication that it was also in part due to a very high sensitivity to experimental error which was accentuated by the particular creep and/or creep recovery testing schedule being employed.

(3) To develop a standard methodology in selecting a creep and/or creep recovery testing schedule. This methodology was to be based upon the results of objective

(2), and it was expected that the procedure developed would be applicable to any viscoelastic material system, and not just graphite-epoxy composites.

(4) To apply the accelerated characterization procedure to the T300/5208 graphite-epoxy material system. The testing program used was to be based upon the guidelines developed as objective (3). Short-term creep and creep recovery tests were to be performed on 90-deg and 10-deg off-axis specimens, at an ambient temperature of 149C (300F). This data would then be used with the program VISLAP to generate long-term compliance predictions.

(5) To obtain long-term experimental measurement of the creep compliance of two distinct T300/5208 laminates at 149C (300F). In previous studies at VPI&SU, compliance measurements were obtained for a maximum time of only 10^4 minutes (6.9 days). Therefore, it was felt that compliance measurements at longer times were required to provide a more rigorous check of predicted long-term behaviour. The two distinct laminate layups were to be selected such that the stress state applied to each layup and hence the viscoelastic response would be significantly different for each layup. Since there was no existing equipment available for such a test, it was also required to design and fabricate a multiple-station creep frame for this purpose.

(6) To compare the long-term experimental measurements obtained as objective (5) with the long-term predictions obtained as objective (4). The accuracy of the predictions at very long times was of particular interest, as was whether a conservative prediction of compliance at relatively short times remained a conservative prediction at very long times.

Background information related to the present study is given in Chapter II, including brief reviews of viscoelastic theory and classical lamination theory. The efforts to achieve each of the above objectives are described in Chapters III through VIII, followed by a summary and conclusions discussion presented in Chapter IX.

II. BACKGROUND INFORMATION

The Theory of Viscoelasticity

Viscoelasticity is the study of materials whose mechanical properties exhibit both a time-dependency and a memory effect. For example, if a tensile specimen of a viscoelastic material is subjected to a constant uniaxial load, the specimen will "creep", and the apparent Young's modulus will steadily decrease with time (or equivalently, the apparent compliance of the material will steadily increase with time). The viscoelastic material will initially remain in a deformed state after unloading, but will "remember" its original configuration and with time will tend to "recover" back towards that configuration.

It is apparent from this definition that many time-dependent phenomena are not necessarily viscoelastic. The mechanical properties of an epoxy change with time during the curing process, for example, but this time-dependency is due to permanent microstructural changes in the molecular chains of the epoxy. Once the cure is complete, there is no tendency for the epoxy to return to its former state, and hence there is no memory effect. Thus, for a phenomenon to be considered viscoelastic, both time-dependency and memory effects must be exhibited.

Three types of experimental tests commonly employed to characterize viscoelastic materials might be considered for use during the present study. These are the creep/creep recovery test, the stress relaxation test, and the constant strain rate test. The creep/creep recovery test is illustrated in Figure 2.1. A uniaxial step load is applied to the specimen, resulting in an axial stress which is held constant for a time t_1. If the test material is viscoelastic, the specimen "creeps" for times in the range of $0 < t < t_1$. After time t_1 the load is removed and the viscoelastic material "recovers" towards its initial configuration.

Strain and stress histories for a stress relaxation test are illustrated in Figure 2.2. In this test, a uniaxial step deformation is applied to the specimen, resulting in an axial strain which is held constant for the duration of the test. The applied deformation induces an initial axial stress σ_o which slowly "relaxes" with time.

The constant strain rate test is illustrated in Figure 2.3. The specimen is subjected to an axial strain which is increased at some constant rate R, and the axial stress induced within the specimen is monitored. If the test material is viscoelastic, the induced stress will not increase linearly with time, as indicated.

In the present study, the creep/creep recovery test was

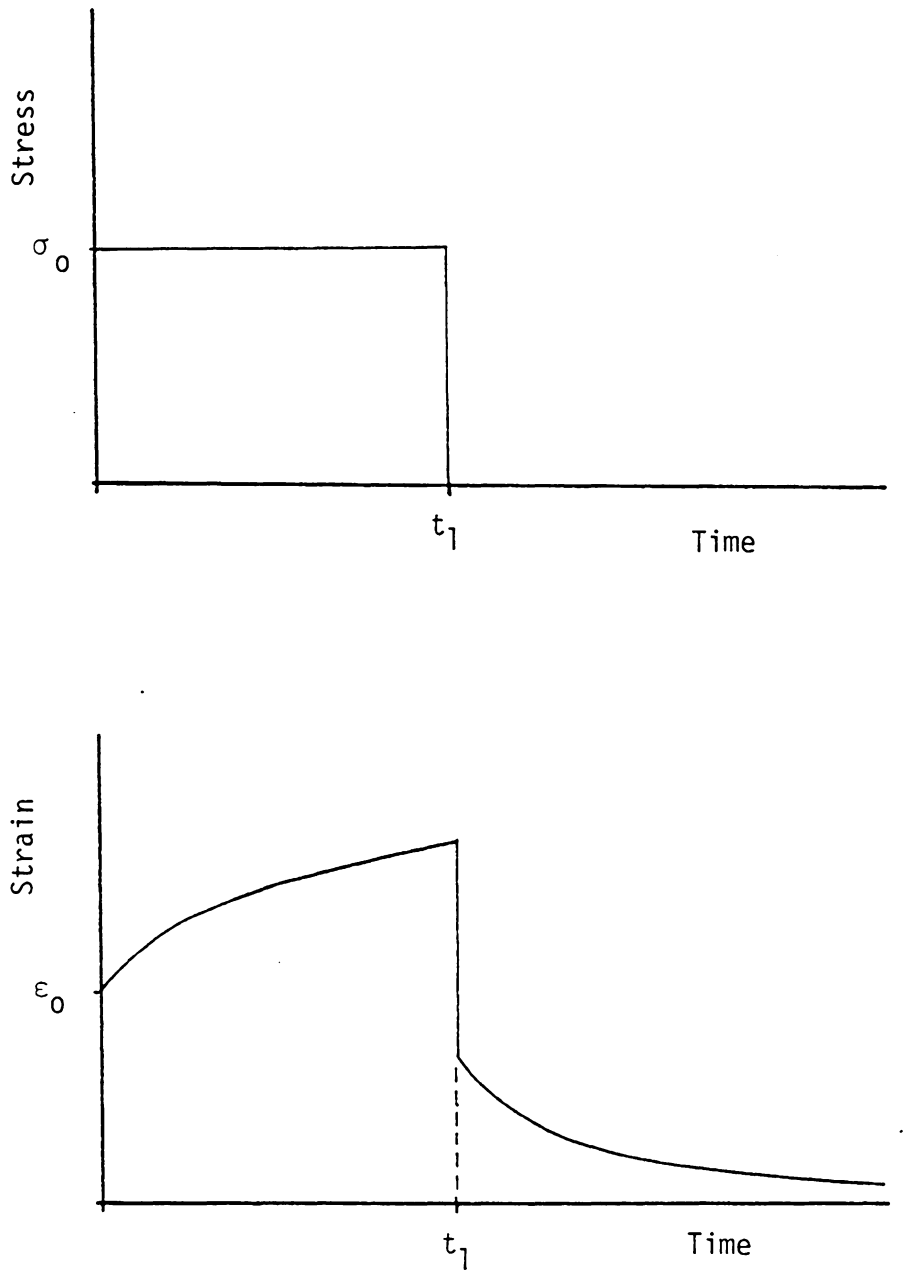

Figure 2.1: Stress and Strain Histories for a Creep/Creep Recovery Test

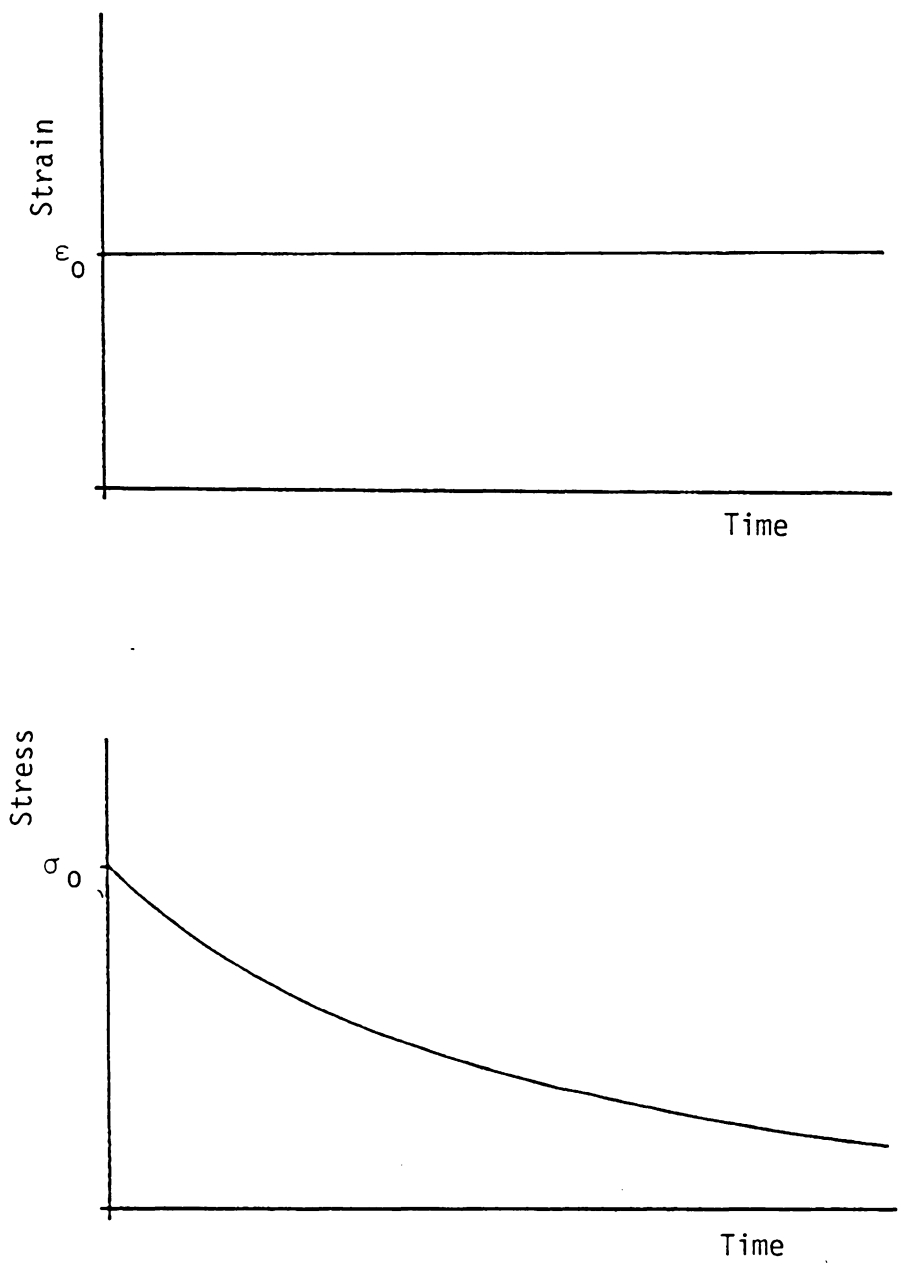

Figure 2.2: Strain and Stress Histories for a Stress Relaxation Test

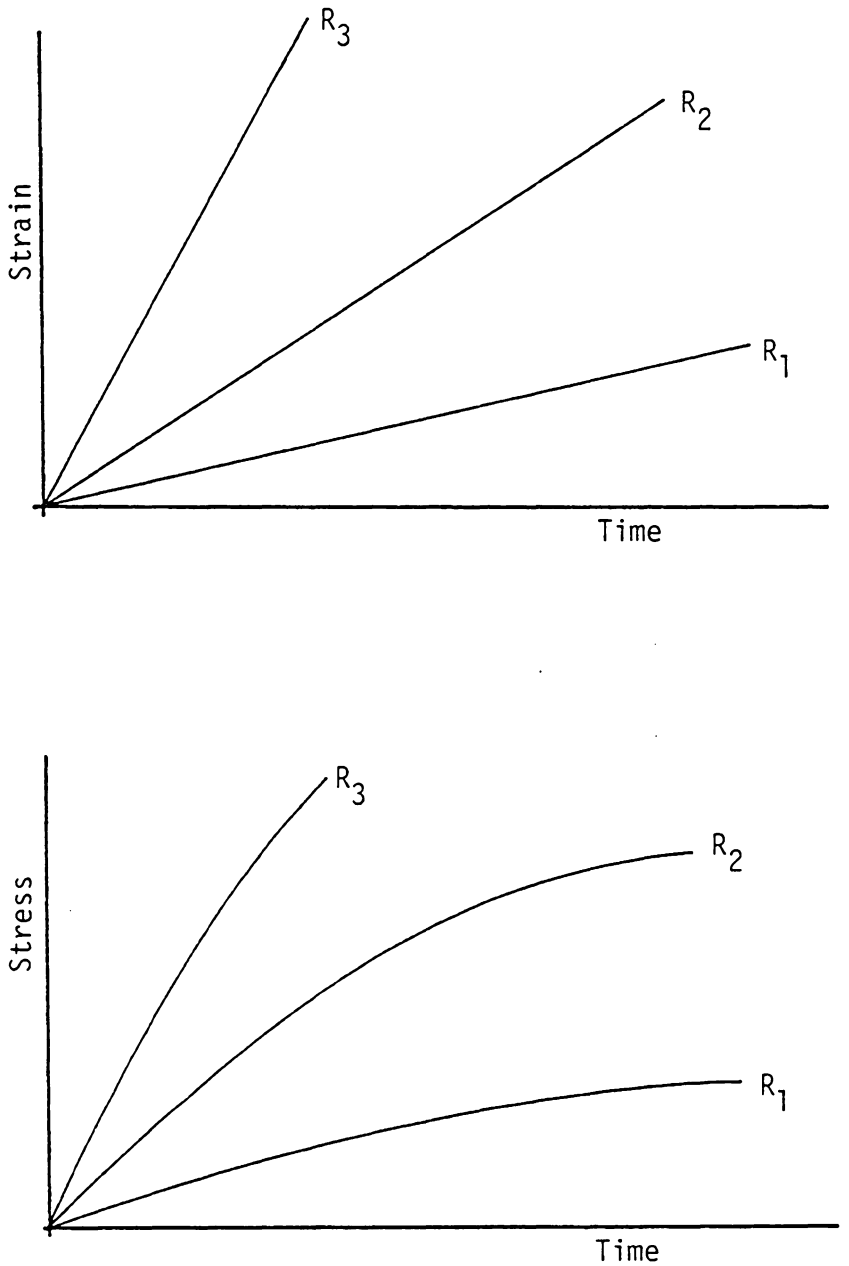

Figure 2.3: Strain and Stress Histories for a Constant Strain Rate Test

used almost exclusively to characterize viscoelastic material behaviour, primarily because creep/creep recovery tests are the easiest to perform. Constant strain rate tests were used occasionally to obtain "instantaneous" modulii, but were not used to obtain any viscoelastic parameters. The stress relaxation test was not used in this study.

Viscoelastic materials are sometimes loosely grouped as viscoelastic "solids" or viscoelastic "fluids". The distinction between these two material types is illustrated in Figure 2.4 for a creep/creep recovery test cycle. For a viscoelastic solid, the creep strain increases from the initial value ε_o towards an asymptotic value ε_∞, and the creep strain rate tends towards zero as time increases. Upon unloading, the recovery strains return asymptotically to zero.

For a viscoelastic fluid, the creep strains do not reach an asymptotic limiting value, and the creep strain rate tends towards a constant as time increases. Upon unloading, the recovery strains return asymptotically to some permanent non-zero strain level, ε_f.

As is the case for elastic materials, viscoelastic materials may be further classified as either linear or nonlinear materials. There are a variety of methods which may be used to distinguish between linear and nonlinear viscoelastic behaviour. A typical technique is illustrated

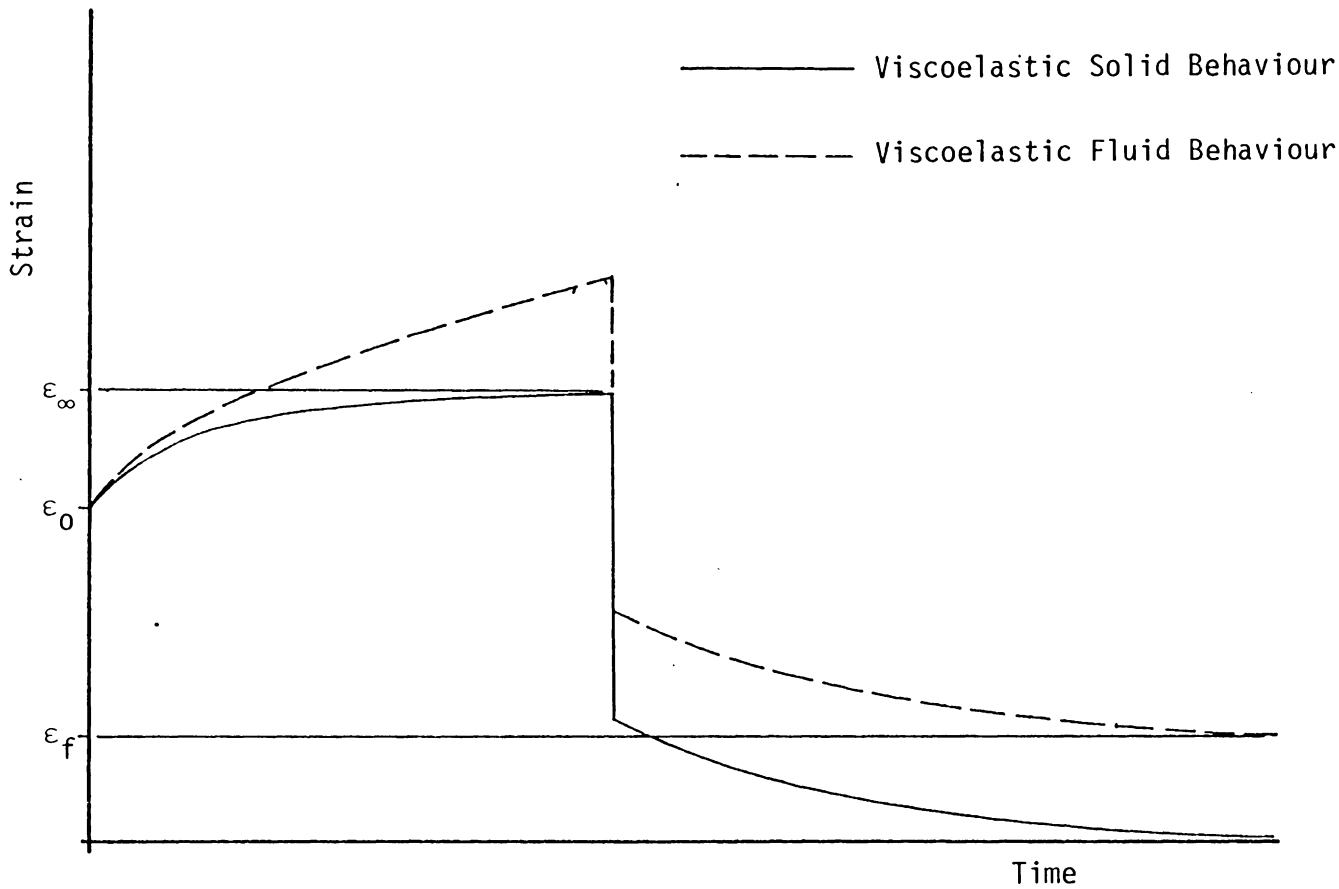

Figure 2.4: Typical Creep/Creep Recovery Behaviour for Viscoelastic Solids and Viscoelastic Fluids

in Figure 2.5, where "isochronous" (i.e., constant time) stress-strain curves are shown for both linear and nonlinear materials. These curves would be generated using data collected during several creep tests. Nonlinear behaviour is readily identified using this technique, as shown.

The mathematical modeling of viscoelastic behaviour is complicated considerably by nonlinear behaviour. As a result, the theory of linear viscoelasticity is very well developed and understood, while nonlinear viscoelasticity theory has received attention only relatively recently and is not as well developed nor understood.

In the present effort, the theory of viscoelasticity will be used to characterize the epoxy matrix used in a composite laminate. An important property which impacts the viscoelastic behaviour of all polymeric materials is the glass transition temperature (T_g). As the temperature of a polymeric material is raised through the T_g, the elastic modulus can decrease by a factor of 10^3 or greater. At temperatures well below the T_g, polymers are generally very brittle, exhibiting little or no viscoelastic response. At temperatures above the T_g, polymers are extremely ductile and "rubbery", exhibiting considerable viscoelastic behaviour. This dramatic change in material behaviour occurs over a narrow temperature range, on the order of 6C (10F). For epoxies, the T_g is usually about 160C (320F).

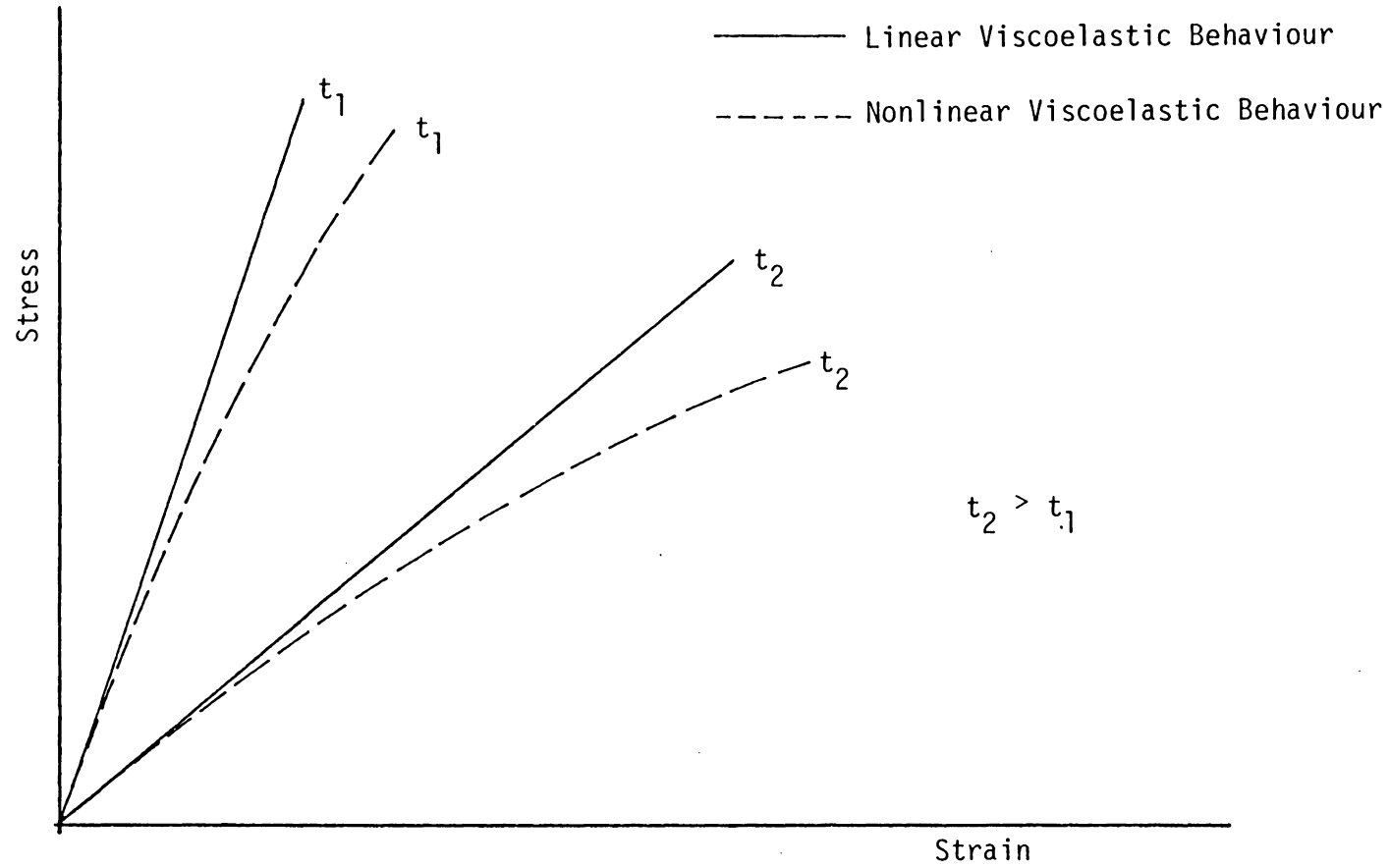

Figure 2.5: Isochronous Stress-Strain Curves Illustrating Linear and Nonlinear Viscoelastic Behaviour

The amount and type (i.e., linear or nonlinear, solid or fluid) of viscoelastic behaviour which is exhibited by polymeric materials is dependent upon a variety of factors, including stress level, temperature, previous thermal history, humidity, and molecular structure.

Linear Viscoelasticity.

Mechanical Models. Perhaps the most familiar concept of linear viscoelasticity is the use of mechanical analogies to model viscoelastic behaviour. The two simplest mechanical models are the Kelvin (or Voigt) element and the Maxwell element. Both elements are simple combinations of a Hookean solid (modeled as a linear spring of stiffness k) and a Newtonian viscous fluid (modeled as a linear dashpot of viscosity μ), as shown in Figure 2.6. Note that for a constant creep load the deformation of the Kelvin element is limited by the elastic spring, and therefore the Kelvin element behaves as a viscoelastic solid. In contrast, for a constant creep load, the deformation of the Maxwell element is not bounded, due to the continued deformation of the ideal dashpot. The Maxwell element therefore behaves as a viscoelastic fluid.

It is easily shown that if at time $t = 0$ a Kelvin element is suddenly subjected to a constant creep stress σ_o, the resulting strain response is given by

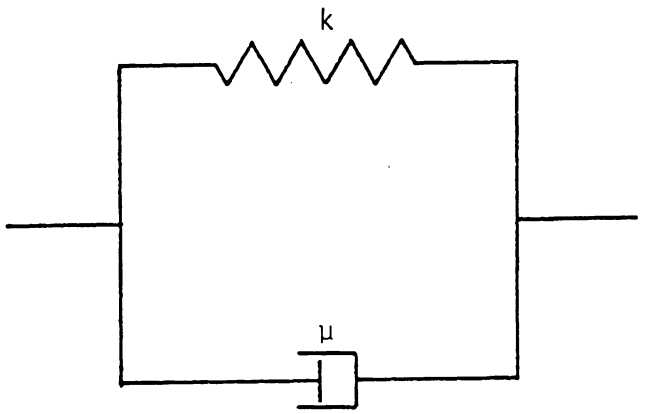

a) Kelvin Viscoelastic Element

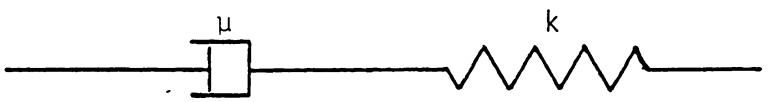

b) Maxwell Viscoelastic Element

Figure 2.6: Simple Mechanical Analogies Used to Model Viscoelastic Behaviour

$$\varepsilon(t) = \frac{\sigma_0}{k} (1 - e^{-t/\tau})$$

where

$$\tau = \frac{\mu}{k} = \text{the "retardation time"}$$

A typical viscoelastic response for a Kelvin element is shown in Figure 2.7. Note that the retardation time τ is determined by the viscosity and stiffness values selected for the dashpot and spring, respectively.

In an analogous fashion, the stress within a Maxwell element which is induced by a suddenly applied constant strain ε_o is given by

$$\sigma(t) = k \varepsilon_o e^{-t/\tau}$$

where

$$\tau = \frac{\mu}{k} = \text{the "relaxation time"}$$

Again, the relaxation time is defined by the viscosity and stiffness values selected.

The behaviour of many viscoelastic materials cannot be modeled by using a single Kelvin or Maxwell element, but can be accurately modeled using the "generalized" Kelvin or Maxwell models. The generalized Kelvin and Maxwell models, shown in Figure 2.8, are composed of many (in some cases an

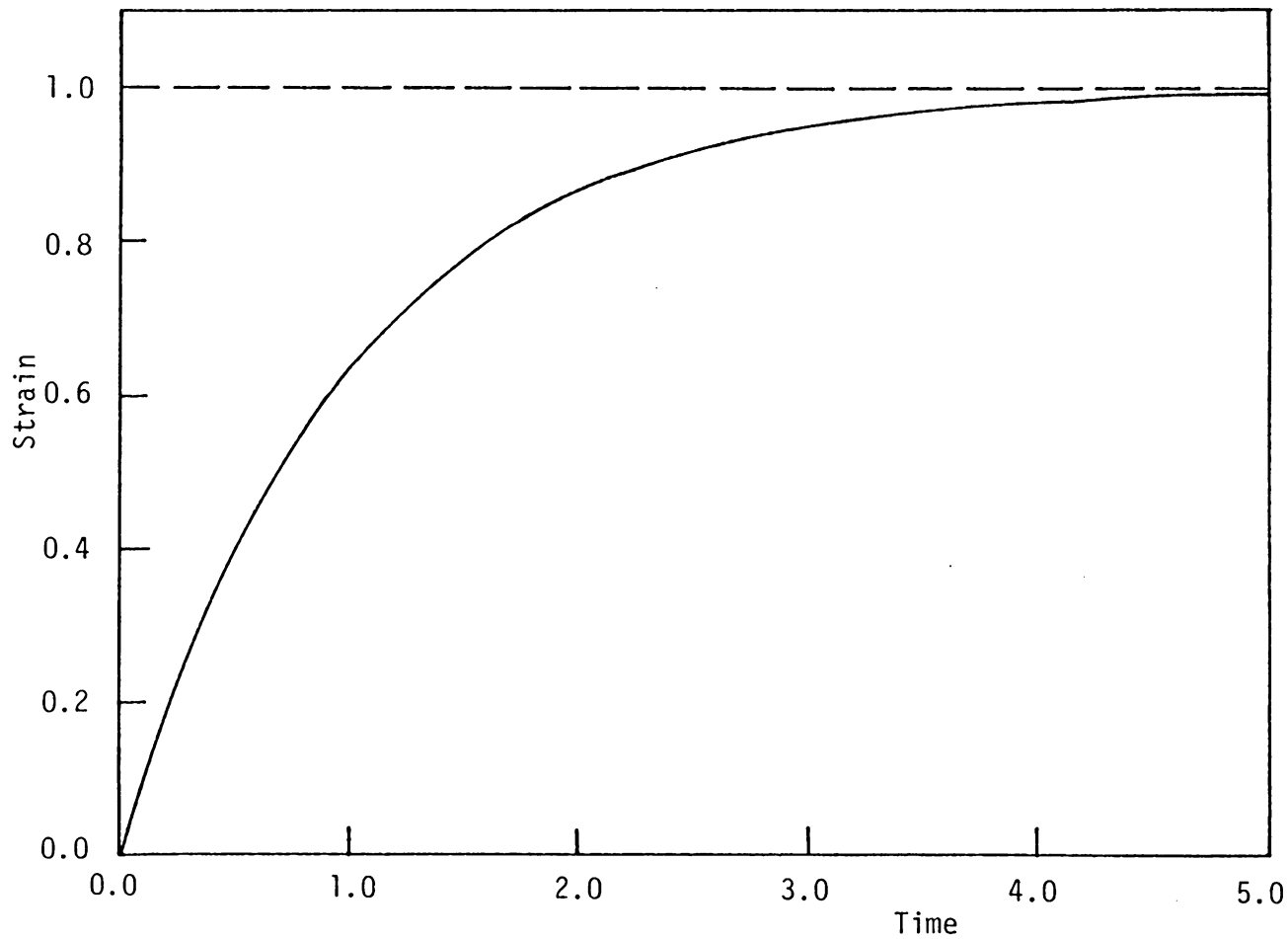

Figure 2.7: Typical Viscoelastic Response for a Kelvin Element; $\tau = 1$, $\frac{\sigma_o}{k} = 1$

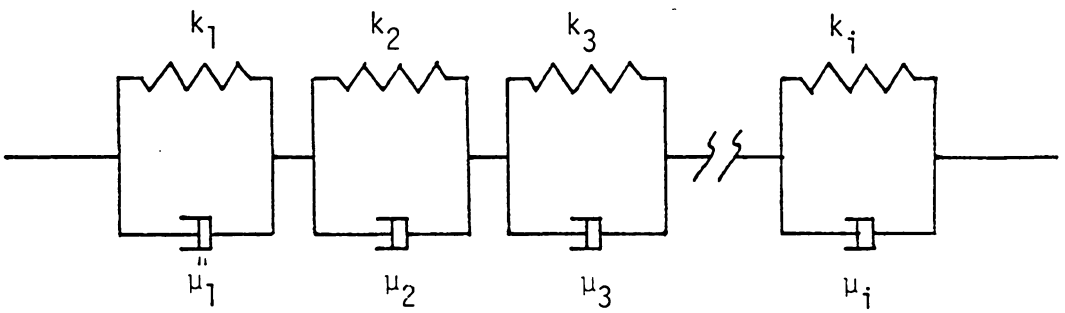

a) Generalized Kelvin Model

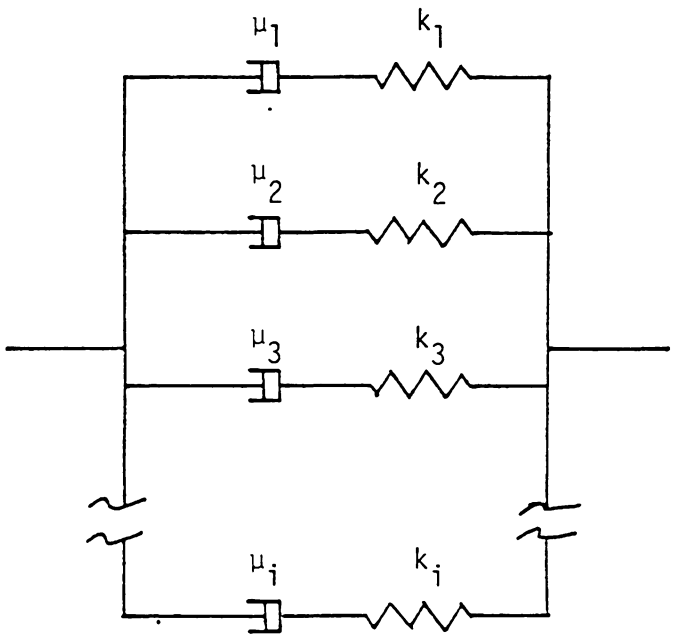

b) Generalized Maxwell Model

Figure 2.8: Generalized Viscoelastic Models

infinite number of) Kelvin or Maxwell elements, acting in concert. For a generalized Kelvin model there is not a single retardation time, but rather many retardation times distributed over several decades in time. Furthermore, a distinct contribution to compliance can be associated with each retardation time. The distribution of these compliance increments over time is called the retardation spectrum and is usually written $L(\tau)$, where $L(\tau)$ has units of area/force. In an analogous fashion, the generalized Maxwell model possesses many relaxation times, and a distinct contribution to stiffness can be associated with each relaxation time. The distribution of these stiffness increments over time is called the relaxation spectrum and is usually written $H(\tau)$, where $H(\tau)$ has units of force/area. In principle, the behaviour of any viscoelastic material can be modeled using the generalized Kelvin or Maxwell models with an infinite number of elements by simply imposing the appropriate retardation or relaxation spectrums. A schematic representation of a continuous retardation spectrum is shown in Figure 2.9. There are also several molecular theories which can be used to approximate the continuous viscoelastic spectra with discrete spectrum lines [28,39], in which case a finite number of Kelvin or Maxwell units is used. For example, the creep response of a generalized Kelvin model consisting of n Kelvin elements is given by

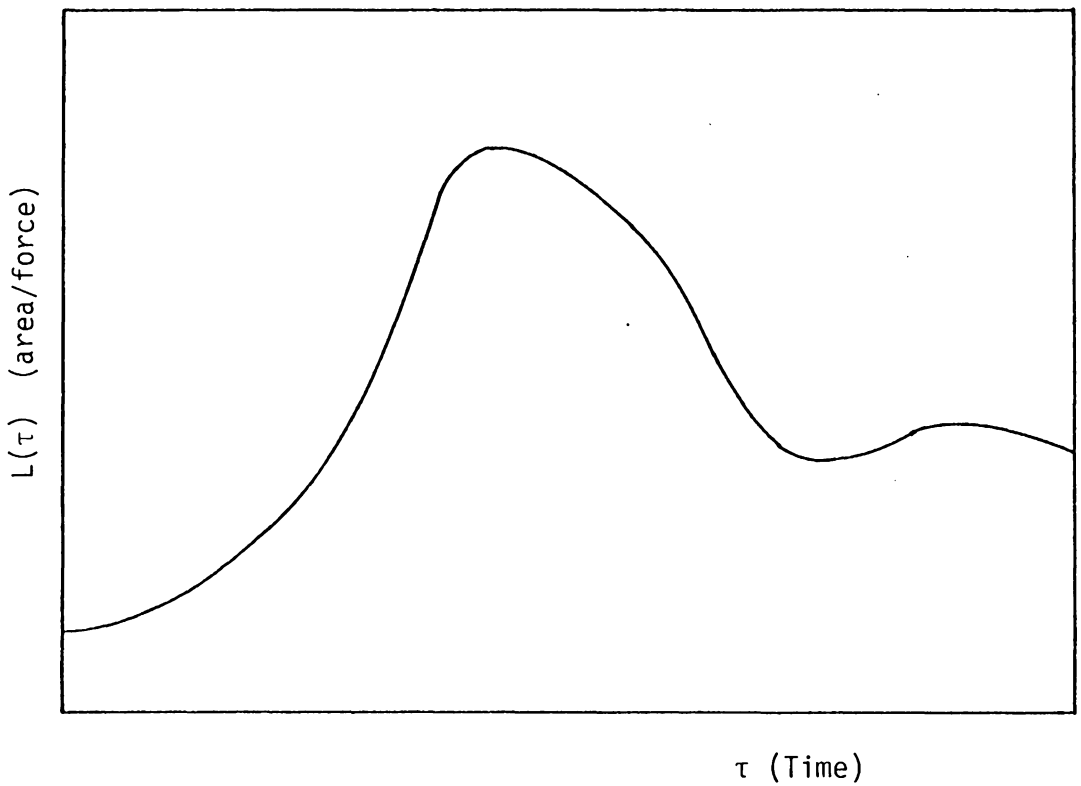

Figure 2.9: Schematic Representation of a Typical Retardation Spectrum

$$\varepsilon(t) = \sigma_0 \sum_{i=1}^{n} \frac{1}{k_i} (1 - e^{-t/\tau_i})$$

As mentioned above, the Kelvin element is associated with the behaviour of a viscoelastic solid and the Maxwell model is associated with the behaviour of a viscoelastic fluid. However, the generalized Kelvin model can be used to model a material exhibiting short-term solid behaviour with long-term fluid behaviour by simply removing an elastic spring, creating a free dashpot in one Kelvin unit. Similarly, the generalized Maxwell model can be used to model short-term fluid behaviour and long-term solid behaviour by removing a linear dashpot in one Maxwell unit.

Boltzman Superposition Principle. The response of a linear viscoelastic material to some arbitrary stress history can be obtained by approximating the stress history using a series of distinct steps in stress, as shown in Figure 2.10. The strain history is given approximately by

$$\varepsilon(t) = D(t)\sigma_0 + D(t-t_1)(\sigma_1-\sigma_0) + D(t-t_2)(\sigma_2-\sigma_1) + \ldots\ldots + D(t-t_i)(\sigma_i-\sigma_{i-1}) \qquad (2.1)$$

where:

$D(t)$ = the appropriate material compliance function

The approximation is, of course, improved as the increments in time $(t_i - t_{i-1})$ are made smaller and smaller. In the

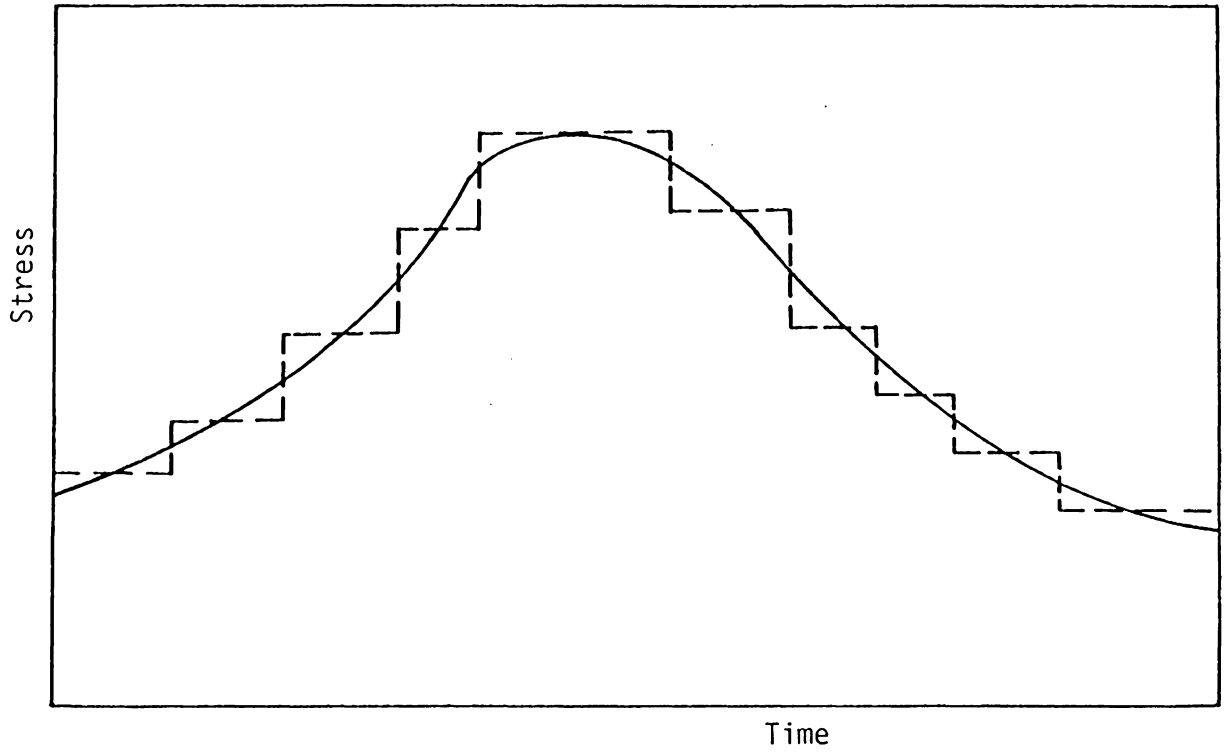

Figure 2.10: Approximation of an Arbitrary Stress History Using a Series of Discrete Steps in Stress

limit eq. 2.1 becomes exact and may be written as

$$\varepsilon(t) = \int_{0^-}^{t} D(t - \tau) \frac{d\sigma}{d\tau} d\tau \qquad (2.2)$$

Equation 2.2 is the well-known Boltzman Superposition Principle, which gives the strain response for a linear viscoelastic material to an arbitrary stress input. Note that it has been assumed that the material has experienced no previous stress or strain histories, i.e., $\sigma = \varepsilon = 0$ for $-\infty < t < 0$.

Time-Temperature Superposition Principle. As discussed in Chapter I, the time-temperature superposition principle (TTSP) was proposed by Leaderman in 1943 [28]. The TTSP is also referred to as the "method of reduced variables" by some researchers. This principle is of fundamental importance to the present investigation because it is an accelerated characterization procedure which has been extensively studied and successfully used for a wide variety of viscoelastic materials. The validity of the TTSP is therefore firmly established, lending credibility to the present efforts to characterize composite materials using an accelerated characterization scheme.

The steps in data reduction involved in the use of the TTSP are summarized in Figure 2.11 for the case of stress relaxation [40]. Short-term stress relaxation data are

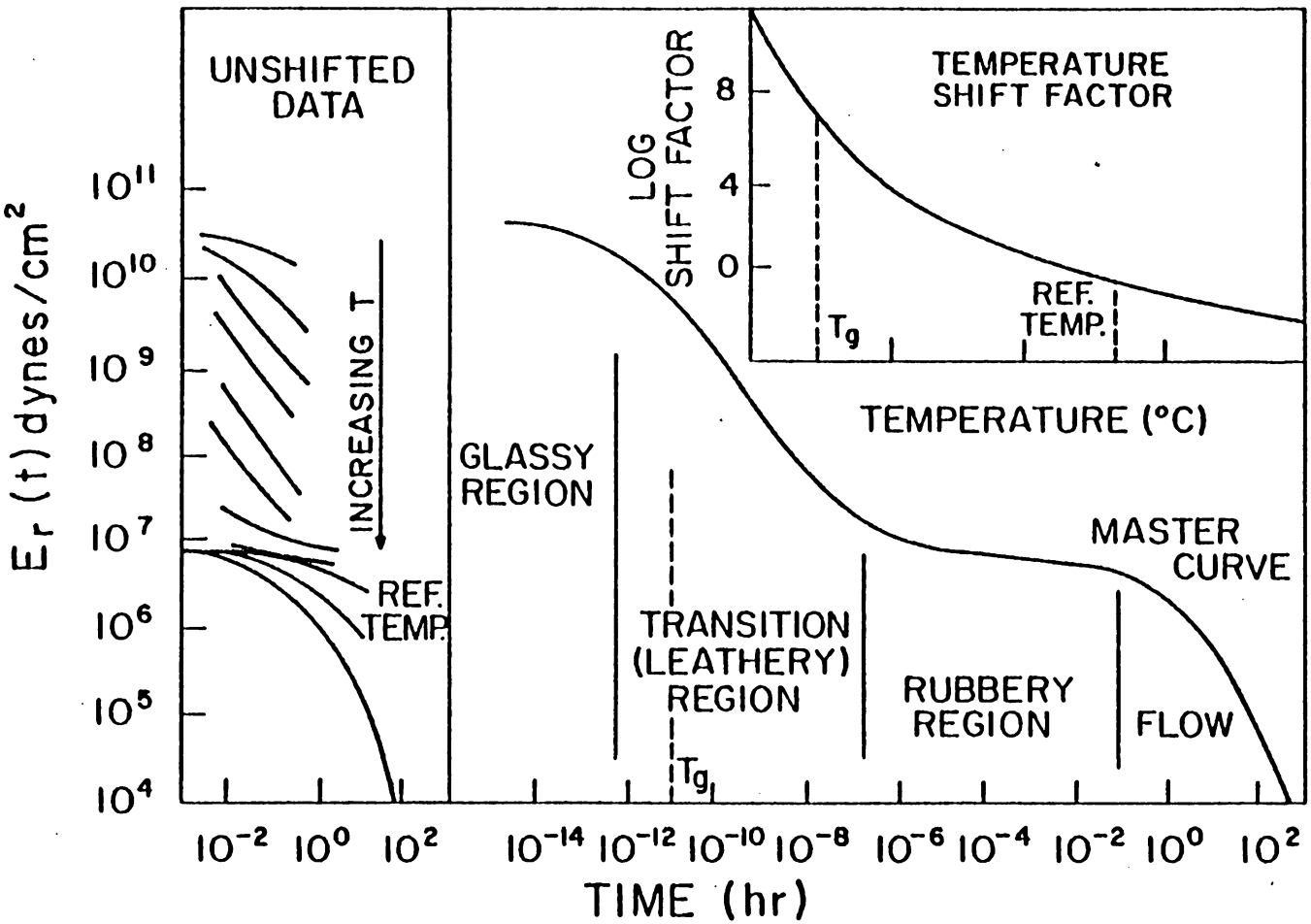

Figure 2.11: TTSP Formation Process As Given By Rosen [40]

obtained at a series of increasing temperatures, as shown at the left of Figure 2.11. The short-term test duration is as long as is convenient, perhaps ranging from a few minutes to 10^4 minutes (6.9 days). A reference temperature is then selected, and a "master curve" is generated by shifting each of the short-term test results horizontally left or right until a smooth curve is produced. In general, short-term data obtained at temperatures lower than the reference temperature are shifted to the left, while data obtained at temperatures higher than the reference temperature are shifted to the right. The master curve is therefore associated with the particular reference temperature selected, and a different master curve would be obtained if a different reference temperature is used.

The horizontal distance each curve is shifted is equal to the log of the so-called "temperature shift factor", a_T, and has also been plotted as a function of temperature in Figure 2.11. At temperatures above the glass transition temperature (T_g), a_T can often be accurately calculated using the Williams-Landel-Ferry (WLF) equation [28]

$$\log a_T = \frac{- C_1 (T - T_o)}{C_2 + T - T_o} \qquad (2.3)$$

C_1 and C_2 are constants for the particular material being investigated and T_o is a reference temperature greater than or equal to the T_g of the material. It has been empirically

observed that for many polymeric materials the WLF equation can be written

$$\log a_T = \frac{-17.44\ (T - T_g)}{51.6 + T - T_g} \tag{2.4}$$

where in equation 2.4:

$T > T_g$

$T,\ T_g$ in degrees Kelvin

$C_1 = 17.44$

$C_2 = 51.6$

A material which can be characterized as described above is referred to as a "thermorheologically simple material" (TSM). For many materials a master curve cannot be formed by means of simple horizontal shifting alone, however, and some vertical shifting of the short-term data prior to horizontal shifting is required. In these cases, the material is referred to as a "thermorheologically complex material" (TCM). Vertical shifting is often associated with environmental effects such as temperature or humidity and also with a nonlinear dependence on stress. Vertical and horizontal shifting procedures have been extensively reviewed by Griffith, et al [19], and will not be discussed in greater detail here. It should be noted however that vertical shifting introduces a significant complication in the use of the TTSP, and is a major reason why alternate

accelerated characterization schemes have been pursued at VPI&SU.

The Findley Power Law Equation. It has been empirically observed that the creep compliance function for many linearly viscoelastic polymeric materials can be accurately modeled using a power law of the form

$$D(t) = A + Bt^n \tag{2.5}$$

where

A, B, n = material constants

t = time after creep loading

For a creep test, the stress history may be expressed as

$$\sigma = \sigma_o H(t), \text{ and therefore}$$
$$\frac{d\sigma}{dt} = \sigma_o \delta(t) \tag{2.6}$$

where

σ_o = constant

H(t) = the Heaviside unit step function $= \begin{cases} 0, & t < 0 \\ 1, & t > 0 \end{cases}$

$\delta(t) = \frac{dH(t)}{dt}$ = the Kronecker-Delta function $= \begin{cases} \infty, & t = 0 \\ 0, & t \neq 0 \end{cases}$

Substituting equations 2.5 and 2.6 into equation 2.2 results in the so-called "Findley power law equation":

$$\varepsilon(t) = \varepsilon_o + mt^n \qquad (2.7)$$

where

$$\varepsilon_o = A\,\sigma_o$$

$$m = B\,\sigma_o$$

Note from these definitions that ε_o and m are also considered material constants.

Equation 2.7 has been used by Findley and his co-workers to successfully characterize the viscoelastic behaviour of a variety of amorphous, crystalline, and crosslinked polymers. As presented here, it is valid only for linearly viscoelastic behaviour. However, Findley has presented a slightly modified form of eq. 2.7 for use with nonlinear viscoelastic materials. This nonlinear Findley power law will be described in the next section.

Nonlinear Viscoelasticity

Mechanical Models. It is theoretically possible to modify the linear generalized Kelvin or Maxwell models to account for nonlinear viscoelastic behaviour through the use of nonlinear springs and/or dashpots. Since the retardation (relaxation) times τ_i for the Kelvin (Maxwell) model are equal to the ratio μ_i/k_i, this implies that τ_i is not a constant for each Kelvin (Maxwell) element but rather a

function of stress level. Alternatively, nonlinear behaviour can be introduced through the use of nonlinearizing functions of stress as follows

$$\varepsilon(t) = \sigma_0 \sum_{i=1}^{n} \frac{1}{k_i} (1 - e^{-t/\tau_i}) f_i(\sigma_0)$$

where

$f_i(\sigma_0)$ = nonlinearizing functions of stress

Hiel et al report [22] that Bach has used this approach to model the nonlinear viscoelastic behaviour of wood. Generalized mechanical models are rather cumbersome even in the linear case however, and have not been used to model nonlinear behaviour to any great extent.

Multiple-Integral Approaches. The viscoelastic constitutive equation relating the strain and stress tensors can be written in the most general form as

$$\varepsilon_{ij}(t) = F_{ijkl} \left[\sigma^{t}_{kl}(\tau)\right]_{\tau=0} \qquad (2.8)$$

where

$\varepsilon_{ij}(t)$, $\sigma_{kl}(\tau)$ = strain and stress tensors, respectively

F_{ijkl} = continuous nonlinear compliance tensor

t = present time

τ = arbitrary time

Equation 2.8 implies that the current strain state is dependent upon the entire previous stress history, i.e., from $0 < \tau < t$. Thus, a material which can be described by eq. 2.8 exhibits a memory effect and is viscoelastic.

In a series of publications [41-43], Green, Rivlin, and Spencer presented an analysis which shows that eq. 2.8 can be approximated to any degree of accuracy by a series of multiple-integrals. This approach involves the use of convoluted integrals containing n-th order terms of stress. The final multiple-integral expression for three-dimensional stress states is quite lengthy and will not be presented here. A simpler expression derived by Onaran and Findley [44] will be used to illustrate the fundamental concept. Their expression is applicable for a uniaxial stress, and only two orders of stress are retained. Using this approach the following relation is obtained

$$\varepsilon(t) = \int_0^t \Phi_1(t-\tau)\,\sigma(\tau)\,d\tau + \int_0^t \int_0^t \Phi_2(t-\tau, t-\tau)[\sigma(\tau)]^2\,d\tau d\tau + 2\int_0^t \int_0^t \Phi_2(t-\tau_1, t-\tau_2)\sigma(\tau_1)\sigma(\tau_2)\,d\tau_1 d\tau_2 \qquad (2.9)$$

The functions Φ_1 and Φ_2 which appear in eq. 2.9 are called kernel functions and must be determined experimentally. If a third order of stress were used in the derivation of eq. 2.9, a triple integral would appear involving a third kernel

function Φ_3. Therefore, the number of tests required to characterize a viscoelastic material using this technique depends upon both the type of loading and the desired degree of accuracy. If a general three-dimensional stress state were assumed and only the first, second, and third orders of stress terms are retained, there are still thirteen independent kernel functions which must be evaluated. This requires over 100 tests involving various combinations of uniaxial, biaxial, and triaxial loading conditions. Such extensive and difficult testing is impractical in most instances. The multiple-integral approach has therefore not been used to any extent in practice, even though it is probably one of the most accurate and versatile nonlinear viscoelastic theories available.

The Nonlinear Findley Power Law Equation. The linear Findley power law was described in the previous paragraph and is given by eq. 2.7. As discussed, the parameters ε_o, m, and n are considered material constants for the linear case. In the nonlinear case, these parameters are not constant with stress, but rather are assumed to follow an expression of the form

$$\begin{aligned} \varepsilon_o &= \varepsilon'_o \sinh (\sigma/\sigma_\varepsilon) \\ m &= m' \sinh (\sigma/\sigma_m) \\ n &= \text{constant} \end{aligned} \tag{2.10}$$

where

ε_o', σ_ε, m', σ_m = material constants

By substituting eqs. 2.10 into eq. 2.7 the nonlinear Findley power law equation is obtained

$$\varepsilon(t) = \varepsilon_o' \sinh(\sigma/\sigma_\varepsilon) + m' t^n \sinh(\sigma/\sigma_m) \qquad (2.11)$$

In eq. 2.11 the nonlinear dependence upon stress is assumed to follow a hyperbolic sine variation in stress. Apparently this assumption was originally based upon empirical observation, although theoretical justification has since been suggested [21,34,39]. This approach has been used successfully by Findley and his coworkers to characterize the viscoelastic response of many materials, including canvas, paper, and asbestos laminates [30,31], polyvinylchloride [32,44,45], and polyethylene, monochlorotriflouroethylene, and polystyrene [45].

Equation 2.11 was developed for the case of constant uniaxial creep loadings. Findley has also extended this concept to account for nonlinear viscoelastic response to a varying uniaxial load. This technique is called the Modified Superposition Principle (MSP), and has been applied by Findley et al to many of the materials mentioned above [30,32,45]. More recently, MSP has been applied by Dillard et al to characterize T300/934 graphite/epoxy laminates [21], and by Yen to characterize SMC-R50 sheet molding

compound [46].

The Modified Superposition Principle will be illustrated by considering the nonlinear viscoelastic response to a two-step uniaxial loading. Consider the creep response at time t_2 of a material which has been subjected to a constant stress σ_1 from time $t = 0$ to $t = t_1$, and subsequently to a second stress σ_2 from time t_1 to t_2. According to the MSP the creep response at time t_2 is equal to the sum of the creep response due to σ_1 from $t = 0$ to $t = t_1$ and the creep response due to $(\sigma_2 - \sigma_1)$ from $t = t_1$ to $t = t_2$. Hence, by using eq. 2.11, the creep response at time t_2 as predicted by the MSP is given by

$$\varepsilon(t_2) = \varepsilon_o' \sinh (\sigma_1/\sigma_\varepsilon) + m' t_2^n \sinh (\sigma_1/\sigma_m) + \varepsilon_o' \sinh \left(\frac{\sigma_2 - \sigma_1}{\sigma_\varepsilon}\right) + m' (t_2 - t_1)^n \sinh \left(\frac{\sigma_2 - \sigma_1}{\sigma_m}\right) \quad (2.12)$$

The Schapery Nonlinear Single-Integral Theory. As mentioned in Chapter I, Schapery's nonlinear single-integral viscoelastic theory can be derived from fundamental principles using the concepts of irreversible thermodynamics [33,34]. A thorough review of the thermodynamic basis of the Schapery theory was recently presented by Hiel et al [22]. In the present study, the Schapery theory was integrated with the accelerated characterization scheme developed

during previous research efforts at VPI&SU [21]. A detailed description of the Schapery equations and the application of these equations during the present study will be presented in Chapter III, so further discussion of the Schapery theory will be delayed until that point.

Classical Lamination Theory

A composite "lamina" or "ply" is a single membrane of composite material in which strong and stiff, continuous (i.e., very long) fibers have been embedded within a relatively weak and flexible "matrix" material. All fibers are aligned in the same direction, and the matrix serves to bind the individual fibers together to form a single unit. For polymer-matrix composites, laminae thicknesses are usually on the order of 0.13 mm (0.005 inch). A composite "laminate" is the bonded assemblage of several layers of composite laminae. The number of laminae or plies within a laminate can vary from a very few (say 4 or 5) to very many (say 150), depending upon application.

Since all fibers within a lamina are orientated in the same direction, a lamina is highly orthotropic and exhibits very high strength and stiffness properties parallel to the fibers and very low strength and stiffness properties perpendicular to the fiber direction. A composite laminate

is therefore normally designed so that fiber orientation relative to some reference direction varies from ply-to-ply, providing good overall strength and stiffness characteristics in more than one direction. An eight-ply composite laminate is shown schematically in Figure 2.12. This laminate is described as a $[0/90]_{2s}$ laminate, meaning that the 0-deg/90-deg lamina pairs are repeated twice and symmetrically about the middle surface of the laminate. Note that the individual ply directions are referenced to the x-axis.

Since a composite laminate may consist of any number of plies, and each ply may be orientated in a different direction, some method of predicting the overall elastic mechanical properties of the laminate based upon the properties of a single ply is required. Such a method has been developed and is known as "classical lamination theory" (CLT). The principal assumptions made in CLT are the plane-stress assumption and the Kirchoff hypothesis, i.e., a line which is initially straight and normal to the laminate middle surface is assumed to remain straight and normal to the middle surface after deformation. In addition, no out-of-plane extensional strains are considered. A brief review of the conventional equations used in CLT will be given below. Notation will follow that of Jones [24].

A composite lamina is shown schematically in Figure

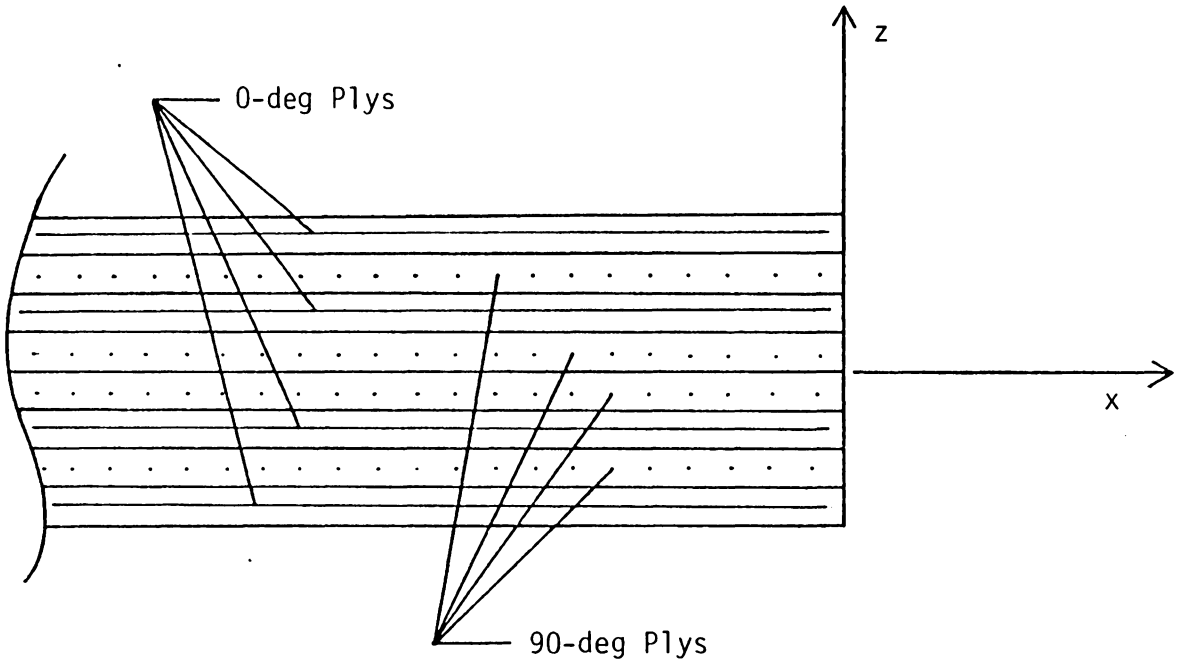

Figure 2.12: Ply Orientation for a $[0/90]_{2s}$ Composite Laminate

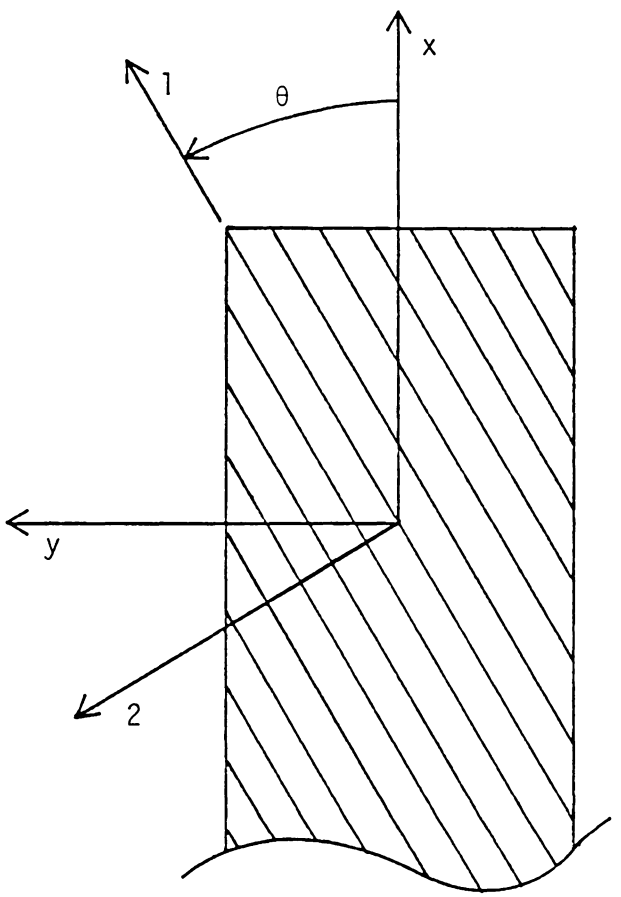

Figure 2.13: Coordinate Systems Used to Describe a Composite Lamina

2.13. The coordinate systems used to describe the lamina are the principal material coordinate system, axes 1 and 2, and the reference coordinate system, axes x and y. The 1,2 coordinate system is rotated an angle θ away from the x,y system. Under plane-stress conditions the stress-strain relations in the 1,2 coordinate system are given by the orthotropic form of Hooke's law

$$\begin{Bmatrix} \sigma_1 \\ \sigma_2 \\ \tau_{12} \end{Bmatrix} = \begin{bmatrix} Q_{11} & Q_{12} & 0 \\ Q_{12} & Q_{22} & 0 \\ 0 & 0 & Q_{66} \end{bmatrix} \begin{Bmatrix} \varepsilon_1 \\ \varepsilon_2 \\ \gamma_{12} \end{Bmatrix} \tag{2.13}$$

where

Q_{ij} = the "reduced stiffness matrix"

$$Q_{11} = \frac{E_1}{1 - \nu_{12}\,\nu_{21}} \qquad Q_{22} = \frac{E_2}{1 - \nu_{12}\,\nu_{21}}$$

$$Q_{12} = Q_{21} = \frac{\nu_{12}\,E_2}{1 - \nu_{12}\nu_{21}} = \frac{\nu_{21}\,E_1}{1 - \nu_{12}\,\nu_{21}}$$

$$Q_{66} = G_{12}$$

In the x,y coordinate system, the stress-strain relations are given by

$$\begin{Bmatrix} \sigma_x \\ \sigma_y \\ \tau_{xy} \end{Bmatrix} = \begin{bmatrix} \bar{Q}_{11} & \bar{Q}_{12} & \bar{Q}_{16} \\ \bar{Q}_{12} & \bar{Q}_{22} & \bar{Q}_{26} \\ \bar{Q}_{16} & \bar{Q}_{26} & \bar{Q}_{66} \end{bmatrix} \begin{Bmatrix} \varepsilon_x \\ \varepsilon_y \\ \gamma_{xy} \end{Bmatrix} \tag{2.14}$$

where

$\bar{Q}_{ij}$ = the "transformed reduced stiffness matrix"

$$\bar{Q}_{11} = Q_{11} m^4 + 2(Q_{12} + 2Q_{66})m^2n^2 + Q_{22} n^4$$

$$\bar{Q}_{22} = Q_{11} n^4 + 2(Q_{12} + 2Q_{66})m^2n^2 + Q_{22} m^4$$

$$\bar{Q}_{12} = \bar{Q}_{21} = (Q_{11} + Q_{22} - 4Q_{66})m^2n^2 + Q_{12}(m^4 + n^4)$$

$$\bar{Q}_{16} = \bar{Q}_{61} = (Q_{11} - Q_{12} - 2Q_{66})m^3n + (Q_{12} - Q_{22} + 2Q_{66})mn^3$$

$$\bar{Q}_{26} = \bar{Q}_{62} = (Q_{11} - Q_{12} - 2Q_{66})mn^3 + (Q_{12} - Q_{22} + 2Q_{66})m^3n$$

$$\bar{Q}_{66} = (Q_{11} + Q_{22} - 2Q_{12} - 2Q_{66})m^2n^2 + Q_{66}(m^4 + n^4)$$

$m = \cos\theta$ $\qquad$ $n = \sin\theta$

A completely equivalent treatment is to consider the strain-stress relations. In the 1,2 coordinate system, the strain-stress relations are given by

$$\begin{Bmatrix} \varepsilon_1 \\ \varepsilon_2 \\ \gamma_{12} \end{Bmatrix} = \begin{bmatrix} S_{11} & S_{12} & 0 \\ S_{12} & S_{22} & 0 \\ 0 & 0 & S_{66} \end{bmatrix} \begin{Bmatrix} \sigma_1 \\ \sigma_2 \\ \tau_{12} \end{Bmatrix} \qquad (2.15)$$

where

S_{ij} = the "reduced compliance matrix"

$$S_{11} = \frac{1}{E_1} \qquad S_{22} = \frac{1}{E_2}$$

$$S_{12} = S_{21} = \frac{-\nu_{12}}{E_1} = \frac{-\nu_{21}}{E_2}$$

$$S_{66} = \frac{1}{G_{12}}$$

In the x,y coordinate system, the strain-stress relations

are given by

$$\begin{Bmatrix} \sigma_x \\ \sigma_y \\ \gamma_{xy} \end{Bmatrix} = \begin{bmatrix} \bar{S}_{11} & \bar{S}_{12} & \bar{S}_{16} \\ \bar{S}_{12} & \bar{S}_{22} & \bar{S}_{26} \\ \bar{S}_{16} & \bar{S}_{26} & \bar{S}_{66} \end{bmatrix} \begin{Bmatrix} \sigma_x \\ \sigma_y \\ \tau_{xy} \end{Bmatrix} \tag{2.16}$$

where

$\bar{S}_{ij}$ = the "transformed reduced compliance matrix"

$$\bar{S}_{11} = S_{11}\, m^4 + (2S_{12} + S_{66})m^2n^2 + S_{22}\, n^4$$

$$\bar{S}_{22} = S_{11}\, n^4 + (2S_{12} + S_{66})m^2n^2 + S_{22}\, m^4$$

$$\bar{S}_{12} = \bar{S}_{21} = S_{12}(m^4 + n^4) + (S_{11} + S_{22} - S_{66})m^2n^2$$

$$\bar{S}_{16} = \bar{S}_{61} = (2S_{11} - 2S_{12} - S_{66})m^3n - (2S_{22} - 2S_{12} - S_{66})mn^3$$

$$\bar{S}_{26} = \bar{S}_{62} = (2S_{11} - 2S_{12} - S_{66})mn^3 - (2S_{22} - 2S_{12} - S_{66})m^3n$$

$$\bar{S}_{66} = 2(2S_{11} + 2S_{22} - 4S_{12} - S_{66})m^2n^2 + S_{66}(m^4 + n^4)$$

$m = \cos\theta$ $\qquad$ $n = \sin\theta$

The above relations are derived from the principles of orthotropic elasticity, subject to the plane-stress assumption. In practice, S_{11} and S_{22} are commonly determined using strain data obtained during uniaxial tensile tests of 0-deg and 90-deg specimens, respectively. Probably the most common strain-measuring device is an axially mounted resistance foil strain gage, although other measurement techniques such as extensometers or moire interferometry could also be used. Theoretically, S_{12} can be determined by mounting a transverse strain gage to either a 0-deg or

90-deg specimen. However, the value of ν_{21} is normally in a range of about 0.01 to 0.05, and consequently the strains measured using a transverse gage mounted to a 90-deg specimen are very low. This can lead to relatively high experimental error. In practice, it is preferable to determine S_{12} using a transverse gage mounted on a 0-deg specimen.

A variety of techniques have been proposed to determine S_{66}, including the rail-shear tests, picture-frame specimen tests, and off-axis tensile specimen tests. In particular, the 10-deg off-axis tensile test has been proposed by Chamis and Sinclair [47] as a standard test specimen for intralaminar shear characterization. Several proposed shear characterization techniques were reviewed by Yeow and Brinson [48], and it was concluded that of those methods reviewed the 10-deg off-axis test was best suited for use, primarily because it is inexpensive and easily performed, while still providing an accurate measure of the shear compliance. This technique was used during the present study. Additional details of the 10-deg off-axis test will be presented in Chapter VI.

The mechanical response of a composite lamina to in-plane external loadings can be described as presented above. The mechanical response of a composite laminate to external loading can be described through the use of CLT, in

conjunction with the orthotropic elasticity relations embodied in eqs. 2.13-16. Some results of CLT pertinent to the present study will now be presented; readers desiring a more detailed treatment are referred to the text by Jones [24].

The resultant forces N_i and resultant moments M_i acting along the edges of a composite laminate can be expressed in terms of the middle surface strains ε_j^o and curvatures κ_j as follows

$$\left\{\begin{array}{c} N_i \\ \hline M_i \end{array}\right\} = \left[\begin{array}{c|c} A_{ij} & B_{ij} \\ \hline B_{ij} & D_{ij} \end{array}\right] \left\{\begin{array}{c} \varepsilon_j^o \\ \hline \kappa_j \end{array}\right\} \tag{2.17}$$

where

$$N_i = \int_{-t/2}^{t/2} \sigma_i \, dz$$

$$M_i = \int_{-t/2}^{t/2} \sigma_i \, z \, dz$$

$$A_{ij} = \sum_{k=1}^{n} (\bar{Q}_{ij})_k \, (z_k - z_{k-1})$$

$$B_{ij} = \frac{1}{2} \sum_{k=1}^{n} (\bar{Q}_{ij})_k \, (z_k^2 - z_{k-1}^2)$$

$$D_{ij} = \frac{1}{3} \sum_{k=1}^{n} (\bar{Q}_{ij})_k \, (z_k^3 - z_{k-1}^3)$$

ε_j^o = normal and shear strains induced at laminate middle surface

κ_j = surface curvatures induced at middle surface

The z-direction is defined in a direction normal to the middle surface. Hence, the quantity $(z_k - z_{k-1})$ equals the thickness of the kth ply within the laminate. The resultant forces N_i are defined as the force per unit length acting along the edge of the laminate. Similarly, the resultant moments M_i are defined as the moment per unit length acting along the edge of the laminate. The strain state of any ply within the laminate can be expressed in terms of the middle surface strains ε_j^o and curvatures κ_j [24].

Through inspection of eq. 2.17, it can be seen that a coupling exists between the in-plane forces N_i and the out-of-plane curvatures κ_j, due to the B_{ij} matrix. Similarly, a coupling exists between the out-of-plane bending moments M_i and the in-plane middle surface strains ε_j^o, again due to the B_{ij} matrix. Such coupling is a major difference between the behaviour of composite materials and more conventional isotropic materials, since such coupling between in-plane and out-of-plane forces and deformations does not occur for isotropic materials. It can be shown that if a composite laminate is "symmetric", such as the laminate shown in Figure 2.12, then all elements of the B_{ij} matrix are zero, and no coupling between in-plane and out-of-plane forces and deformations occurs. During the present study, only symmetric laminates were considered. In addition, the only

external loads considered during the present study were in-plane normal loads; i.e., $M_i = 0$. Therefore, eq. 2.17 can be simplified for the present case to

$$\{N_i\} = [A_{ij}]\{\varepsilon_j^o\}$$

or

$$\{\varepsilon_j^o\} = [A_{ij}]^{-1}\{N_i\} \qquad (2.18)$$

Since neither out-of-plane bending loads nor coupling between the in-plane loads and out-of-plane curvatures are considered in the present case, the middle surface strains ε_j^o are equal to the elastic laminate strains ε_j^e

$$\{\varepsilon_j\}^e = \{\varepsilon_j^o\}$$

The elastic laminate strains ε_j^e as calculated above are referenced to the x,y coordinate system. These strains can be transformed to the 1,2 coordinate system of any individual ply using the standard transformation equation

$$\begin{Bmatrix} \varepsilon_1 \\ \varepsilon_2 \\ \gamma_{12}/2 \end{Bmatrix} = \begin{bmatrix} m^2 & n^2 & 2mn \\ n^2 & m^2 & -2mn \\ -mn & mn & m^2-n^2 \end{bmatrix} \begin{Bmatrix} \varepsilon_x \\ \varepsilon_y \\ \gamma_{xy}/2 \end{Bmatrix}$$

where

$$m = \cos\theta$$

$$n = \sin\theta$$

The elastic stresses acting within the kth ply, referenced to the 1,2 coordinate system, can be calculated using eq. 2.13

$$\{\sigma_i\}^k_{1,2} = [Q_{12}]^k\{\varepsilon_j\}^e_{1,2}$$

The elastic strains are considered to be the difference between the total laminate strains ε^t_j and any residual strains ε^r_j present

$$\{\varepsilon_j\}^e_{1,2} = \{\varepsilon_j\}^t_{1,2} - \{\varepsilon_j\}^r_{1,2}$$

In the present case, the residual strains considered will be those due to viscoelastic creep. Residual strains can also be caused by thermal expansion or water absorption (hygroscopic strains).

Finally, it should be noted that the above relations are contingent upon the underlying assumptions of CLT, namely the plane-stress assumption and the Kirchoff hypothesis. Accordingly, this analysis is not valid for very thick laminates or for regions near a free-edge. In both of these latter cases, a three-dimensional stress state is induced, including interlaminar shear stresses [1-3].

III. THE SCHAPERY NONLINEAR VISCOELASTIC THEORY

One of the objectives of this study was to integrate the Schapery nonlinear viscoelastic model with the accelerated characterization scheme previously developed at VPI&SU. This principally involved the inclusion of the Schapery equations in an existing computer program called VISLAP, written by Dillard [21]. The efforts to attain this objective will be described in this chapter. In the following section, the Schapery model will be reviewed, and the methods used to incorporate the appropriate equations into the present analysis will be described. This discussion is followed by a section describing the program VISLAP, as modified for use during the present study.

It should be noted that VISLAP is capable of predicting both the long-term creep response and creep rupture times of symmetric composite laminates. In the present study, creep rupture was not considered, and so in the following discussion creep rupture will be mentioned only to provide an overall review of the VISLAP program.

The Schapery Viscoelastic Model

As mentioned in Chapter I, the Schapery nonlinear viscoelastic theory can be derived from fundamental principles using the concepts of irreversible thermodynamics

[33,34], and a comprehensive review of the thermodynamic basis of the Schapery theory has recently been presented by Hiel et al [22]. The theory has been successfully applied to a variety of materials, including glass fiber-epoxy composites [35], T300/934 graphite-epoxy composites [22], nitrocellulose film, fiber-reinforced phenolic resin, and polyisobutylene [49], and FM-73 structural adhesives [37,50,51].

For the case of uniaxial loading at constant temperature, the Schapery theory reduces to the following single-integral expression

$$\varepsilon(t) = g_0 A_o \sigma + g_1 \int_{0^-}^{t} \Delta A(\psi-\psi') \frac{dg_2\sigma}{d\tau} d\tau \qquad (3.1)$$

where

A_o, $\Delta A(\psi)$ = initial and transient components of the linear viscoelastic creep compliance, respectively

$$\psi = \psi(t) = \int_{0^-}^{t} \frac{dt}{a_\sigma}$$

$$\psi' = \psi'(t) = \int_{0^-}^{\tau} \frac{dt}{a_\sigma}$$

g_0, g_1, g_2, a_σ = stress-dependent nonlinearizing material parameters

Several points should be noted regarding eq. 3.1. First, the initial and transient components of the creep compliance, A_o and $\Delta A(\psi)$, are assumed to be independent of stress level. That is, at a given temperature both A_o and $\Delta A(\psi)$ are assumed constant for any stress level, and all nonlinear behaviour is introduced through the four stress-dependent nonlinearizing parameters g_0, g_1, g_2, and a_σ. Secondly, no assumption is implied regarding the form of A_o and $\Delta A(\psi)$, and theoretically any form suitable for use with the material being investigated may be used. It is often assumed that $\Delta A(\psi)$ can be approximated by a power law in time (as will be discussed below), but this is not an implicit assumption within the Schapery theory. Thirdly, if the material is linearly viscoelastic, then $g_0 = g_1 = g_2 = a_\sigma = 1$ and eq. 3.1 reduces to the familiar Boltzman Superposition Principle (eq. 2.2). Finally, the effect of the stress-dependent parameter a_σ, embedded within the expressions defining the "reduced time" parameters ψ and ψ', is to "shift" the viscoelastic time scale, depending upon stress level. The a_σ parameter can therefore be considered to be a "stress shift factor", analogous to the familiar "temperature shift factor", a_T, used in the TTSP and discussed in Chapter II. In this light the Schapery theory can be considered to be an analytical form of a Time-Stress Superposition Principle (TSSP).

If closed-form expressions for g_0, g_1, g_2, and a_σ as functions of stress are available, and if the form of A_o and $\Delta A(\psi)$ are known, then it is theoretically possible to integrate eq. 3.1 and obtain an expression for the viscoelastic response $\varepsilon(t)$ for any uniaxial stress history $\sigma(t)$. In general such closed-form expressions are not available however, and subsequently simple stress histories must be assumed in order to integrate eq. 3.1. However, during the present study a procedure was developed whereby the viscoelastic response to a complex uniaxial stress history can be approximated to any desired degree of accuracy by using a series of discrete steps in stress. This approach will be described below and is similar in concept to the Modified Superposition Principle proposed by Findley and his colleagues, which was discussed in Chapter II.

The first step in the application of the Schapery theory is to establish an analytic form of the transient component of the creep compliance, $\Delta A(\psi)$, which is suitable for use with the material being investigated. In previous applications of the Schapery theory, $\Delta A(\psi)$ has been modeled using a power law approximation of the form

$$\Delta A(\psi) = C\psi^n \qquad (3.2)$$

This form was also used in the present study. In eq. 3.2

both C and n are assumed to be material constants at any stress level, for a constant temperature. Substituting eq. 3.2 into eq. 3.1 results in

$$\varepsilon(t) = g_0 A_o \sigma + g_1 C \int_{0^-}^{t} (\psi-\psi')^n \frac{dg_2 \sigma}{d\tau} d\tau \qquad (3.3)$$

Now consider the stress history applied during a creep/creep recovery test cycle, as previously illustrated in Figure 2.1. This stress history can be expressed mathematically as

$$\sigma(t) = \sigma_o[H(\tau) - H(\tau - t_1)]$$

and therefore

$$\frac{dg_2 \sigma}{d\tau} = g_2 \sigma_0 [\delta(\tau) - \delta(\tau - t_1)]$$

For times $0 < t < t_1$, the stress is a constant, $\sigma = \sigma_o$, and therefore

$$\frac{dg_2 \sigma}{d\tau} = g_2 \sigma_0 \delta(\tau)$$

$$\psi = \int_{0^-}^{t} \frac{dt}{a_\sigma} = \frac{t}{a_\sigma}$$

$$\psi' = \int_{0^-}^{\tau=0} \frac{dt}{a_\sigma} = 0$$

Substituting these relations into eq. 3.3 results in

$$\varepsilon_c(t) = \left[g_0 A_o + \frac{g_1 g_2 C t^n}{a_\sigma^n} \right] \sigma_0 \qquad (3.4)$$

Equation 3.4 is the Schapery equation for creep, and is applicable for times $0 < t < t_1$. The values of g_0, g_1, g_2, and a_σ are dependent upon the applied creep load σ_o. The instantaneous response at time $t = 0$ will be of interest in the following discussion. From eq. 3.4 the response at time $t = 0$ is calculated as

$$\Delta\varepsilon(0) = g_0 A_o \sigma_0$$

Now consider the recovery strains during times $t > t_1$. The current applied stress is now $\sigma = 0$, and hence $g_0 = g_1 = 1$, and eq. 3.3 becomes

$$\varepsilon_r(t) = C \int_{0^-}^{t} (\psi - \psi')^n \frac{dg_2\sigma}{d\tau} d\tau \qquad (3.5)$$

Since the stress history $\sigma(t)$ is discontinuous, eq. 3.5 must be broken into two parts

$$\varepsilon_r(t) = C \int_{0^-}^{t_1^-} (\psi - \psi')^n \frac{dg_2\sigma}{d\tau} d\tau + C \int_{t_1}^{t} (\psi - \psi')^n \frac{dg_2\sigma}{d\tau} d\tau \qquad (3.6)$$

for $\int_{0^-}^{t_1^-}$:

$$\frac{dg_2\sigma}{d\tau} = g_2\sigma_0\ \delta(\tau)$$

$$\psi = \int_{0^-}^{t} \frac{dt}{a_\sigma} = \int_{0^-}^{t_1^-} \frac{dt}{a_\sigma} + \int_{t_1}^{t} \frac{dt}{1} = \frac{t_1}{a_\sigma} + t - t_1$$

$$\psi' = \int_{0}^{\tau=0} \frac{dt}{a_\sigma} = 0$$

for $\int_{t_1}^{t}$:

$$\frac{dg_2\sigma}{d\tau} = -\ g_2\sigma_0\ \delta(\tau - t_1)$$

$$\psi = \int_{0^-}^{t} \frac{dt}{a_\sigma} = \frac{t_1}{a_\sigma} + t - t_1$$

$$\psi' = \int_{0^-}^{\tau=t_1} \frac{dt}{a_\sigma} = \frac{t_1}{a_\sigma}$$

Substituting the above relations into eq. 3.6 results in

$$\varepsilon_r(t) = g_2\, C\, \sigma_0 \left[\left\{ \frac{t_1}{a_\sigma} \left(\frac{t_1 + a_\sigma t - a_\sigma t_1}{t_1} \right) \right\}^n - \left\{ \frac{t_1}{a_\sigma} \left(\frac{a_\sigma t - a_\sigma t_1}{t_1} \right) \right\}^n \right] \qquad (3.7)$$

The following quantities are next defined

$$\psi_1 = \frac{t_1}{a_\sigma}$$

$$\lambda = \frac{t - t_1}{t_1}$$

$$\Delta\varepsilon_1 = g_1 g_2\, C\, \psi_1^n\, \sigma_o$$

and equation 3.7 is rewritten in a simpler form as

$$\varepsilon_r(t) = \frac{\Delta\varepsilon_1}{g_1} [(1 + a_\sigma\lambda)^n - (a_\sigma\lambda)^n] \qquad (3.8)$$

In the literature, Schapery has presented the recovery equation in the form of eq. 3.8.

An interesting consequence of the Schapery theory involves the instantaneous change in strain following removal of the creep load at time t_1. If the recovery strain predicted immediately after t_1 (calculated using eq. 3.8) is subtracted from the creep strain predicted immediately before t_1 (calculated using eq. 3.4), the following expression is obtained

$$\Delta\varepsilon(t_1) = g_0 A_o \sigma_0 + (g_1 - 1) g_2 \frac{C\, t_1^n}{a_\sigma^n} \sigma_0$$

The instantaneous response to the creep load has already been shown to be

$$\Delta\varepsilon(0) = g_0 A_o \sigma_0$$

Thus, the instantaneous change in strain following removal of the creep load at time t_1 equals the instantaneous

response at time t = 0 only if the material is linear, i.e., if $g_1 = 1.0$. If $g_1 > 1.0$, then $\Delta\varepsilon(t_1) > \Delta\varepsilon(0)$, and the resulting nonlinear recovery curve is "flatter" than the corresponding linear recovery curve. If $g_1 < 1.0$, then $\Delta\varepsilon(t_1) < \Delta\varepsilon(0)$ and the nonlinear recovery curve is "steeper" than the linear recovery response.

The viscoelastic response to the two-step loading illustrated in Figure 3.1 can be derived using similar mathematical procedures [49]. For example, for times $t > t_1$, the viscoelastic response is given by

$$\varepsilon(t) = g_0^2 A_o \sigma_2 + g_1^2 C \left[g_2^1 \sigma_1 \psi^n + (g_2^2 \sigma_2 - g_2^1 \sigma_1) \left(\psi - \frac{t_1}{a_\sigma^1} \right)^n \right] \qquad (3.9)$$

where

$$\psi = \frac{t_1}{a_\sigma^1} + \frac{t - t_1}{a_\sigma^2}$$

In eq. 3.9, the superscripts associated with each of the nonlinearizing parameters denote the stress level at which these parameters are to be evaluated. For example, g_2^2 indicates that g_2 is to be evaluated at stress σ_2.

During the present study, the Schapery theory was to be used to predict the viscoelastic response of individual plies within a composite laminate. In previous efforts, the

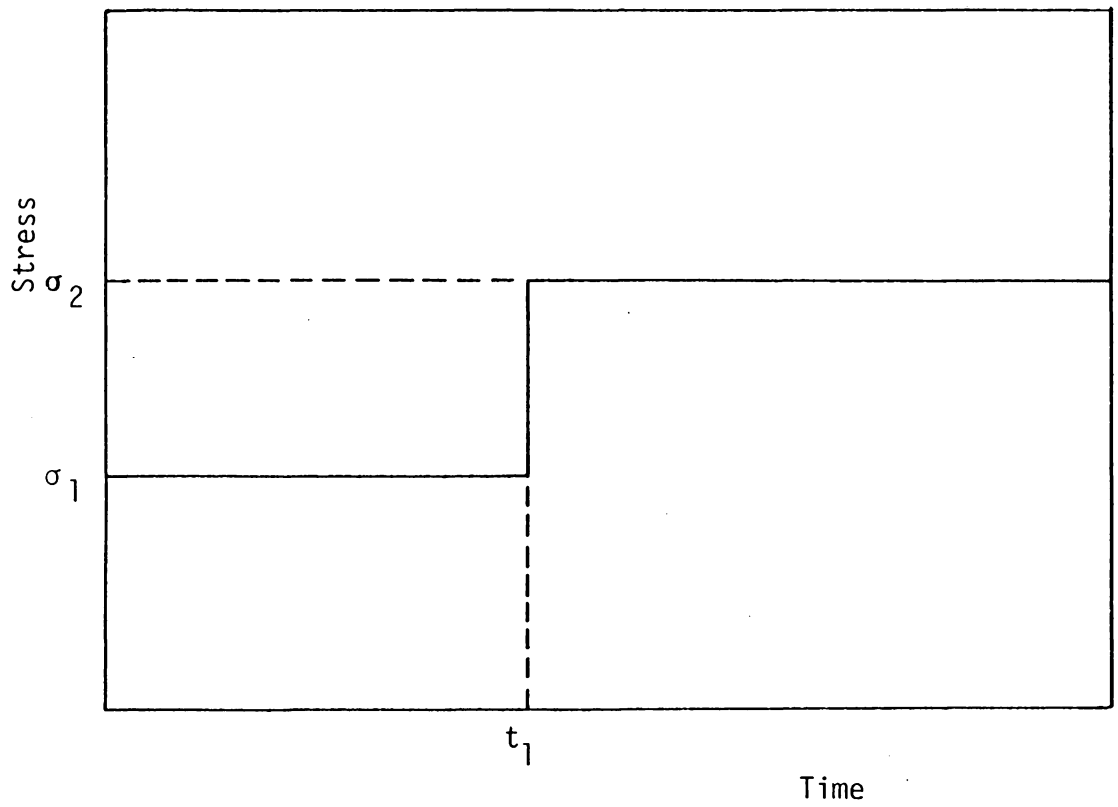

Figure 3.1: Two-Step Uniaxial Load History

stress applied to a given ply over time had been approximated in discrete steps in stress, as illustrated in Figure 3.2. Therefore, an expression for the viscoelastic response after an arbitrary number of steps in stress was required for the present effort. To the author's knowledge, such an expression has not been published in the literature. Expressions for three-step and four-step loadings were derived, using the same mathematical procedures as described above, and a predictable pattern began to emerge. By inspection, the following recursive relation was obtained for the viscoelastic response at time t_j, following j steps in stress

$$\begin{aligned}\varepsilon_j = g_0^j A_o \sigma_j + g_1^j C \Bigg\{ & g_2^1 \sigma_1 [\psi]^n + (g_2^2 \sigma_2 - g_2^1 \sigma_1) \left[\psi - \left(\frac{t_1}{a_\sigma^1} \right) \right]^n \\ & + (g_2^3 \sigma_3 - g_2^2 \sigma_2) \left[\psi - \left(\frac{t_2 - t_1}{a_\sigma^2} + \frac{t_1}{a_\sigma^1} \right) \right]^n \\ & + \\ & \vdots \\ & + (g_2^j \sigma_j - g_2^{j-1} \sigma_{j-1}) [\psi - \psi 1]^n \Bigg\}\end{aligned} \tag{3.10}$$

where

$$\psi = \sum_{k=1}^{j} \frac{t_k - t_{k-1}}{a_\sigma^k}$$

$$\psi 1 = \sum_{k=1}^{j} \frac{t_k - t_{k-1}}{a_\sigma^k}$$

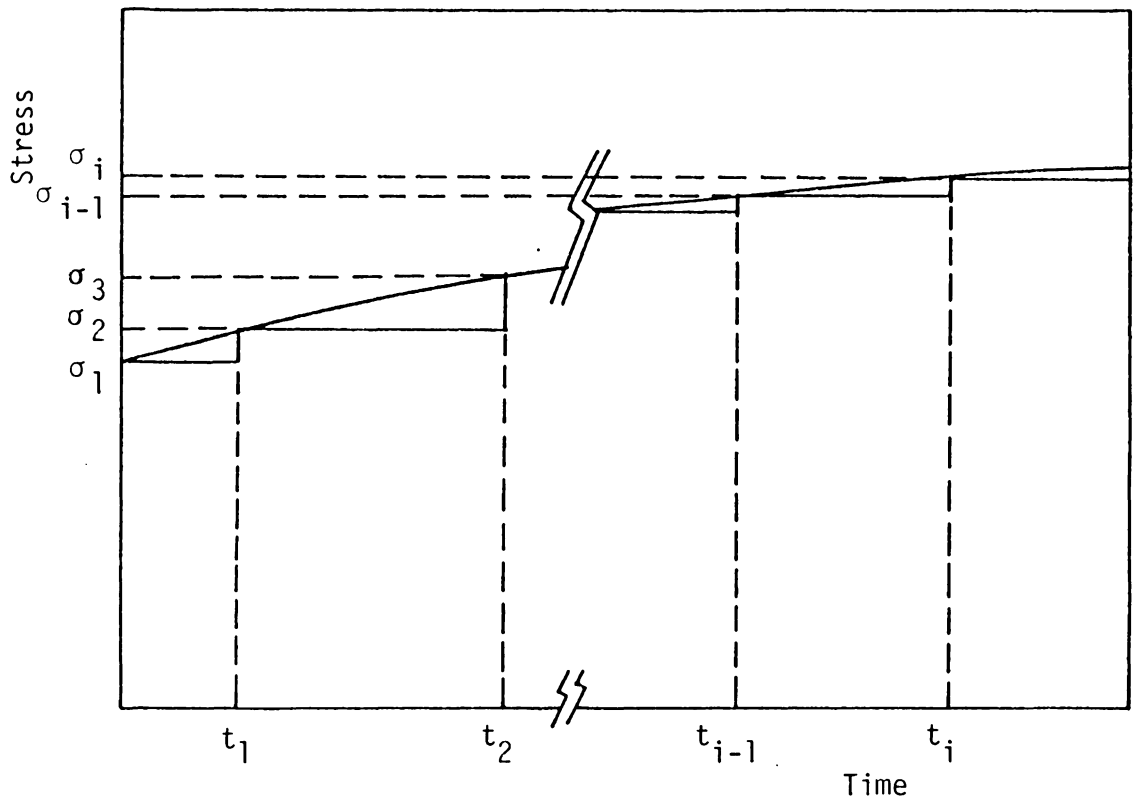

Figure 3.2: Approximation of Ply Stress History Using Discrete Steps in Stress

As before, the superscripts associated with the nonlinearizing parameters g_0, g_1, g_2, and a_σ indicate the stress level at which these quantities are to be evaluated.

In the preceding discussion a uniaxial normal stress, σ, has been used to illustrate the Schapery theory. An equivalent treatment can be presented for a constant applied shear stress , τ, and any of the above expressions can be converted to the corresponding relationship for shear by simply replacing σ with τ and ε with $\gamma/2$. For example, the recursive relationship given as eq. 3.10 becomes for the case of shear

$$\begin{aligned}\frac{1}{2}\gamma_j = g_0^j A_o \tau_i + g_1^j C \Bigg\{ & g_2^1 \tau_1 [\psi]^n + (g_2^2\tau_2 - g_2^1\tau_1)\left[\psi - \left(\frac{t_1}{a_\sigma^1}\right)\right]^n \\ & + (g_2^3\tau_3 - g_2^2\tau_2)\left[\psi - \left(\frac{t_2 - t_1}{a_\sigma^2} + \frac{t_1}{a_\sigma^1}\right)\right]^n \\ & + \\ & \vdots \\ & + (g_2^j\tau_j - g_2^{j-1}\tau_{j-1})[\psi - \psi 1]^n \Bigg\}\end{aligned} \tag{3.11}$$

where

$$\psi = \sum_{k=1}^{j} \frac{t_k - t_{k-1}}{a_\sigma^k}$$

$$\psi 1 = \sum_{k=1}^{j-1} \frac{t_k - t_{k-1}}{a_\sigma^k}$$

Experimental Measurement of the Schapery Parameters

The above presentation has indicated that to characterize the behaviour of a viscoelastic material using the Schapery theory, seven material parameters are required. These are the elastic compliance term A_o, the power law parameter C, the power law exponent n, and the four nonlinearizing functions of stress, $g_0(\sigma)$, $g_1(\sigma)$, $g_2(\sigma)$, and $a_\sigma(\sigma)$. These parameters are customarily determined through a series of creep/creep recovery tests at sequentially higher creep stress levels. At relatively low stress levels, linear viscoelastic behaviour is usually observed, and hence $g_0 = g_1 = g_2 = a_\sigma = 1$. Therefore, at low stress levels the Schapery single-integral (eq. 3.1) reduces to the Boltzman Superposition Principle (eq. 2.2), and the Schapery equation for creep (eq. 3.4) is equivalent to the Findley power law equation (eq. 2.7). The results of the low stress level creep tests can therefore be used to determine A_o, C, and n.

Nonlinear viscoelastic behaviour is often initiated at relatively high stress levels, and in general $g_0 \neq g_1 \neq g_2 \neq$

$a_\sigma \neq 1$. These four parameters are determined using the results of high stress level creep tests, where it is assumed that A_o, C, and n have been previously determined.

Lou and Schapery [35] have presented a technique whereby these seven material parameters are determined graphically. Since graphical techniques are inherently time-consuming and subject to graphical error, computer-based routines have been developed which determine these parameters by performing a least-error-squared fit between the experimental data and the appropriate analytic expression. Two such numerical schemes where used in the present study. The first of these was written by Bertolloti et al [52], and is called the SCHAPERY program, since it is based upon the Schapery nonlinear equations. The second was written by Yen [46], and is called the FINDLEY program, since it is based upon the Findley power law equation. As discussed above, under conditions of linear viscoelastic behaviour the Schapery creep equation and the linear Findley power law equation are equivalent. FINDLEY was used in the present study only for linear viscoelastic stress levels.

Both the SCHAPERY and FINDLEY programs utilize a commercially available least-error-squared fitting routine called ZXSSQ, which is an ISML library routine available on the VPI&SU computer system. This routine is capable of fitting a user-supplied analytic expression involving N

unknowns to a set of M experimental measurements. The details of the ZXSSQ routine are proprietary to ISML, and in any case are irrelevent to the present discussion since routines which can provide the same function are available on most computer systems.

Some details regarding the SCHAPERY and FINDLEY programs are described below.

Program SCHAPERY

The computer program SCHAPERY is used to perform two distinct analyses, the linear viscoelastic analysis and the nonlinear viscoelastic analysis. For the linear case three unknowns are required; namely A_o, C, and n. For the nonlinear case it is assumed that A_o, C, and n are known, and the four remaining unknowns g_0, g_1, g_2, and a_σ are required. It is easiest to discuss the program by first considering a linear analysis and then considering a nonlinear analysis.

Linear Analysis. For the linear case the Schapery equations for creep and recovery are reduced to:

$$\varepsilon_c(t) = A_o\sigma + C\sigma t^n \tag{3.12}$$

and

$$\varepsilon_r(t) = \Delta\varepsilon_1[(1 + \lambda)^n - \lambda^n] \tag{3.13}$$

where

$$\Delta\varepsilon_1 = C\sigma t_1^n$$

$$\lambda = \frac{t - t_1}{t}$$

The three unknowns in these equations are the instantaneous compliance A_o, and the power law parameters C and n.

The SCHAPERY program uses linear creep and recovery data to determine these parameters as shown in the flow chart given in Figure 3.3. First information defining the data set is input. This includes the number of recovery points, NREC, the number of creep points, NCR, the creep unloading time, t_1, the creep stress level, σ, and initial estimates for the transient creep strain, $\Delta\varepsilon_1$, and power law parameter n. Note that in the linear case the transient creep strain is directly proportional to the power law parameter C

$$C = \frac{\Delta\varepsilon_1}{\sigma_0 \, t_1^n} \tag{3.14}$$

Therefore, the initial estimate for $\Delta\varepsilon_1$ is an initial estimate for C as well.

Next the recovery data pairs are input, consisting of the recovery time, TREC(M), and the measured recovery strain, REC(M). The linear recovery curve, eq. 3.13, is then fit to the data using ZXSSQ, and estimates for the two unknowns $\Delta\varepsilon_1$

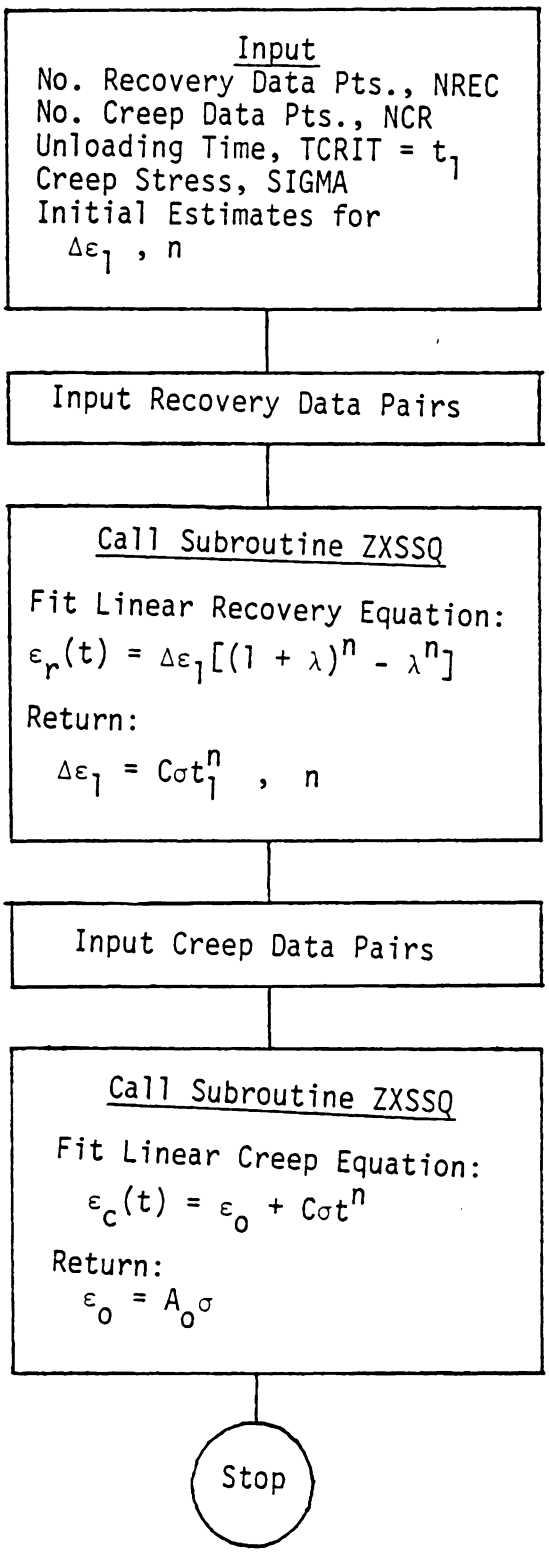

Figure 3.3: Flow Chart for Program SCHAPERY - Linear Analysis

and n are obtained. C is then calculated using eq. 3.14.

The creep data pairs are then input, TCR(M) and CR(M). Since C and n have been determined using the recovery data, the only unknown which remains is the instantaneous compliance A_o. The value of A_o is calculated by fitting the creep data to the linear equation for creep, eq. 3.12, again using the library routine ZXSSQ.

Nonlinear Analysis. In the nonlinear case, the Schapery equations for creep and recovery are

$$\varepsilon_c(t) = g_0 A_o \sigma_0 + \frac{g_1 g_2}{a_\sigma^n} C\, t^n \sigma_o \tag{3.15}$$

and

$$\varepsilon_r(t) = \left(\frac{\Delta\varepsilon_1}{g_1}\right) \left[(1 + a_\sigma \lambda)^n - (a_\sigma \lambda)^n\right] \tag{3.16}$$

where, for the nonlinear case,

$$\Delta\varepsilon_1 = \frac{g_1 g_2}{a_\sigma^n} C\, \sigma\, t_1^n$$

Since it is assumed that a linear analysis has been performed to determine A_o, C, and n, there are only four unknowns remaining in eqs. 3.15 and 3.16. These are g_0, g_1, g_2, and a_σ. Program SCHAPERY uses nonlinear creep and creep recovery data to determine these parameters as shown in the flow chart given in Figure 3.4. First, information defining the data set is input, which includes the number of recovery

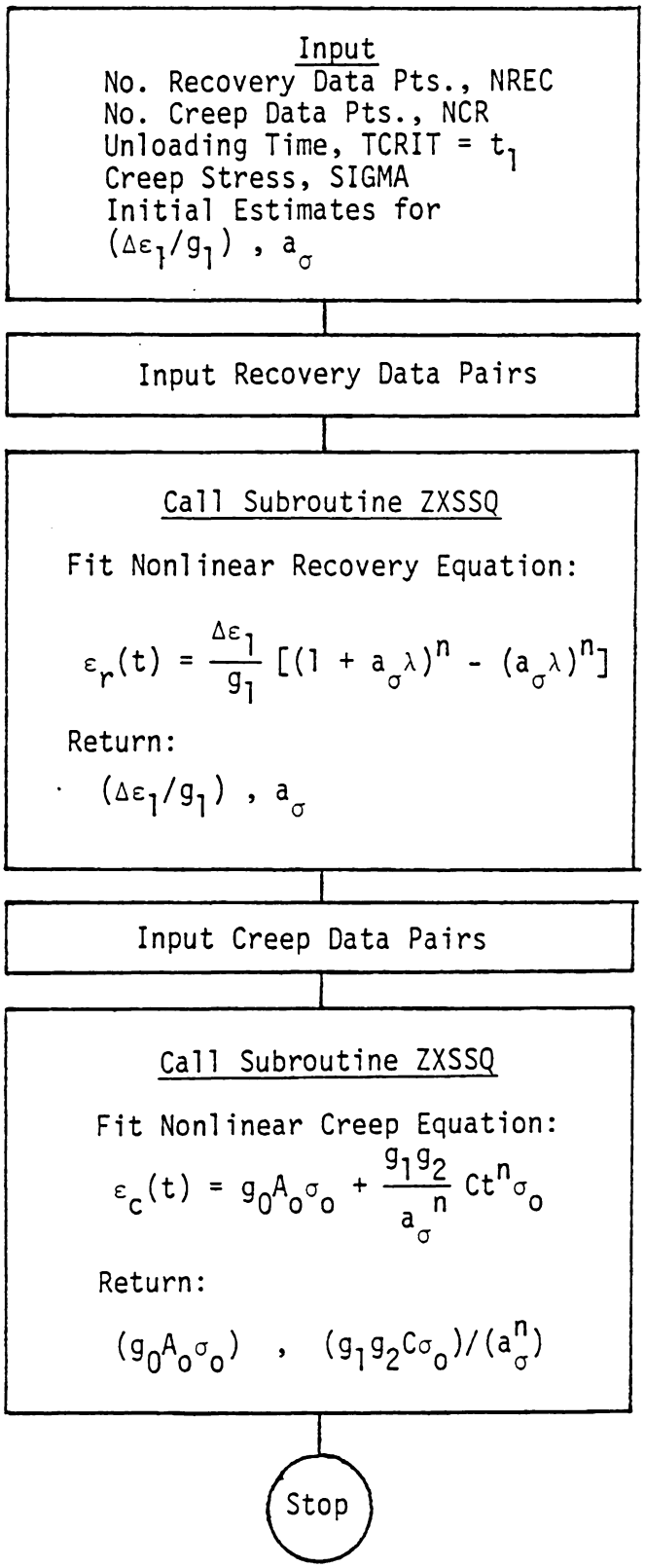

Figure 3.4: Flow Chart for Program SCHAPERY - Nonlinear Analysis

points, NREC, the number of creep points, NCR, the creep stress unloading time, t_1, and initial estimates for the transient recovery strain, $(\Delta\varepsilon_1/g_1)$, and the parameter a_σ. The recovery data pairs are then input, which consists of the recovery time, TREC(M), and the measured recovery strain at that time, REC(M). The nonlinear recovery curve, eq. 3.16, is then fit to the data using ZXSSQ and estimates for the two curve-fitting parameters, $(\Delta\varepsilon_1/g_1)$ and a_σ, are obtained.

Next, the creep data pairs are input, TCR(M) and CR(M). The nonlinear creep curve, eq. 3.15, is then fit to the creep data using ZXSSQ. Estimates for the quantities $(g_0 A_o \sigma)$ and $(g_1 g_2 C\sigma/a_\sigma^n)$ are obtained. This completes the analysis, since all of the Schapery parameters may now be calculated as follows:

$$g_0 = \frac{(g_0 A_o \sigma_0)}{A_o \sigma_0}$$

$$\Delta\varepsilon_1 = \left[\frac{g_1 g_2}{a_\sigma^n} C\,\sigma\right] t_1^n$$

$$g_1 = \frac{\Delta\varepsilon_1}{(\Delta\varepsilon_1/g_1)}$$

$$g_2 = \frac{\left[\left[\frac{g_1 g_2}{a_\sigma^n} C\,\sigma\right] a_\sigma^n\right]}{g_1 C\,\sigma}$$

Program FINDLEY

Since the program FINDLEY is used only for the case of linear viscoelastic behaviour, there are only three unknowns, A_o, C, and n. These parameters are determined using creep data only. The creep data is fit to the Findley power law equation

$$\varepsilon(t) = \varepsilon_o + mt^n$$

where

$$\varepsilon_o = A_o\sigma$$

$$m = C\sigma \qquad (3.17)$$

A flow chart for the FINDLEY program is given in Figure 3.5. Information defining the data set is input first, including the number of creep data points, initial estimates for ε_o, m, and n, and the time and creep data sets. The Findley power law is then fit to the data, and best-fit estimates for ε_o, m, and n are returned. A_o and C are then calculated using eqs. 3.17.

Average Matrix Octahedral Shear Stress

A final consideration is the effect of stress

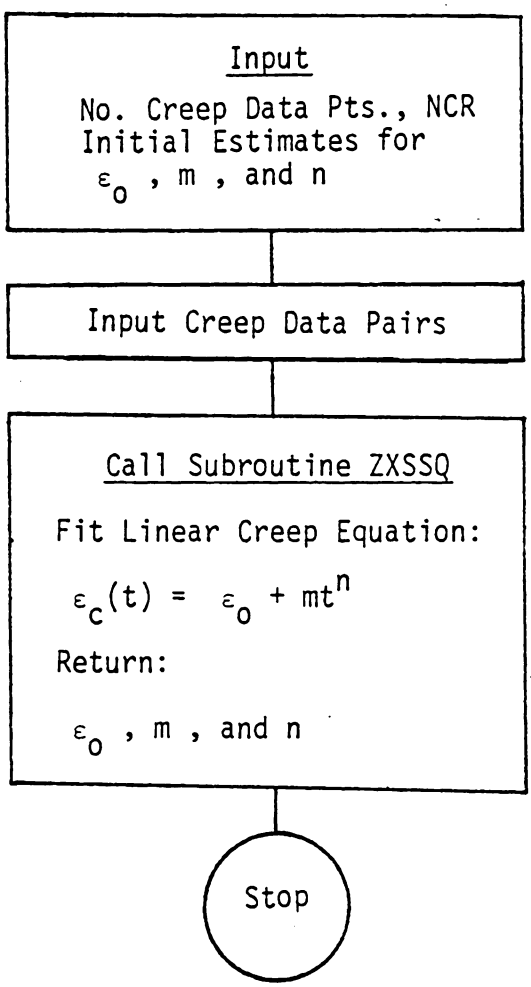

Figure 3.5: Flow Chart for Program FINDLEY

interaction in the case of multiaxial stress states. During experimental characterization of a viscoelastic material the various parameters are often determined under conditions of a uniaxial normal stress. In the present case the $S_{22}(t,\sigma)$ compliance term was determined based on a uniaxial stress σ_2, for example. However, an individual ply within a composite laminate is in general subjected to a plane-stress state consisting of the three stress components σ_1, σ_2, and τ_{12}. The effects of stresses σ_1 and τ_{12} on viscoelastic parameters which have been determined under uniaxial stress σ_2 only must therefore be considered. Lou and Schapery [35] and Dillard, Morris, and Brinson [21] have accounted for such interaction through the use of the "average matrix octahedral shear stress", τ_{oct}. This approach uses a simple rule of mixtures approximation to calculate τ_{oct}. The resulting expression for τ_{oct} is [21]

$$\tau_{oct} = \frac{1}{3}\left[(\sigma_1^m - \sigma_2^m)^2 + (\sigma_1^m)^2 + (\sigma_2^m)^2 + 6(\tau_{12}^m)^2\right]^{\frac{1}{2}} \qquad (3.17)$$

where the matrix stresses σ_1^m, σ_2^m, and τ_{12}^m are given in terms of the applied ply stresses σ_1, σ_2, and τ_{12} by

$$\begin{Bmatrix} \sigma_1^m \\ \sigma_2^m \\ \tau_{12}^m \end{Bmatrix} = \begin{bmatrix} \left(\frac{E_m}{E_{11}}\right) & \left(\nu_m - \frac{E_m}{E_{11}}\nu_{12}\right) & 0 \\ 0 & 1 & 0 \\ 0 & 0 & 1 \end{bmatrix} \begin{Bmatrix} \sigma_1 \\ \sigma_2 \\ \tau_{12} \end{Bmatrix} \qquad (3.18)$$

and

$$E_{11} = E_f v_f + E_m(1 - v_f)$$

$$\nu_{12} = \nu_f v_f + \nu_m(1 - v_f)$$

ν_m = matrix Poisson's ratio

E_f = fiber modulus

E_m = matrix modulus

v_f = fiber volume fraction

Note that it is assumed that both the ply normal stresses perpendicular to the fibers and the ply shear stresses are supported entirely by the matrix, i.e., $\sigma_2^m = \sigma_2$ and $\tau_{12}^m = \tau_{12}$.

Some of the above properties were not available for the graphite-epoxy used in this study, as the manufacturer had only supplied the volume fraction. The properties required were obtained by measuring E_{11}, E_{22}, and ν_{12}, and assumimg a value for ν_m. With the additional rule of mixtures relation

$$E_{22} = \frac{E_f E_m}{(1 - v_f) E_f + v_f E_m}$$

it was possible to calculate an appropriate value for each of the required material properties. The values obtained and used in the analysis were

E_{11} = 132.2 GPa (19.16 X 10^6 psi)

ν_{12} = 0.273

ν_m = 0.35

E_f = 201.3 GPa (29.2 X 10^6 psi)

E_m = 3.42 GPa (0.497 X 10^6 psi)

v_f = 0.65

The ply strain-stress relationships as used in the present analysis can now be written in the form of eq. 2.15 as

$$\begin{Bmatrix} \varepsilon_1(t) \\ \varepsilon_2(t) \\ \gamma_{12}(t) \end{Bmatrix} = \begin{bmatrix} S_{11} & S_{12} & 0 \\ S_{12} & S_{22}(t,\tau_{oct}) & 0 \\ 0 & 0 & S_{66}(t,\tau_{oct}) \end{bmatrix} \begin{Bmatrix} \sigma_1(t) \\ \sigma_2(t) \\ \tau_{12}(t) \end{Bmatrix} \qquad (3.19)$$

Lamination Program VISLAP

The computer program VISLAP provides long-term predictions of both the creep compliance and the creep rupture times of composite laminates of symmetric layup. This program was modified during the present study by inserting the Schapery viscoelastic model into the program as described above. The program will be briefly described

in this paragraph. The reader is referred to Reference 21 if additional details regarding program structure are desired.

The analysis performed by VISLAP is based upon classical lamination theory, either the Findley MSP or the Schapery viscoelastic model, and the Tsai-Hill failure criterion [24]. The Tsai-Hill failure criterion is normally applied to elastic materials, but has been modified for use with viscoelastic materials during previous research efforts [21]. A linear cumulative damage law is used to account for time-varying ply stresses.

A flow diagram of VISLAP is given in Figure 3.6. The program proceeds as follows: The laminate layup and initial lamina properties are input, (A). The current elastic laminate strain is determined using CLT, (B) through (G). The total laminate strain is then calculated as the sum of the current elastic laminate strain plus the current equivalent laminate creep strain, (H). The individual ply stresses are next calculated, based upon the total laminate strain minus the individual ply creep strain, (I). If the ply stresses have changed significantly since the previous time step, a nonlinear iteration procedure cycles through steps (B) through (I) to assure that the ply stresses have converged to the actual current stress state, (J). This stress state is then stored in a stress history array and

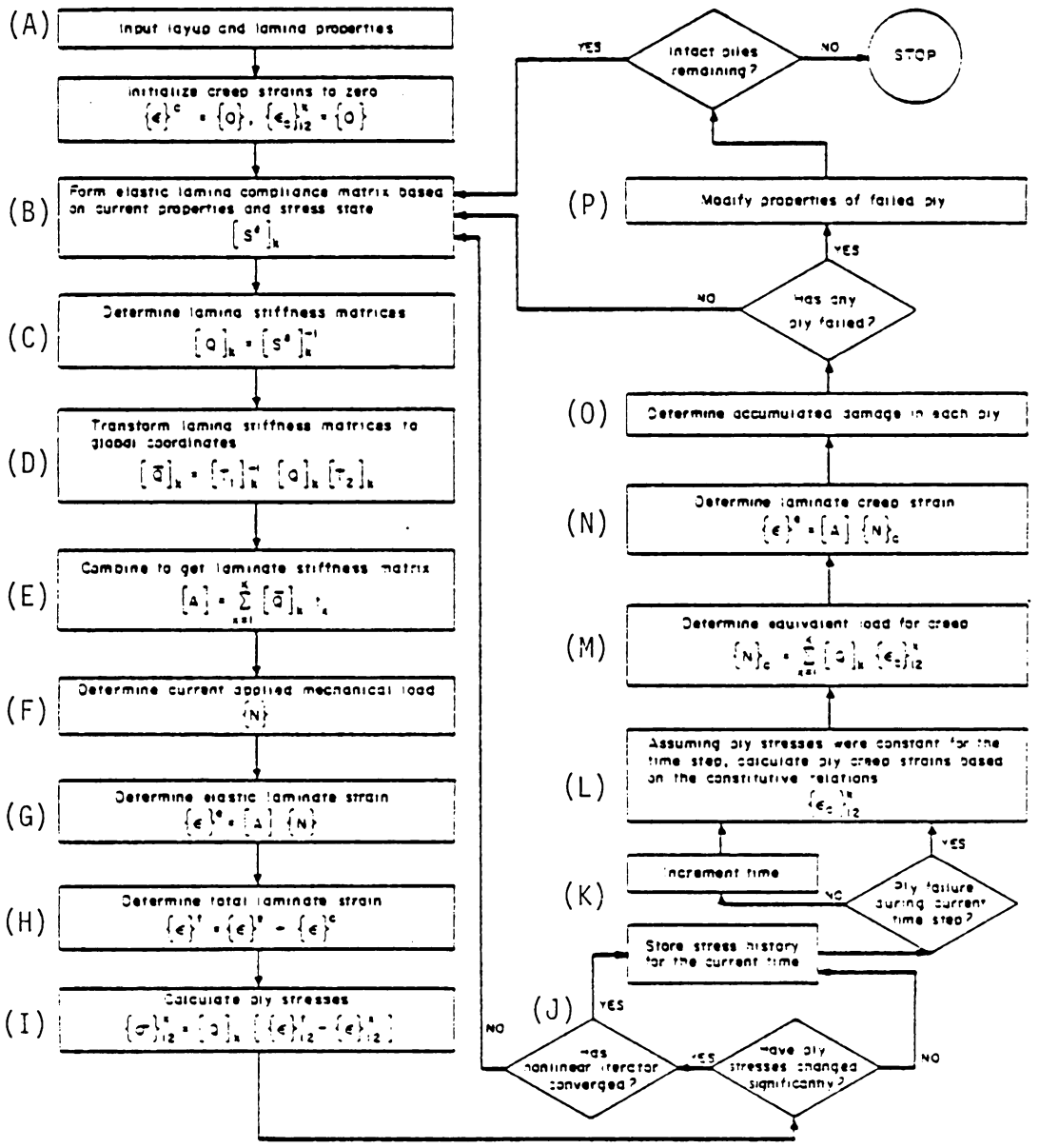

Figure 3.6: Flow Chart for Viscoelastic Laminated Analysis VISLAP [21]

time is incremented, (K). The current ply creep strains which would be produced by the stresses stored in the stress history array are then calculated, (L). The modified version of VISLAP allows the user to select either the Findley MSP viscoelastic model or the Schapery viscoelastic model to calculate these ply creep strains. An "equivalent mechanical load" which equals the summation of the loads required to produce ply elastic strains of the same magnitude as the current ply creep strains is next calculated (M). This equivalent load is then used to calculate the equivalent laminate creep strain (N). The modified Tsai-Hill failure criterion is used to predict any lamina failures, together with the cumulative damage law and the stress history array. Should a ply fail, the ply properties are modified to account for the type of ply failure (i.e., either a fiber or a matrix failure), (O) and (P). The entire procedure is repeated until either all plies have failed or the user-specified maximum time is reached.

A subtle point in the analysis which should be noted is that the equivalent laminate creep strains calculated in step (N) do not in general equal the individual ply creep strains calculated in step (L). The differences between the equivalent laminate creep strains and the individual ply creep strains are added to the original elastic ply strains,

resulting in ply stresses which vary with time. As viscoelastic deformations occur, a greater percentage of the externally applied loading is supported by the fibers, whereas the matrix load is decreased. Thus, the ply stresses change with time even though the externally applied creep load is constant.

IV. SENSITIVITY ANALYSIS

Early in the experimental portion of this study, it became apparent that the linear viscoelastic parameters A_o, C and n were very sensitive to small errors in measured strain data. High sensitivity to measurement errors have also been reported by Dillard [21], Hiel [22], Rochefort [37], and Yen [46]. Both Dillard and Yen concluded that a stable value for the power law exponent n could not be obtained through short-term creep tests; long-term tests of a duration of 10^4 minutes (6.9 days) or greater were required. The major difficulty encountered by Hiel during his application of the Schapery theory was that "damage" accumulated within the test specimen during the creep portion of the creep/creep recovery testing cycle. This resulted in a permanent strain reading after the recovery period, i.e., the recovery strains did not return to zero but rather approached some permanent strain level in an asymptotic manner. Similar difficulties have been discussed by others, including Lou and Schapery [35], Caplan and Brinson [36], and Peretz and Weitzman [50]. From these efforts, it appears that damage accumulated during the creep portion of the testing cycle is the major potential source of error in application of the Schapery theory. Hiel used his recovery data to calculate various viscoelastic

parameters, but could obtain stable values only by first subtracting the permanent strain from the recovery data recorded at each point in time. This procedure effectively translates the entire recovery curve down towards zero strain.

It should be noted that many researchers subject viscoelastic specimens to a "mechanical conditioning cycle" prior to the creep/creep recovery test [35,37,46]. The assumption is that such a conditioning cycle produces a stable damage state within the specimen, and no further damage is accumulated during the creep/creep recovery test. Apparently this approach avoids the difficulties associated with permanent recovery strains encountered by Hiel. However, Hiel argues [22] that mechanical conditioning results in a fundamental change in the material being investigated, and therefore results obtained from mechanically conditioned specimens do not reflect the behaviour of the material which would occur in a practical situation. Specifically, it was felt that mechanical conditioning results in plastic deformation of the matrix material which alters the initial stress-strain constitutive relationship of the virgin matrix material. A further complication arises in the present case, since results obtained using unidirectional specimens were to be used to predict the response of laminates with arbitrary layup.

Since ply stress states vary with layup, the appropriate mechanical conditioning cycle would depend upon the specific laminate being studied. Due to the above considerations, no mechanical conditioning was performed in the present study.

Two areas of concern arose during the present efforts due to the above observations. First, the level of accuracy required when determining the values of the seven Schapery viscoelastic parameters was not clear. Since these parameters were to be used to predict long-term viscoelastic behaviour, such errors could obviously impact the predicted response. Therefore, until the impact of these errors on predicted response was evaluated, the severity of such errors could not be properly appreciated. Secondly, it appeared that some viscoelastic parameters were more sensitive to experimental error than others. For example, the values obtained for the power law exponent n by Dillard [21] at various stress levels exhibited a significant scatter, whereas the values for the power law parameter m (where in the linear case $m = C\sigma$) were relatively smooth and uniform with stress (see Figure 1.3). An attempt was made to determine the origin of this sensitivity. It was felt that such information would indicate the level of stability which could be expected for each parameter during reduction of actual experimental data, and might also be useful in selecting appropriate testing cycles and data reduction

techniques.

Impact on Long-Term Predictions

One of the major objectives of this study was to predict the long-term behaviour of a composite laminate based solely upon the results of short-term tests of unidirectional composite specimens. Specifically, the creep compliance of a composite laminate was monitored for a period of 10^5 minutes (69.6 days). Therefore, the impact of error over a 10^5 minute period was considered.

Consider a nonlinear viscoelastic material subjected to a uniaxial creep load, and assume that the material follows the Schapery theory exactly. Thus, the viscoelastic response is given by eq. 3.4, restated here for convenience

$$\varepsilon_c(t) = \left[g_0 A_o + \frac{g_1 g_2 \, C \, t^n}{a_\sigma^n} \right] \sigma_0 \qquad (3.4)$$

Further suppose that the exact values for each of the seven viscoelastic parameters involved in eq. 3.4 are as follows

$A_o = 0.0978/\text{GPa}$ $(0.674 \times 10^{-6}/\text{psi})$

$C = 0.00210/\text{GPa-min}^n$ $(0.0145 \times 10^{-6}/\text{psi-min}^n)$

$n = 0.33$

$g_0 = 1.10$

$g_1 = 1.10$

$g_2 = 0.90$

$a_\sigma = 0.90$

The values for the nonlinearizing parameters correspond to values expected for a slightly nonlinear viscoelastic material. They were selected because previous results indicated that the 90-deg unidirectional T300/5208 graphite-epoxy specimens used in this study were either linearly viscoelastic or only slightly nonlinearly viscoelastic at a temperature of 300F. The values for A_o, C, and n were estimated using the results of a few initial tests at low stress levels.

Now suppose that an experimental program has been conducted, and all viscoelastic parameters have been calculated exactly except for one, say g_2^e. The superscript "e" denotes that the experimental g_2 value is in error. The creep strain which would be expected based upon these experimental results is given by

$$\varepsilon_c^e(t) = \left[g_0 A_o + \frac{g_1 g_2^e \, C \, t^n}{a_\sigma^n} \right] \sigma_0$$

The error in predicted strain at any time t can now be expressed as

$$\text{error}(t) = \frac{\varepsilon_c^e(t) - \varepsilon_c(t)}{\varepsilon_c(t)} \times 100\%$$

The impact on predicted strain levels at any time t due to

an error in one of the viscoelastic parameters can be isolated using this approach. Based upon previous results, a deviation of $\pm 10\%$ from the average measured value of the linear viscoelastic parameters is not uncommon, so this level of error was used in the analysis. A creep stress level of 13.8 MPA (2000 psi) was assumed.

Note from eq. 3.4 that g_0 and A_o are both linearly related to the creep strain $\varepsilon_c(t)$, and therefore a $\pm 10\%$ error in either g_0 or A_o has the same affect on $\varepsilon_c(t)$. Similarly, $\pm 10\%$ errors in g_1, g_2, or C affect the predicted creep strains in identical fashion. Therefore, only four analyses were required: the first to account for errors in g_0 or A_o, the second to account for errors in g_1, g_2, or C, the third to account for errors in n, and the fourth to account for errors in a_σ.

Results are summarized in Figures 4.1-4.4. Figure 4.1 illustrates the error in predicted creep strains due to a $\pm 10\%$ error in either g_0 or A_o. An error of this type is confined entirely to the instantaneous creep strain, i.e., the transient creep strains are not affected by an error in either g_0 or A_o. Therefore, the percentage error is equal to $\pm 10\%$ at time t = 0, and slowly decreases with time as transient strains develop. After 10^5 minutes, the error has been reduced to about $\pm 7\%$.

The effects of a $\pm 10\%$ error in g_1, g_2, or C are

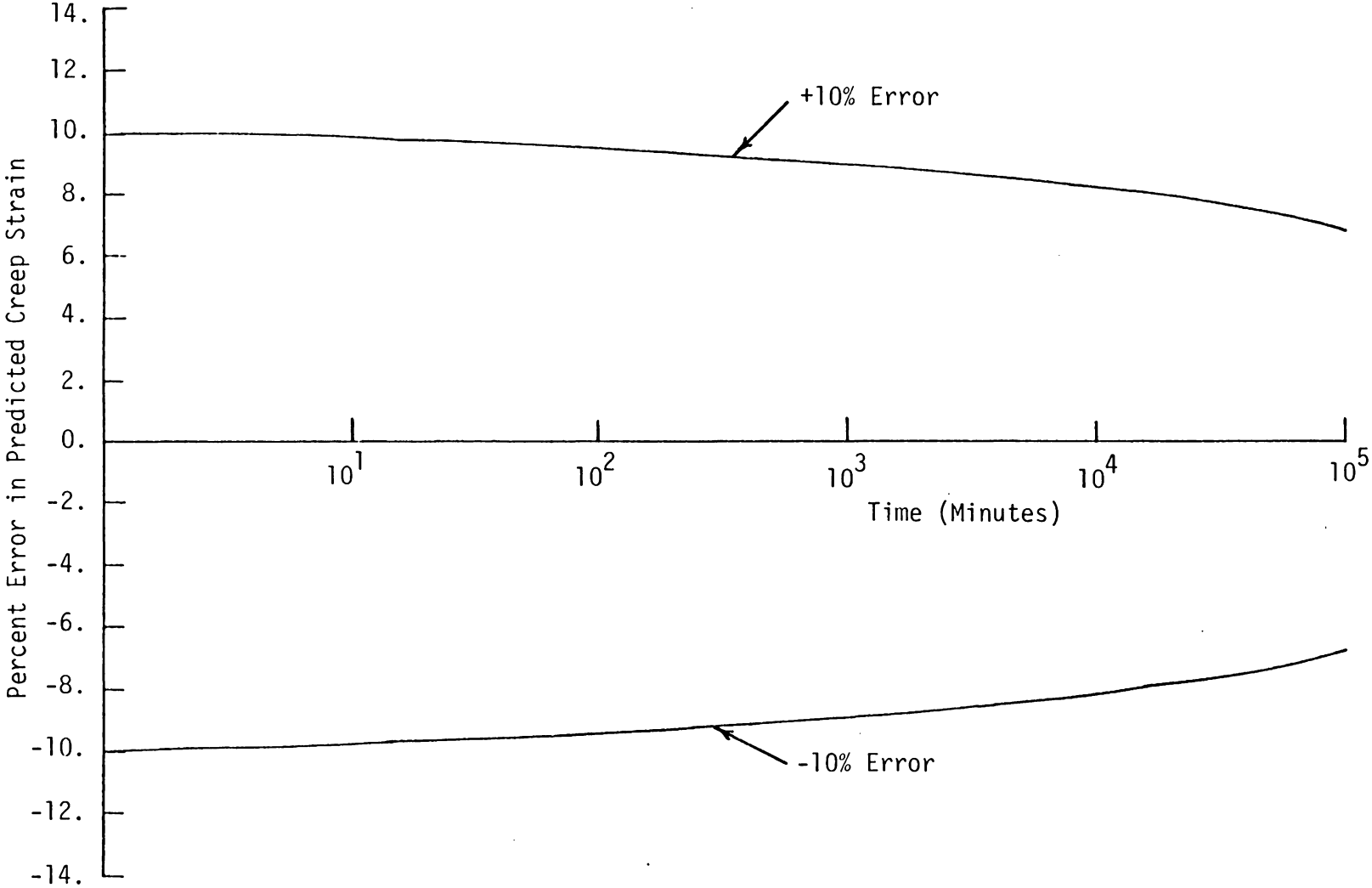

Figure 4.1: Percent Error in Predicted Creep Strains Due to a $\pm$10% Error in A_o or g_o

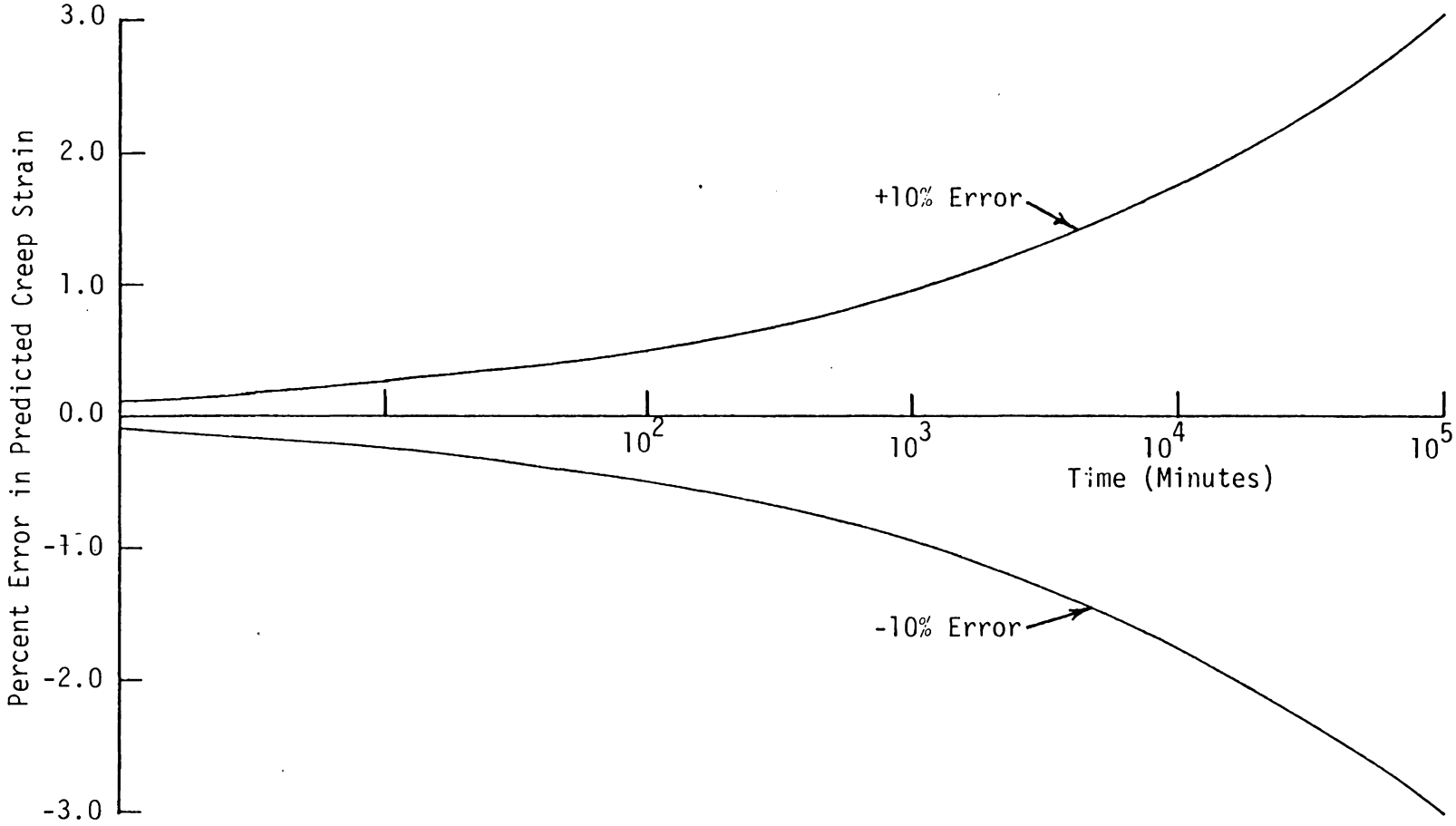

Figure 4.2: Percent Error in Predicted Creep Strains Due to a $\pm$10% Error in C, g_1, or g_2

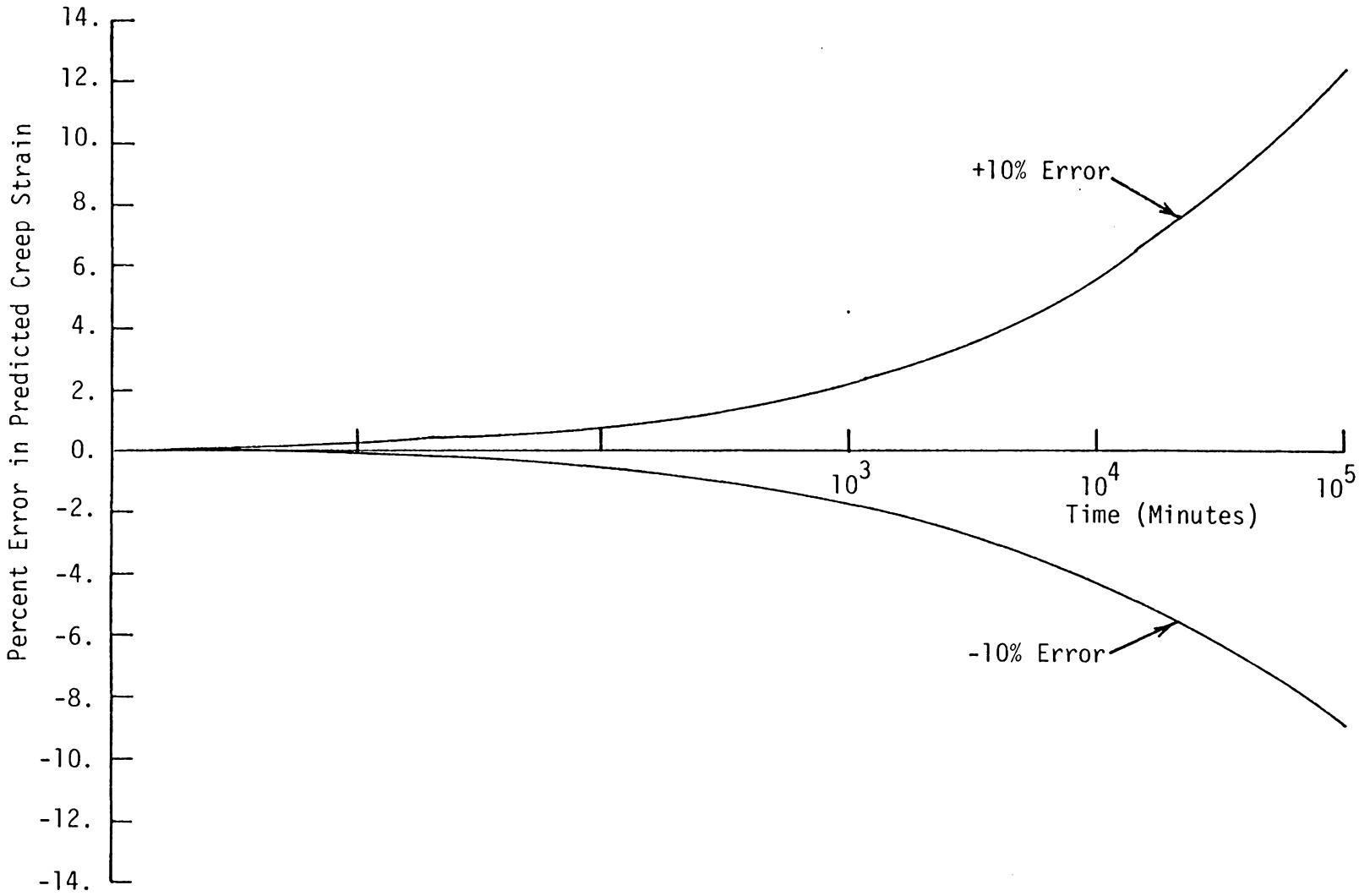

Figure 4.3: Percent Error in Predicted Creep Strains Due to a $\pm$10% Error in n

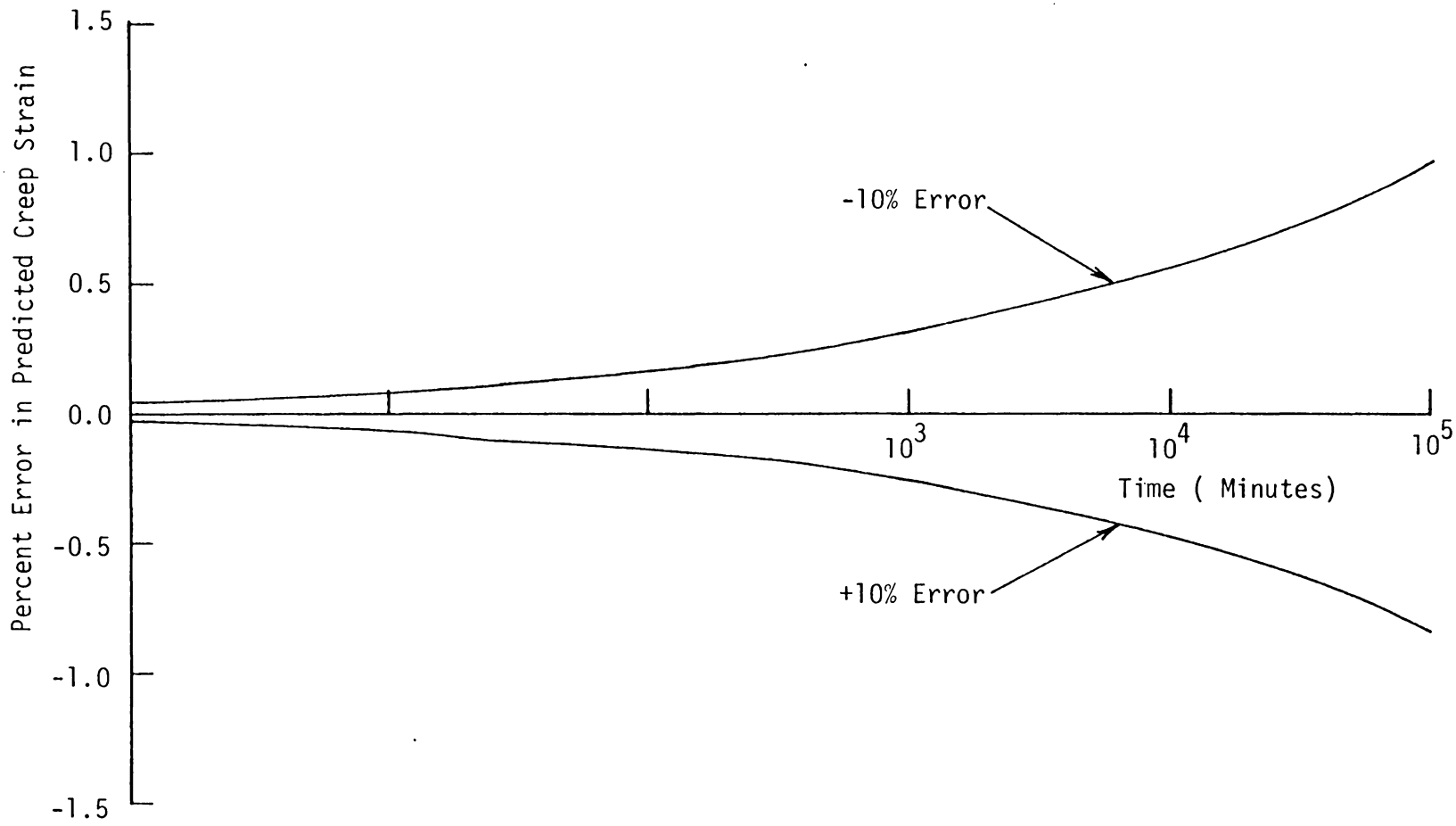

Figure 4.4: Percent Error in Predicted Creep Strains Due to a $\pm$10% Error in a_σ

illustrated in Figure 4.2. Since an error of this type impacts only the transient component of the total creep response, the percentage error is very low at short times, and in fact is zero at time t = 0. As indicated, the percentage error reaches $\pm 3\%$ after 10^5 minutes.

Figure 4.3 illustrates percentage error due to a $\pm 10\%$ error in n. This error again impacts only the transient strain response, and hence the error is very low at short times. At long times however, the error becomes appreciable and obviously increases dramatically for times greater than 10^5 minutes. A 10% error in n results in a 12% error in $\varepsilon_c(t)$ after 10^5 minutes, while a -10% error in n results in a -9% error in $\varepsilon_c(t)$ after 10^5 minutes.

A $\pm 10\%$ error in a_σ is illustrated in Figure 4.4. The error curve for a_σ is very similar to that for error in n, but as indicated the predicted values for $\varepsilon_c(t)$ are much less sensitive to error in a_σ than to error in n. The error in $\varepsilon_c(t)$ due to a +10% error in a_σ is less than $\pm 1\%$ after 10^5 minutes.

It should be noted that Figures 4.1-4.4 are based upon the specific values selected for A_o, C, n, g_0, g_1, g_2, and a_σ. Different results would obviously be obtained if the material properties were different, and the results reported here should not be considered to be representative of the response of all viscoelastic materials. It is considered

that the results presented are reasonably accurate for a 90-deg unidirectional specimen of T300/5208 graphite-epoxy, however.

Sensitivity to Experimental Error

In this paragraph, efforts to determine which of the viscoelastic parameters are most sensitive to experimental error will be described. As presented in Chapter III, these seven parameters are determined using a two-step process. First A_o, C, and n are calculated using creep and recovery data obtained at relatively low stress levels such that linear viscoelastic behaviour is observed. Once estimates for A_o, C, and n are obtained the remaining four parameters g_0, g_1, g_2, and a_σ are determined using nonlinear data recorded at higher stress levels. The sensitivity analysis followed this same format. An analysis was first performed which considered the sensitivity of A_o, C, and n to errors in linear viscoelastic data. A second analysis then considered the sensitivity of g_0, g_1, g_2, and a_σ to errors in nonlinear viscoelastic data.

The first step in both analyses was to generate an "exact" creep and creep recovery data set. This data set was generated analytically using the Schapery equations. That is, strain data were calculated at specified times using eqs. 3.4 and 3.8 and subsequently used as the exact

data set. Values assumed for the various viscoelastic parameters were the same as those listed in the preceding paragraph, and as noted are appropriate for a slightly nonlinear viscoelastic material. A 30 minute/60 minute creep/creep recovery testing cycle was assumed. A testing cycle of this duration is typical of those used in previous studies [18-22,35-37,46,50,51]. During the present study, a 480 minute/120 minute creep/creep recovery test cycle was used, partially due to the results of the present sensitivity analysis. Selection of the testing cycle employed in this study will be further discussed in Chapter V.

Once the exact data was obtained as described above, it was neccessary to define the errors within the data set. Two types of error were considered, a "percentage error" and an "offset error". For the percentage error case, the strain data used in the analysis was in error by some constant percentage of the exact strain value at each point in time. The $\pm$10% error case for creep recovery is shown in Figure 4.5. Note that a percentage error causes a change in shape of the strain history curve, since the numerical value of the error changes as the value of the exact strain data changes.

For the case of an offset error, the strain data used in the analysis was in error by some constant amount at any

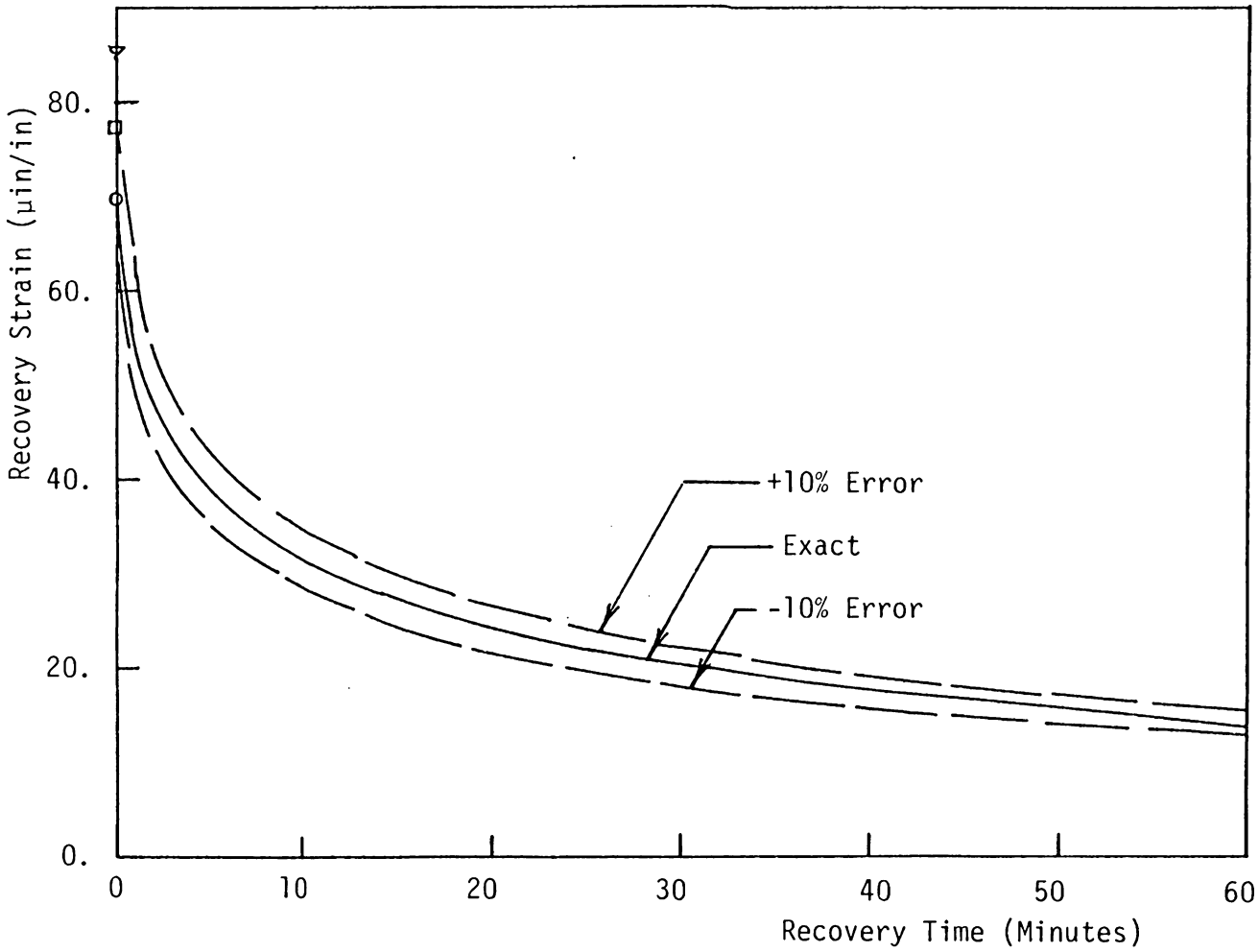

Figure 4.5: Recovery Strain Histories Used in Sensitivity Analysis for a Constant ±10% Error

time. That is, some constant strain value was added to or subtracted from the exact data set at all times. The +5 μin/in offset error case is shown for creep recovery in Figure 4.6. An offset error does not change the shape of the strain history curve, but rather rigidly translates the entire curve up or down the vertical axis. Note that Hiel [22] reduced his recovery data as if an offset error had occurred. That is, the permanent strain reading recorded after recovery was subtracted from the recovery strain data at each point in time, translating the entire curve down the strain axis.

Both the percentage and offset error types have been defined as an artificially smooth deviation from exact behaviour. Simple random error probably occurs most frequently in practice, where "random error" refers to small errors in strain measurement which occur in no discernible pattern and at intermittent times throughout the test period. Due to their very nature, random errors are difficult to model. The effects of random error are most often accounted for through the use of some least-error-squared smoothing technique. Such techniques were used during the present study as described in Chapter III, to minimize the effects of any random experimental error.

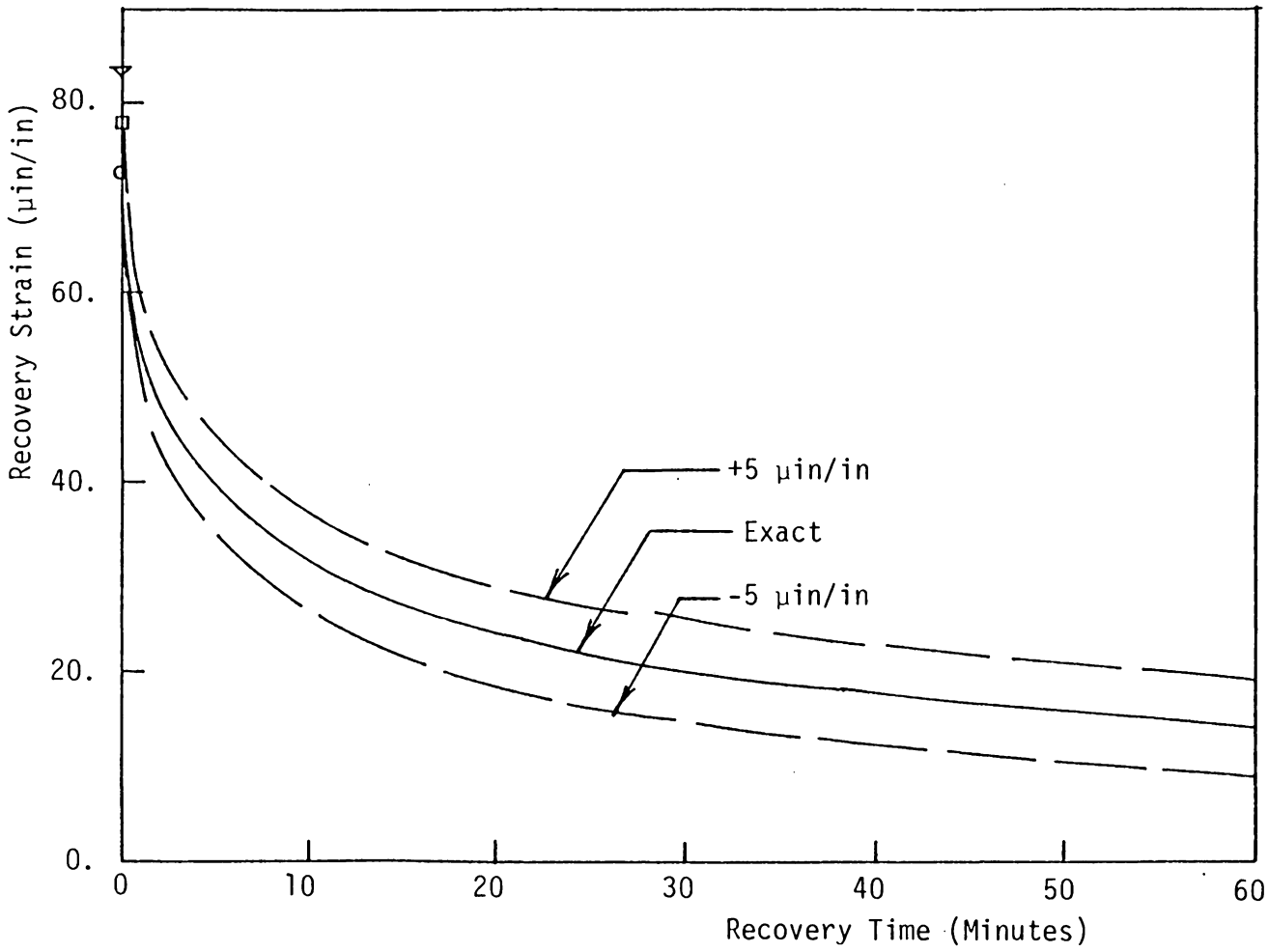

Figure 4.6: Recovery Strain Histories Used in Sensitivity Analysis for a Constant ±5 μin/in Offset Error

Linear Viscoelastic Analysis

As discussed in Chapter III, two computer-based fitting routines were available to obtain the linear viscoelastic parameters A_o, C, and n. The SCHAPERY program utilizes linear creep recovery data to calculate C and n, and linear creep data to calculate A_o. The FINDLEY program uses only linear creep data to calculate A_o, C and n. These programs were used to generate the results presented below.

Calculations Using Creep Data. A_o, C, and n were calculated using creep data which contained percentage errors ranging from -10% to +10%. The results of these calculations are summarized in Figure 4.7. It was found that n is completely independent of percentage errors, as n was calculated correctly as 0.33 in all cases. A_0 and C were influenced dramatically by percentage errors, however. Furthermore, it was found that a percentage error in strain data causes the same percentage error in A_o and C. For example, a +10% error in strain measurement causes the same +10% error in both A_o and C.

A_o, C, and n were next calculated using creep data which contained offset errors ranging from -100 μin/in to +100 μin/in. These results are summarized in Figure 4.8. It was found that both C and n are independent of offset errors in creep data, and all error is confined to the estimate for A_o. This is as would be expected, since as previously noted

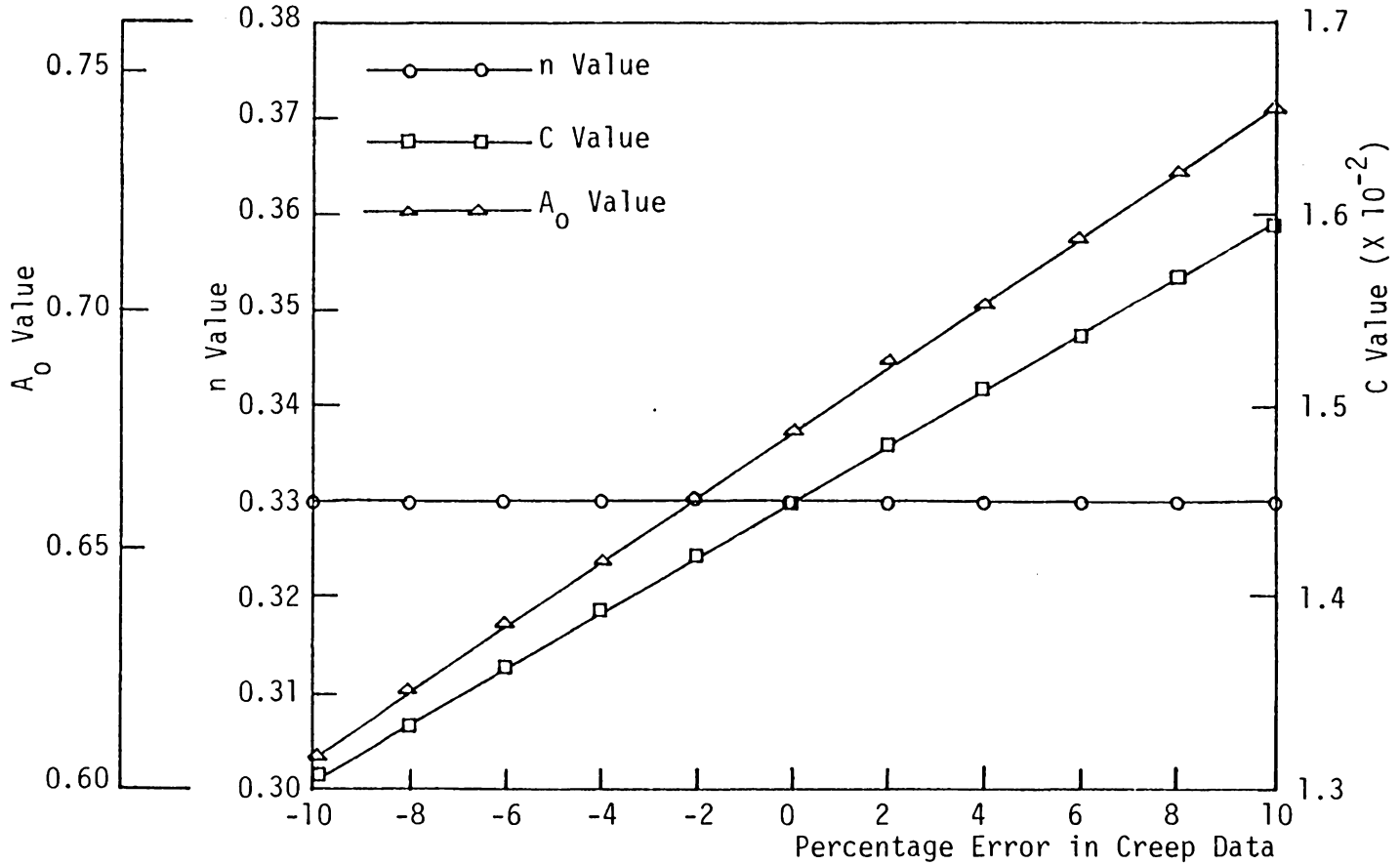

Figure 4.7: Sensitivity of Power Law Parameters A_o, n, and C to Percentage Errors in Creep Strain Data; Stress = 1750 psi, Actual A_o, n, and C Values are 0.674, 0.33, and 0.0145, Respectively

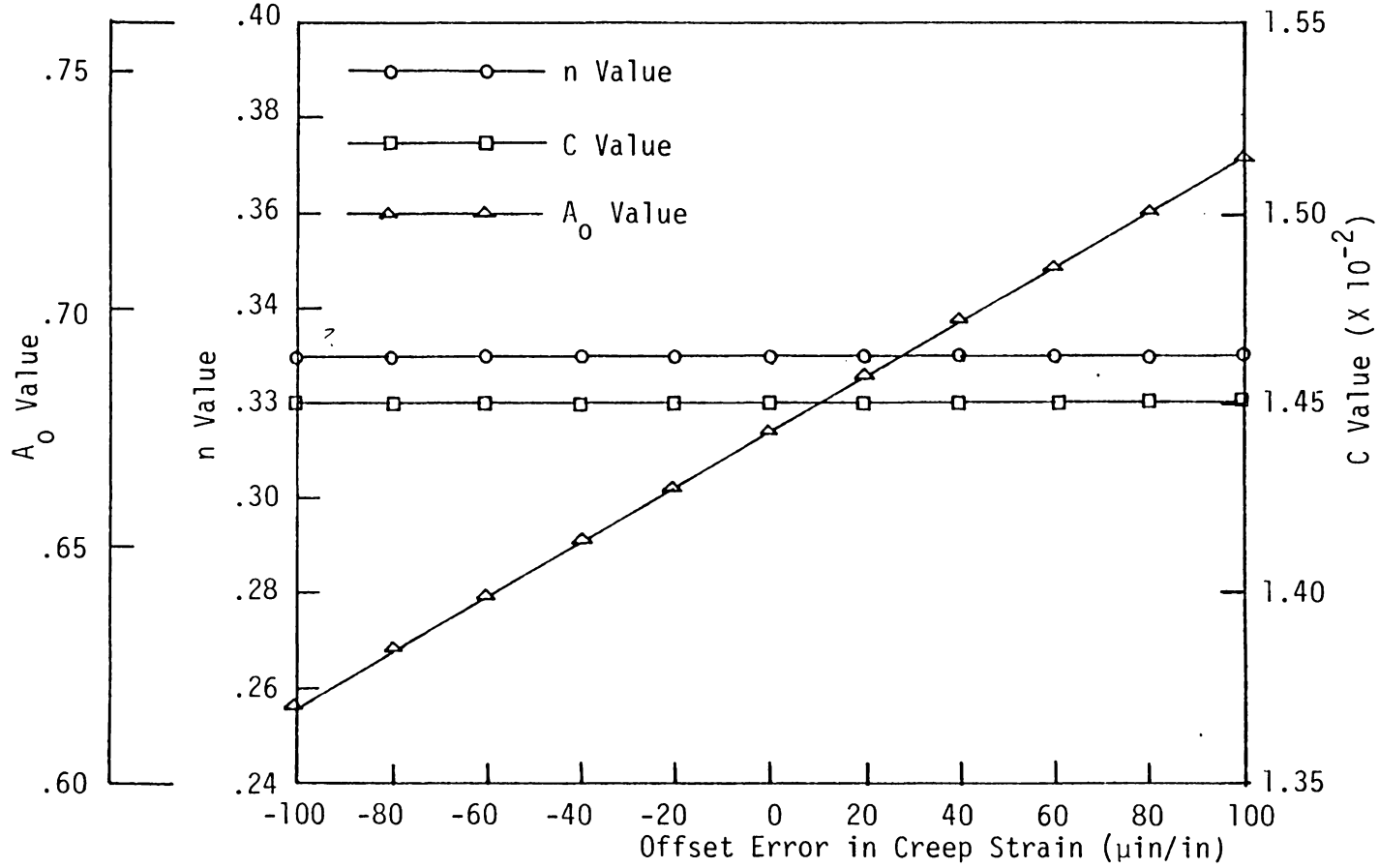

Figure 4.8: Sensitivity of Power Law Parameters A_o, n, and C to Offset Errors in Creep Strain Data; Stress = 1750 psi, Actual A_o, n, and C Values 0.674 , 0.33, and 0.0145, Respectively

an offset error does not change the shape of the creep curve but merely shifts the entire curve up or down the vertical axis. Hence, only the estimate for the initial compliance A_o is affected. These results imply that even in the case of very high offset error accurate measurement of C and n is possible using creep data.

Calculations Using Recovery Data. The parameters C and n were calculated using recovery data which contained percentage errors ranging from -10% to +10%. The results are summarized in Figure 4.9. As before, it was found that n is completely independent of percentage errors, while C is linearly dependent on percentage errors; a +10% error in strain measurement causes a +10% error in the calculated value for C.

In Figure 4.10 the estimates for C and n calculated using recovery data which contained offset errors ranging from -5 μin/in to +5 μin/in are shown. It is seen that both C and n are highly sensitive to offset errors in recovery strain data. This is in direct contrast with the results presented in Figure 4.8, where it was shown that offset errors imbedded within linear creep strain data had no effect on the estimates for C and n, but only on the estimate for A_o. These results indicate that estimates for C and n may be more stable if obtained by using creep data rather than recovery data, especially under conditions in which offset

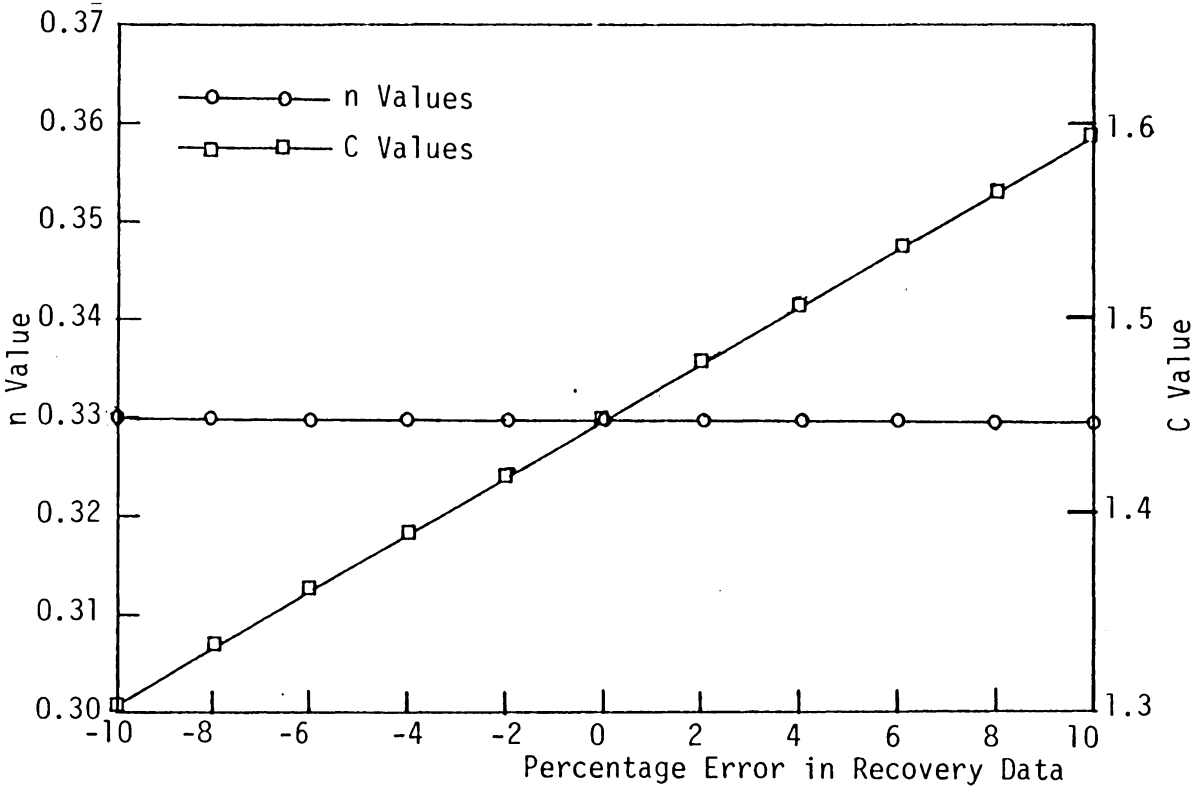

Figure 4.9: Sensitivity of Power Law Parameters C and n to Percentage Errors in Recovery Strain Data; Stress Level = 1750 psi, Actual C and n Values are 0.0145 and 0.33, Respectively

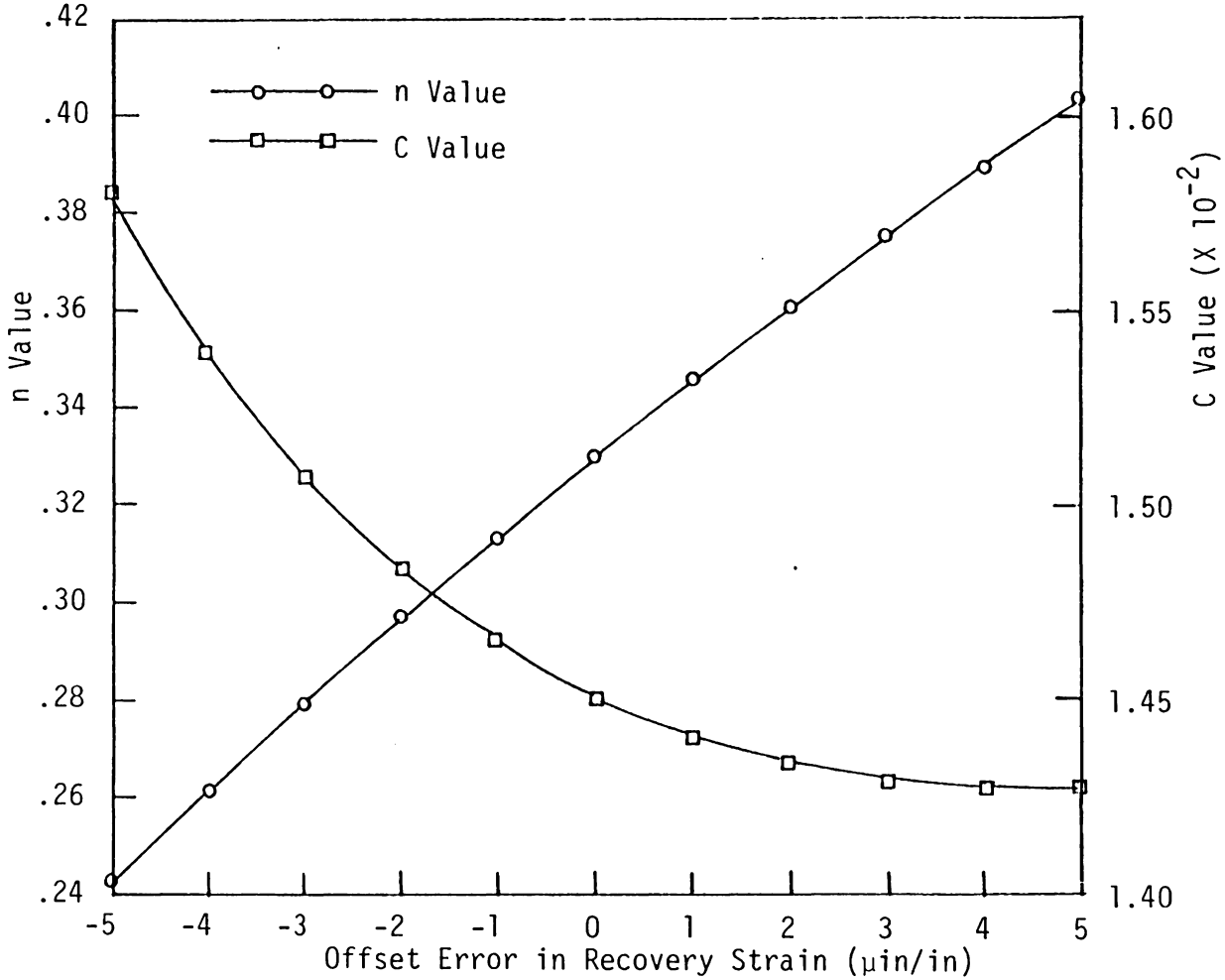

Figure 4.10: Sensitivity of Power Law Parameters C and n to Offset Errors in Recovery Strain Data; Stress = 1750 psi, Actual C and n Values 0.0145 and 0.33, Respectively

errors may be prevalent.

Nonlinear Viscoelastic Analysis

During the nonlinear viscoelastic analysis, the impact of measurement error on the four nonlinearizing parameters g_0, g_1, g_2, and a_σ were investigated. It was assumed that the exact values for A_o, C, and n were known, and the program SCHAPERY was used to calculate the effects of the two types of error considered.

Effects of Percentage Errors. The effects of percentage errors ranging from -10% to +10% are summarized in Figures 4.11-4.14. As indicated, the parameters g_0 and g_2 are most sensitive to percentage errors. The variance of g_0 with percent error was found to be linear, and is very similar to the effects on A_o in the linear case (see Figure 4.7). This simply reflects that error in the initial response is embedded entirely within the g_0 parameter. Errors in the transient response are divided among the g_1, g_2, and a_σ parameters in a manner dictated by the least-squared-error convergence criteria within the program SCHAPERY. This accounts for the rather irregular dependence on percent error exhibited by these three parameters.

Effects of Offset Error. Offset errors were expected to arise mainly due to accumulated damage within the matrix material. Such damage becomes apparent during the recovery

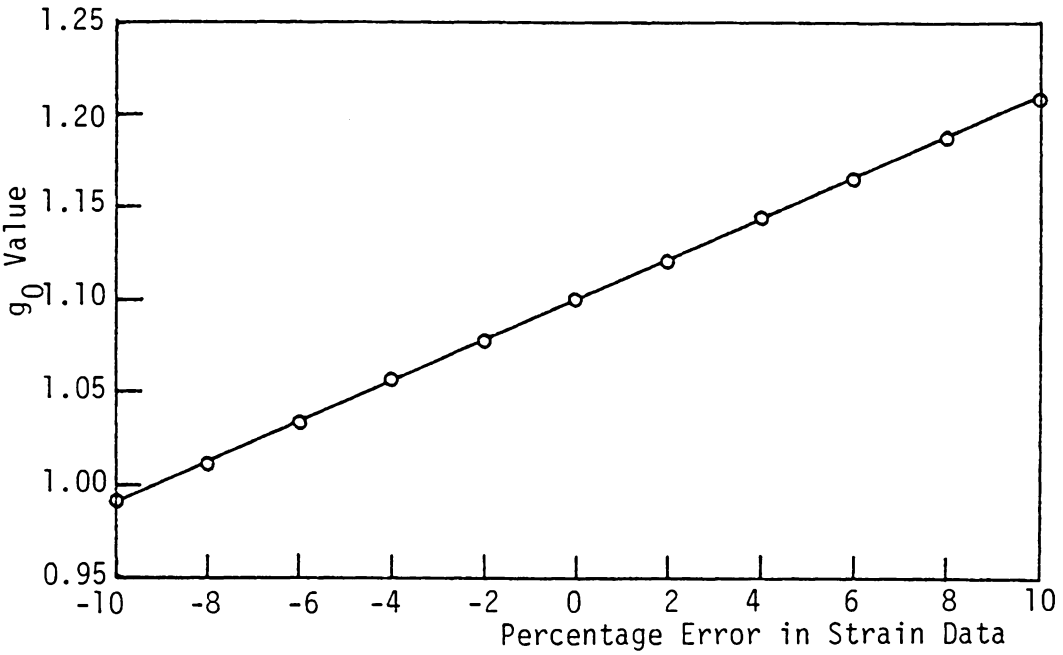

Figure 4.11: Sensitivity of g_0 to Percentage Errors in Strain Data; Stress = 1750 psi, A_0 = 0.674, C = 0.0145, n = 0.33

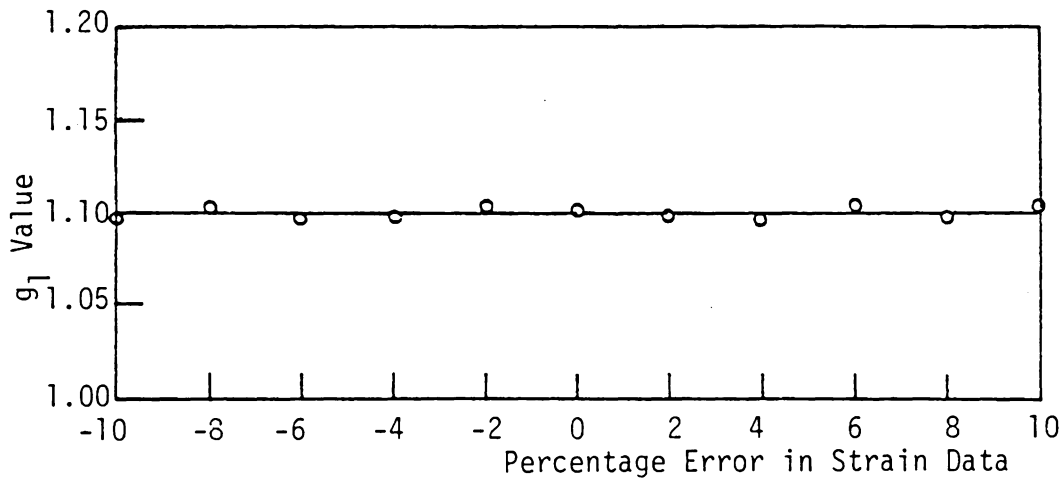

Figure 4.12: Sensitivity of g_1 to Percentage Errors in Strain Data; Stress = 1750 psi, A_0 = 0.674, C = 0.0145, n = 0.33

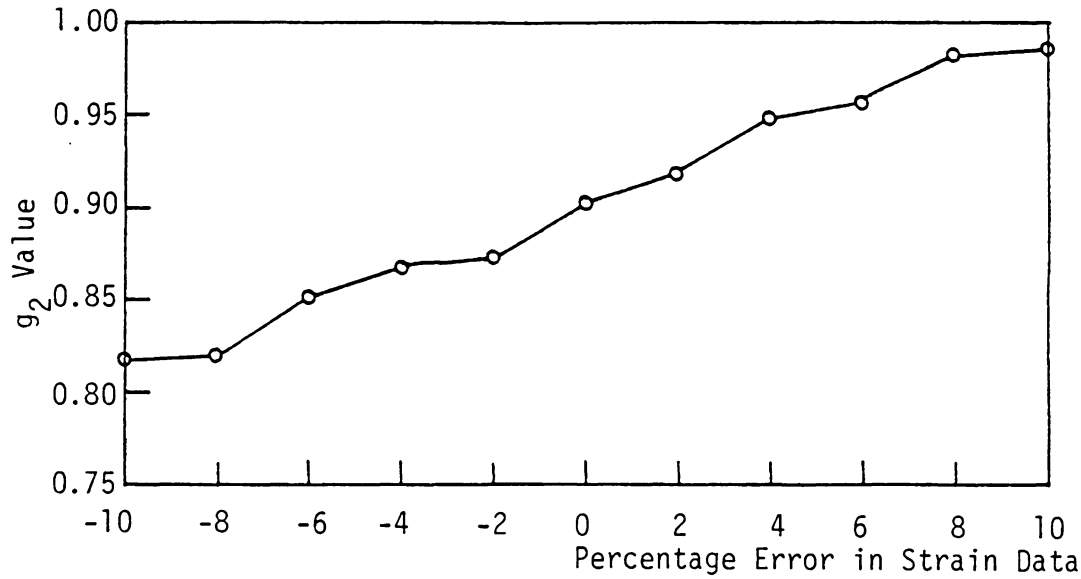

Figure 4.13: Sensitivity of g_2 to Percentage Errors in Strain Data; Stress = 1750 psi, A_o = 0.674, C = 0.0145, n = 0.33

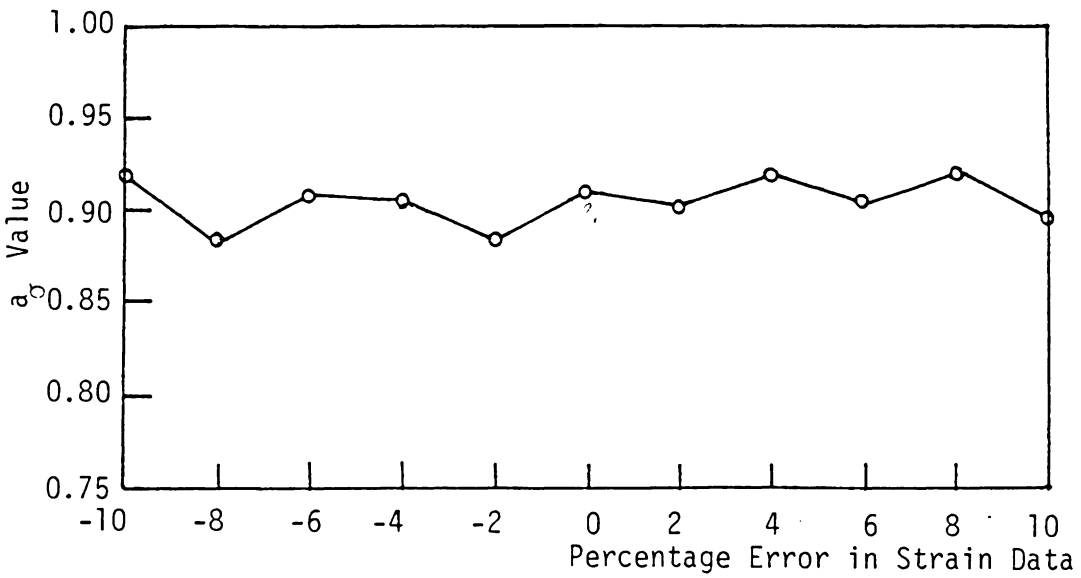

Figure 4.14: Sensitivity of a_σ to Percentage Errors in Strain Data; Stress = 1750 psi, A_o = 0.674, C = 0.0145, n = 0.33

portion of the creep/creep recovery testing cycle in the form of a permanent strain reading. If this permanent strain is subsequently removed from the recovery data, the offset error within the recovery data is presumably decreased to a relatively low level. However, since the mechanism by which damage is accumulated during creep is not apparent, no correction of the creep data has been performed during previous efforts. The offset error within the creep data therefore remains relatively high.

These considerations were taken into account by specifying different levels of offset error in the creep and creep recovery data. Offset errors ranging from -100 μin/in to +100 μin/in were assumed to exist within the creep data, while offset errors ranging from -5 μin/in to +5 μin/in were assumed to exist within the recovery data. While specifying offset error in this manner is admittedly arbitrary, it is believed to reflect the qualitative nature of offset errors which would exist in an experimentally obtained data set.

The results of this analysis are presented in Figures 4.15-4.18. The major impact of the offset errors considered is embedded within the parameters g_0 and a_σ, although all four parameters are affected to a greater extent by offset errors than by percent errors.

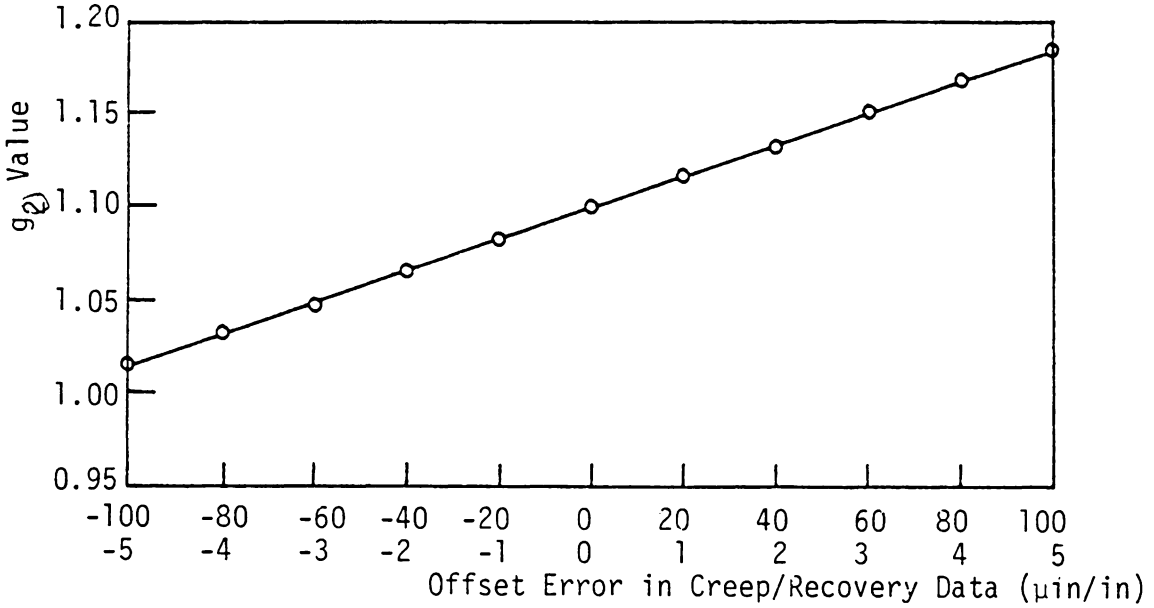

Figure 4.15: Sensitivity of g_0 to Offset Errors in Strain Data; Stress = 1750 psi, A_0 = 0.674, C = 0.0145, n = 0.33

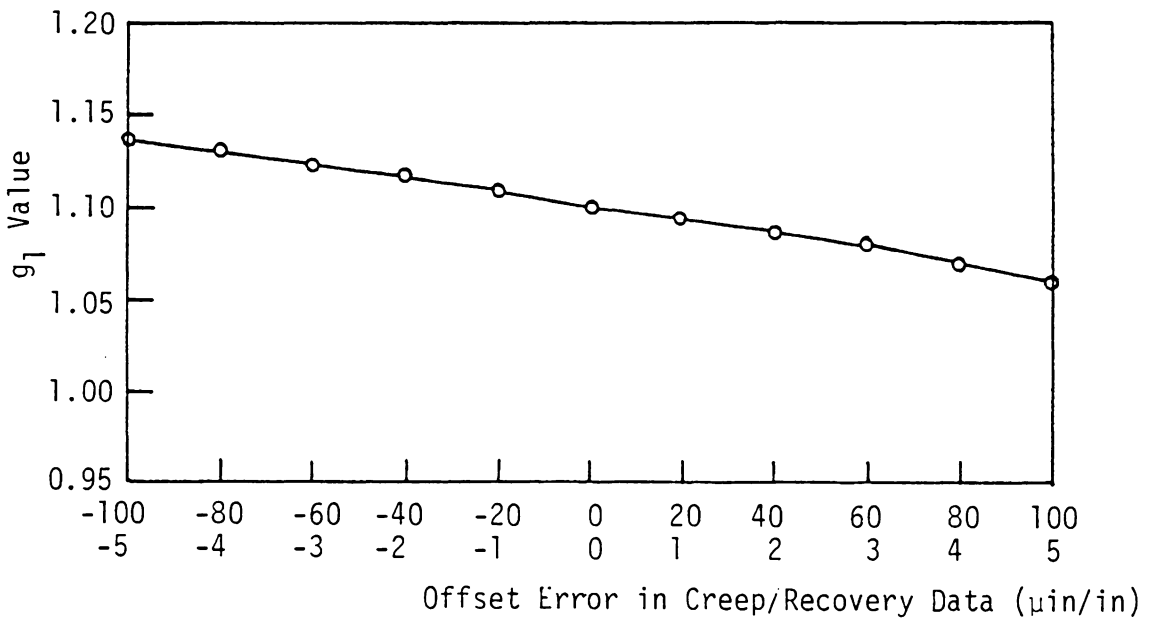

Figure 4.16: Sensitivity of g_1 to Offset Errors in Strain Data; Stress = 1750 psi, A_0 = 0.674, C = 0.0145, n = 0.33

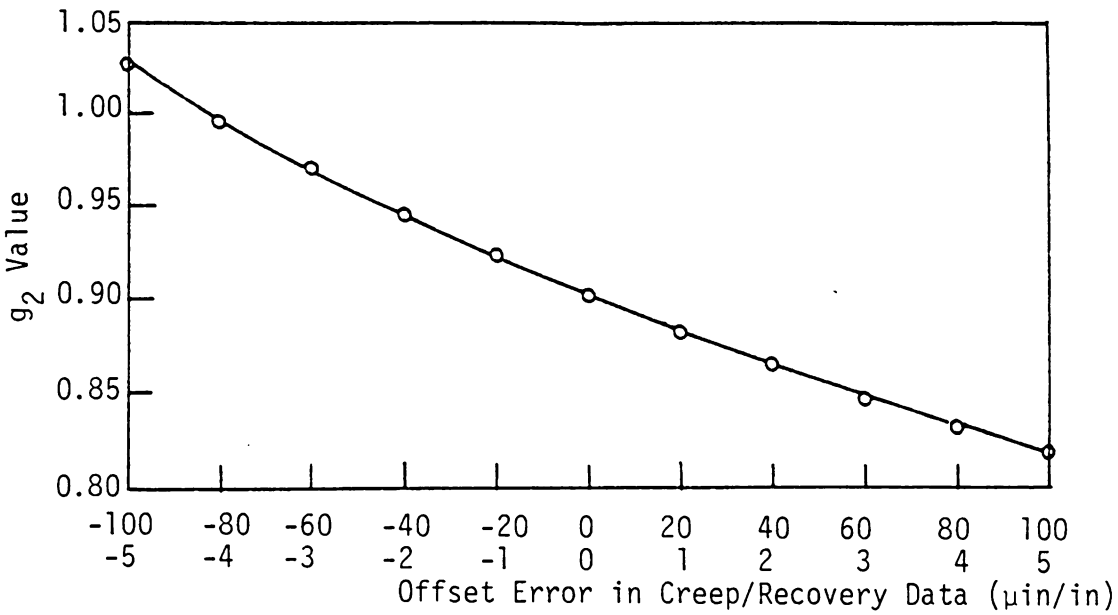

Figure 4.17: Sensitivity of g_2 to Offset Errors in Strain Data; Stress = 1750 psi, A_0 = 0.674, C = 0.0145, n = 0.33

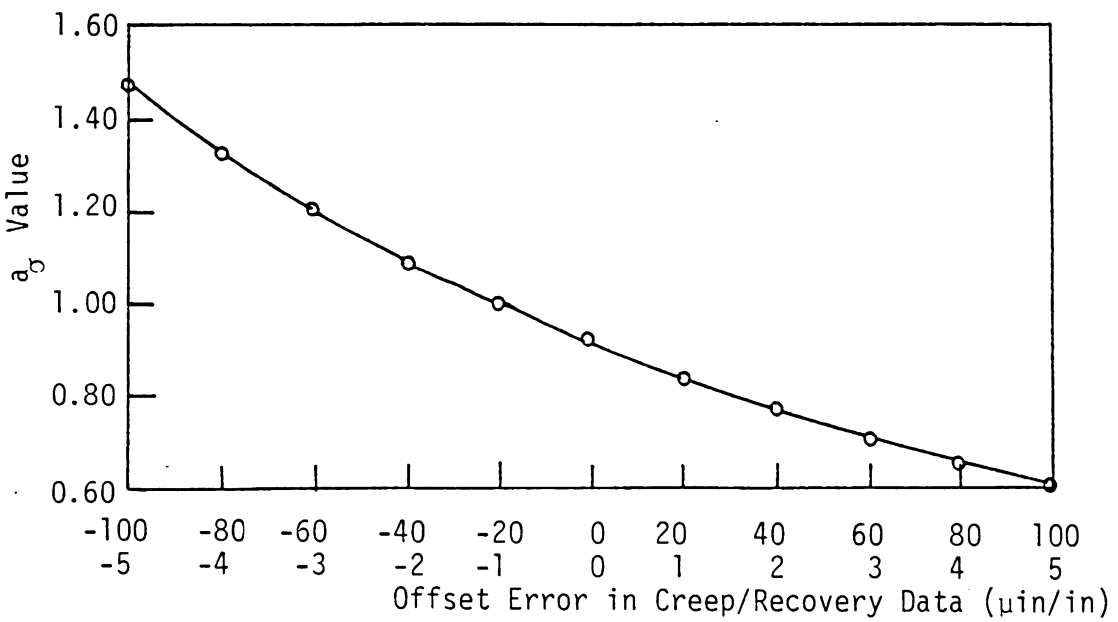

Figure 4.18: Sensitivity of a_σ to Offset Errors in Strain Data; Stress = 1750 psi, A_0 = 0.674, C = 0.0145, n = 0.33

Summary of the Sensitivity Analysis

The results of the sensitivity analysis just described were used to guide the selection of the creep/creep recovery testing cycle used in the present program, which will be discussed in Chapter V. Therefore, it is appropriate to summarize the major results of this analysis at this point.

It is concluded that an accurate measure of n is crucial for reasonable long-term predictions of viscoelastic creep response. Errors in g_1, g_2, C, or a_σ can also be important at very long times, but for the particular time frame used in the present study these are less important than errors in n. It is considered from a practical standpoint that errors in A_o or g_0 are relatively unimportant, first because such errors are apparent immediately and second because the impact of such errors decreases with time.

It is further concluded that the power law exponent n should be calculated using creep data rather than recovery data. As demonstrated, n is insensitive to percentage errors within either creep or creep recovery data, and is also insensitive to offset errors within creep data. This parameter is very sensitive to offset errors within recovery data, however, and it is likely that offset errors will occur due to the accumulation of damage during the creep cycle.

While the sensitivity analysis presented in this chapter

is believed to represent a reasonable approach, it must be admitted that rather arbitrary and subjective assumptions have been made. These are necessitated for the most part by the unknown nature of the damage mechanism believed to be primarily responsible for experimental error. Until further information regarding such damage is available, a more rigorous sensitivity analysis cannot be performed.

V. SELECTION OF THE TESTING SCHEDULE

Preliminary Considerations

The seven viscoelastic parameters involved in the Schapery nonlinear viscoelastic theory are typically determined using data obtained during a series of creep/creep recovery tests. The testing schedule used to determine these parameters must be selected so as to insure that the viscoelastic response predicted at long times is reasonably accurate. This is especially significant in light of the analysis presented in Chapter IV, where it was demonstrated that an error in any of the parameters associated with the transient response (g_1, g_2, a_σ, C, or n) is not apparent at short times but may result in gross error at long times. This implies that prior to selection of the creep/creep recovery testing cycle a conscious decision must be made regarding both the desired length of prediction and desired accuracy of prediction. A testing cycle which results in an acceptable prediction at 10^5 minutes may not result in an acceptable prediction at 10^6 minutes, for example.

A review of the literature indicates that in general the creep/creep recovery testing schedules used during previous applications of the Schapery theory have been of relatively

short duration. For example, some reported creep/creep recovery time schedules are 60 minutes/600 minutes [22], 60 min/120 min [35], 30 min/30 min [36], 30 min/60 min [37], 15 min/5 min [50,51], and 25 min/25 min [53]. In all studies the viscoelastic response was compared to actual measurements and judged to be an accurate prediction. However, in all cases the predicted response was compared over a time span either equal to or only slightly greater than the original creep time. Thus, it is not clear whether the viscoelastic parameters determined using the short-term testing schedules listed are accurate enough to provide viscoelastic predictions at much longer times, say at times greater than 10^4 minutes.

Another consideration is the method of strain measurement used. In this study (and in most previous studies) resistance foil strain gages were used to measure strain. In modern strain gage applications, the strain gage system (including strain gage, amplifier, and readout device) will commonly provide a sensitivity of 1 μin/in. However, there are many inevitable experimental difficulties involved, including amplifier nonlinearities, instabilities, and noise; strain gage thermal compensation; strain gage stability and drift; and tolerances in gage factor and resistance. When these factors are taken into account, measurement accuracy under the best of conditions is

probably no better than about ± 5 μin/in. This potential level of error must also be considered during selection of the test cycle.

The amount of viscoelastic response expected at the temperature and stress levels of interest is also of importance. In general, long-term predictions for highly viscoelastic materials require a very accurate measure of the viscoelastic parameters, whereas predictions for mildly viscoelastic materials require less accurate measurement of these parameters.

A final consideration is applicable for the specific case in which the transient compliance is modeled using the power law (as in the present study). The power law is merely a good approximation to the actual transient compliance function. While the power law is reasonably accurate for many viscoelastic materials, it cannot provide an exact match with measured results at all points in time. Since in practice the viscoelastic response at long times is generally of greatest interest, it is desirable to provide the best fit between analytic and experimental results at long times. Accuracy at long times is often accomplished at the expense of accuracy at short times, however.

Testing Schedule Selected

The test schedule used during this study was selected

with several objectives in mind, in light of the above considerations and the results presented in Chapter IV. The schedule was keyed towards an accurate measure of the power law exponent n. The selection process is described below.

Initial estimates for the linear viscoelastic parameters A_o, C, and n were obtained by conducting a few 30 min/60 min creep/creep recovery tests on a 90-deg specimen of T300/5208 graphite-epoxy. The results of these tests were used in the sensitivity study presented in Chapter IV, and the estimates obtained are restated here for convenience

$$A_o = 0.0978/\text{GPa} \ (0.674 \times 10^{-6}/\text{psi})$$
$$C = 0.00210/\text{GPa-min}^n \ (0.0145 \times 10^{-6}/\text{psi-min}^n)$$
$$n = 0.33$$

The linear viscoelastic creep response at any time t is given by eq. 3.4 (with $g_0 = g_1 = g_2 = a_\sigma = 1$)

$$\varepsilon_c(t) = [A_o + C\, t^n]\, \sigma_0 \tag{5.1}$$

Equation 5.1 can also be rearranged to provide an expression for n, in terms of A_o, C, n, t, and $\varepsilon(t)$

$$n = \frac{\log \left\{ \frac{1}{C} \left[\frac{\varepsilon_c(t)}{\sigma_0} - A_o \right] \right\}}{\log t} \tag{5.2}$$

The approximate creep strain expected at 10^5 minutes for T300/5208 was calculated using eq. 5.1 and the initial estimates for A_o, C, and n, at a stress level 12.1 MPa (1750

psi). The viscoelastic response was expected to be linear at this stress level. The approximate creep strain was calculated as

$$\varepsilon(10^5) = 2313 \text{ μin/in}$$

Next, an accuracy of ±10% at 10^5 minutes was specified. That is, the measured value of n was required to produce a predicted creep response within ±10% of the actual creep strain at 10^5 minutes. A ±10% error implies a predicted response at 10^5 minutes of

$$\varepsilon(10^5)_{+10\%} = 2544 \text{ μin/in}$$

$$\varepsilon(10^5)_{-10\%} = 2082 \text{ μin/in}$$

The error bounds on n can now be calculated using eq. 5.2

$$n_{+10\%} = 0.346$$

$$n_{-10\%} = 0.310$$

Since the "exact" value of n is assumed to be 0.33, the specified ±10% tolerance on predicted creep strain at 10^5 minutes requires that the error in n range between -6.1% to +4.8%. Therefore, the creep time used to determine n must be long enough such that this difference in n can be distinguished. As previously discussed, the accuracy in strain gage measurements is perhaps ±5 μin/in. It was

arbitrarily decided to specify a confidence level in strain measurement of ±20 μin/in for the present study. That is, the creep time was to be long enough such that a variance of ±20 μin/in away from "exact" behaviour could be measured. It was reasoned that this rather conservative confidence level would help to assure an accurate measure of n. The transient response given by each value of n has been plotted in Figure 5.1. As indicated a variance of ±20 μin/in away from the response for n = 0.33 occurs at about 480 minutes. The duration of the creep test chosen for this study was therefore 480 minutes.

Once the length of the creep test was selected it was possible to specify a reasonable recovery period. The predicted recovery curves following 480 minutes of creep at 12.1 MPa are shown in Figure 5.2. Since the material has been assumed to be linearly viscoelastic, the variance from the n = 0.33 curve is initially ±20 μin/in. After 120 minutes this variance has been reduced to about ±13 μin/in. This was judged to be a reasonable recovery time, and so recovery strains were monitored for 120 minutes.

In summary, the creep/creep recovery testing cycle used in this study was keyed towards accurate measure of the power law exponent n, since a sensitivity analysis had indicated that errors in long-term predictions would most likely arise due to errors in n. Based upon the procedure

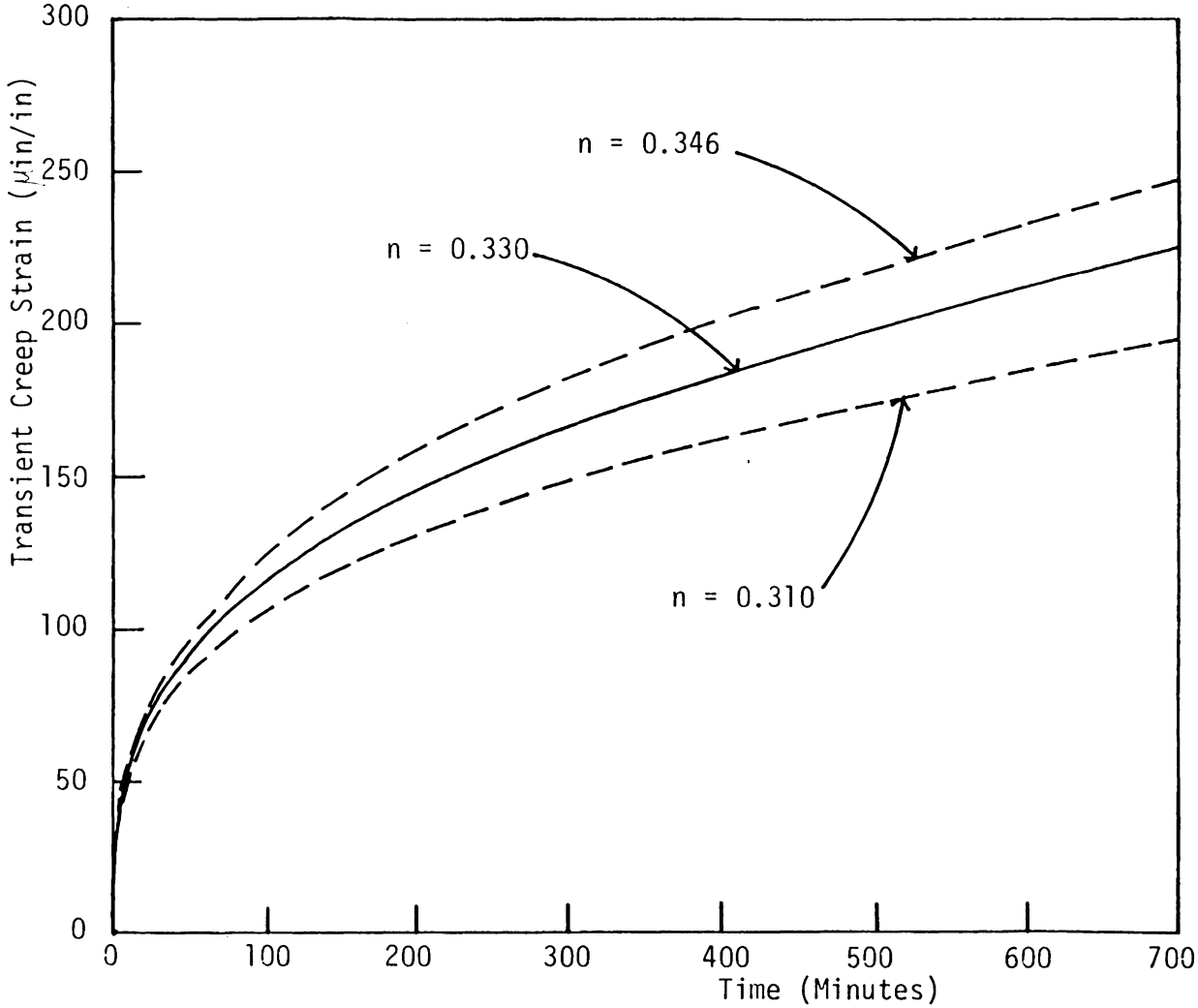

Figure 5.1: Transient Creep Response Predicted for a Creep Stress of 12.1 MPa (1750 psi); A_o = 0.674, C = 0.0145

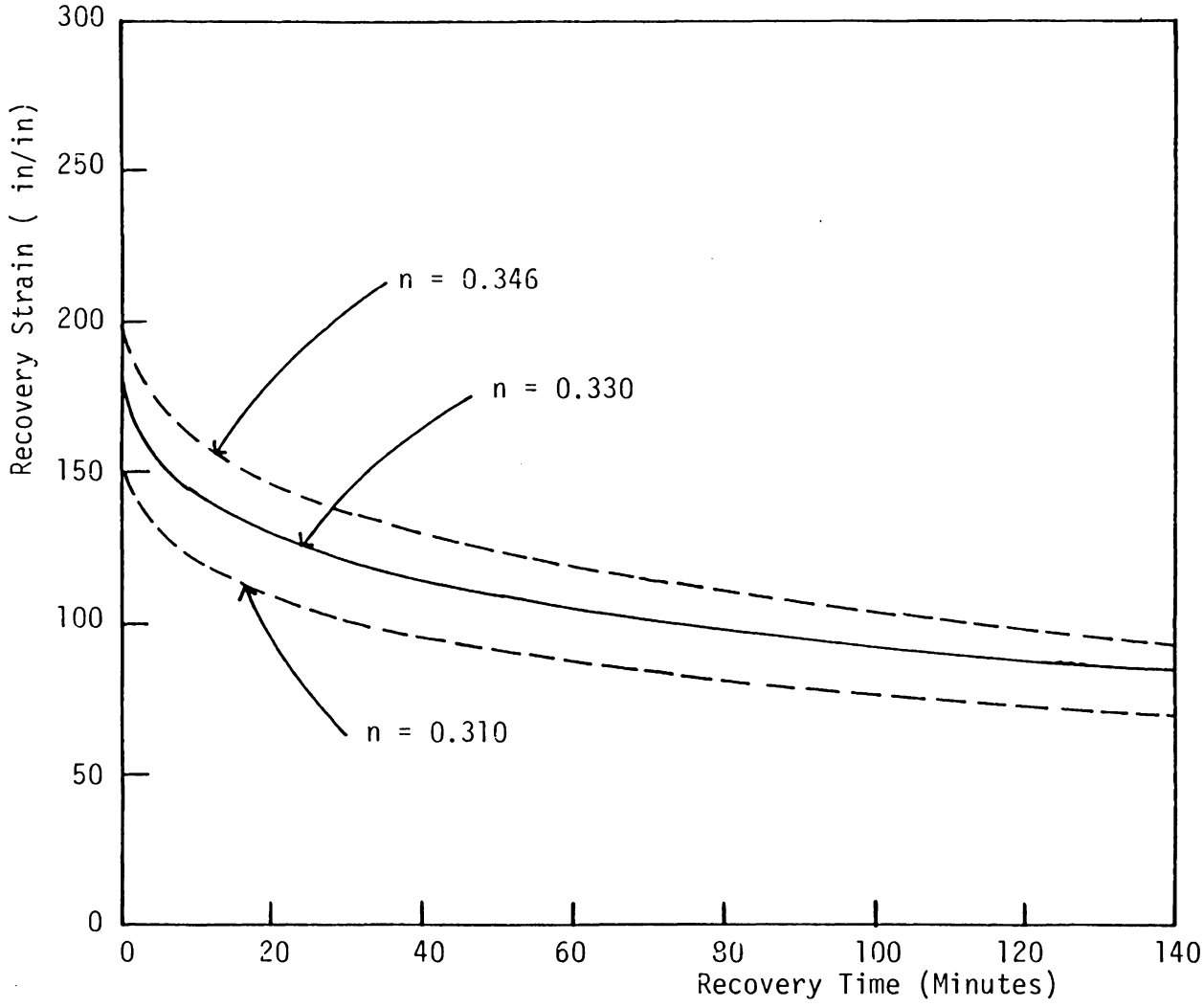

Figure 5.2: Predicted Recovery Response Following 480 Minutes of Creep at 12.1 MPa (1750 psi); A_o = 0.674, C = 0.0145

described above, a 480 minute/120 minute creep/creep recovery test cycle was selected.

Proposed Test Selection Process

The procedures followed in selecting the creep/creep recovery test schedule were intended to assure accurate long-term prediction of viscoelastic response. The test selected depends to a certain extent upon the material being studied, in the present case T300/5208 graphite-epoxy. It is likely that a different test schedule would be selected if a different material were being investigated. Therefore, the test selection process followed during this study has been itemized below. This "standard" procedure would serve to address those variables which are essential for accurate long-term predictions.

- Obtain initial estimates for the linear viscoelastic parameters A_o, C, and n through a few relatively short creep/creep recovery tests at low stress levels.
- Determine the desired maximum time of prediction and desired accuracy at the maximum time. In the present study these were 10^5 minutes and $\pm$10%, respectively.
- Using the initial estimates for A_o, C, and n, calculate the expected "exact" response at the maximum time of prediction (using eq. 5.1) and the acceptable error bounds in predicted creep strain at that time.
- Calculate the acceptable error bounds for the power law exponent n (using eq. 5.2).
- Determine the "confidence" level for the strain measuring system being used. In the present study, this confidence level was specified as $\pm$20 μin/in.

- Determine the creep time required to distinguish the creep response for an n value outside of the acceptable range in n. In the present study, this creep time was determined to be 480 minutes, using Figure 5.1.

- Select a recovery period based upon the expected recovery response after the creep time determined above. In the present study, the recovery period selected was 120 minutes, based upon Figure 5.2.

These general guidelines should be especially helpful to the researcher studying a viscoelastic material which has not been previously investigated.

VI. ACCELERATED CHARACTERIZATION OF T300/5208

During this study, the accelerated characterization scheme described in previous chapters was applied to the T300/5208 graphite-epoxy material system. The viscoelastic response of unidirectional 90-deg and 10-deg off-axis specimens was monitored during 480 minute/120 minute creep/creep recovery tests, conducted at several stress levels. These tests were used to characterize the viscoelastic behaviour of the matrix-dominated properties S_{22} and S_{66}. A few tests were conducted using 0-deg specimens to measure the fiber-dominated properties S_{11} and S_{12}. Specific details including specimen fabrication, equipment used, data collection techniques, typical data obtained, data analysis techniques, and results of the short-term analysis will be presented in this chapter.

Specimen Fabrication

Specimens were fabricated from 8-ply panels of T300/5208. These panels were layed up by hand, using NARMCO RIGIDITE 5208 Carbon Fiber Prepreg tape with a fiber volume fraction of 65%. It is desirable to cure composites in an autoclave, since the resulting composite laminates are generally of a higher quality than those produced by other methods. However, the use of an autoclave could not be

arranged within the time frame of the present study, and therefore the panels were cured using the VPI&SU hot press facility. The heat and pressure cycle used to cure the panels consisted of the following steps:

- Initial heatup from room temperatures to 135C (275F), at an average rate of 2.8C/min (5F/min), at atmospheric pressure
- Hold temperature at 135C for 30 minutes at atmospheric pressure
- Apply 6.89 kPag (100 psig) with platens
- Raise temperature to 179C (355F) at 6.89 kPag and hold for 120 minutes
- Cool in press to 60C (140F) at 6.89 kPag
- Remove from press and air-cool to room temperature

Nominal panel dimensions were 0.10 cm X 30.5 cm X 30.5 cm (0.04 in X 12.0 in X 12.0 in).

A problem experienced throughout the program was a shortage of prepreg tape. The experimental portion of the program was initiated using prepreg on hand, which had a fiber volume fraction of 65%. After a significant amount of testing had been completed, it was learned that additional prepreg with the same fiber volume fraction was not available. Rather than repeating all of the tests which had been conducted up until that time, the program was continued using the limited amount of materials on hand. This caused some difficulty with respect to selection of the laminates used during the long-term creep studies. These problems

will be further discussed in Chapter VII.

The tensile specimens were sawed from the panels using a diamond wheel abrasive disk. Nominal specimen width was 1.3 cm (0.50 inch). Specimen length ranged from 17.8 cm to 33.0 cm (7.0 to 13.0 inches).

It has been shown [20-22,39] that previous thermal history can dramatically affect the viscoelastic behaviour of polymer-based composite materials. Therefore, after being sawed from the panels, all specimens were subjected to a post-cure thermal treatment. This treatment was intended to erase the influence of any previous thermal histories, and to bring all specimens to a common thermodynamic (i.e., viscoelastic) reference state. The post-cure consisted of the following steps:

- Initial heatup from room temperatures to 177C (350F) at an average rate of 2.6C/min (4.7F/min)
- Hold temperature at 177C for four hours
- Cooldown from 177C to approximately 49C (120F) at a closely controlled rate of 2.8C/hr (5F/hr)
- Remove from oven and air-cool to room temperature

After post-cure, all specimens were placed in a desiccator at a relative humidity of 21% $\pm$ 3% until used in testing.

Specimens were strain gaged using gages mounted back-to-back and wired in series, as described by Griffith, et al [20]. Using back-to-back gages in series serves two purposes. First, the effective resistance of the strain gage

is doubled, which allows the use of a relatively high excitation voltage resulting in high sensitivity, while still maintaining low gage current and good gage stability. Secondly, any effects due to specimen bending are electrically averaged and therefore removed from the strain gage signal. Micro-Measurement 350Ω WK-series strain gages were used. The WK gage alloy is especially stable and suited for use at high temperatures [54]. The gages were mounted to the specimens using the M-Bond 600 adhesive system. This is an elevated-temperature adhesive requiring a cure temperature ranging from about 75C (175F) for 4 hours to about 175C (350F) for 1 hour [55]. In the present study, a cure at 82C (180F) for 8 hours was used to assure complete cure of the adhesive while still avoiding any perturbation of the post-cure thermal treatment.

For 0-deg and 90-deg tensile specimens, uniaxial strain gages were mounted along the major axis of the specimen, parallel to the load direction. For 10-deg off-axis specimens, a 3-element strain gage rosette was used, oriented as shown in Figure 6.1. All gages were mounted using a magnifying glass to aid in gage alignment.

Since WK-series gages are provided with preattached leadwire ribbons, lead wires were soldered to the ribbons rather than directly to the gage tabs. This avoided placing the soldering iron tip in direct contact with the specimen,

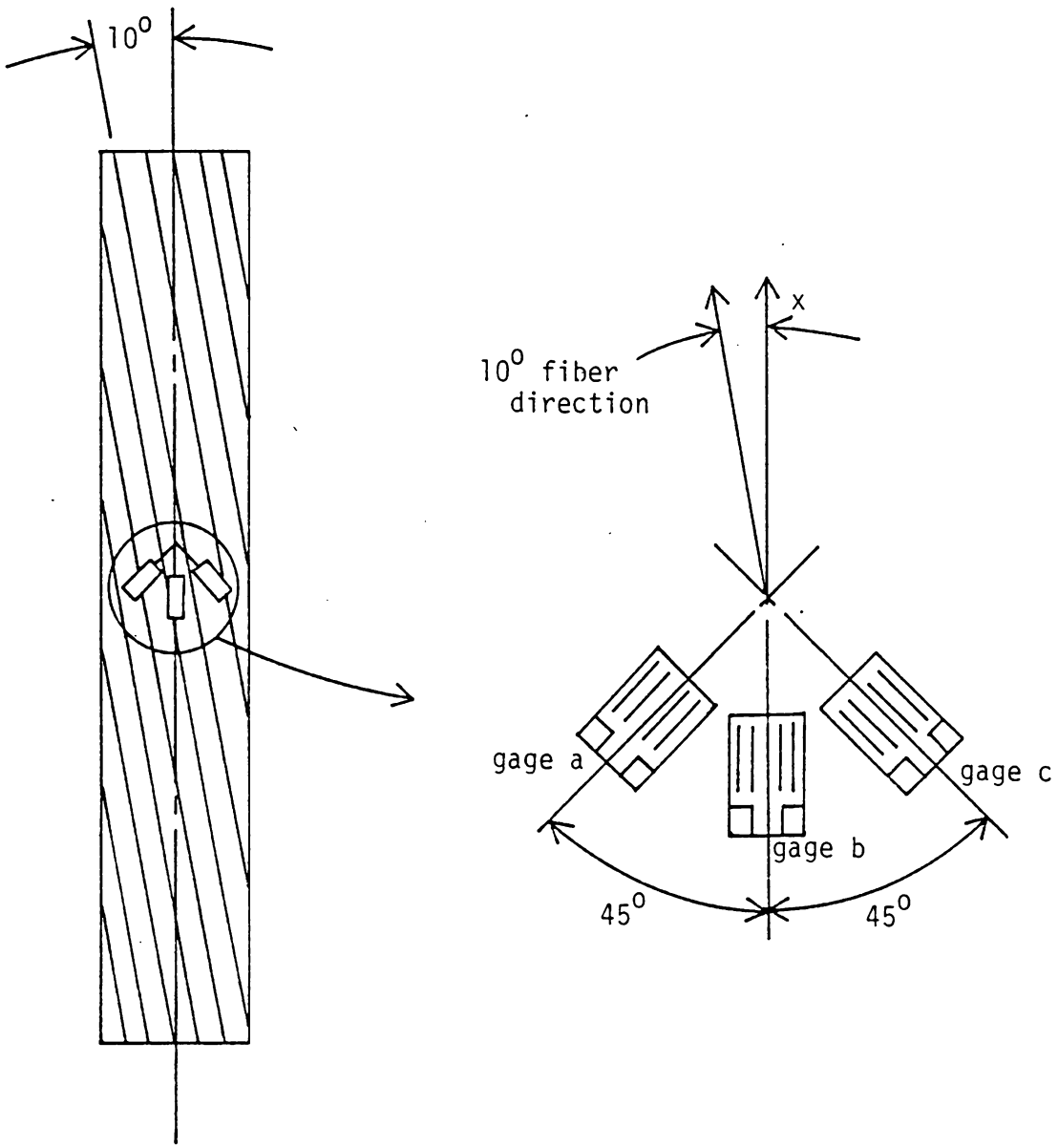

Figure 6.1: 10-deg Off-Axis Tensile Specimen, Indicating Orientation of the 3-Element Strain Gage Rosette

which can cause local damage in the form of broken fibers, damaged epoxy matrix, or both [56]. Micro-Measurements 330-FTE leadwire was used, which is a 3-conductor, stranded silver-plated copper wire with Teflon insulation, suitable for use to 260C (500F).

Thermal compensation of the strain gage signal was accomplished using the dummy gage technique [57]. In this method, a gaged "dummy" specimen is placed immediately adjacent to the mechanically-loaded "active" specimen. In all cases, the dummy specimen was identical to the active specimen with respect to gage type and gage/fiber orientation. The two specimens were wired in adjacent arms of a Wheatstone bridge circuit. Ideally, the dummy specimen experiences the same thermal history as the active specimen. Due to the characteristics of the Wheatstone bridge circuit, any gage response to temperature is cancelled and the remaining gage signal is entirely due to the mechanical load.

Equipment Used

Tensile creep loads were applied using one of three different dead-weight creep frames. All frames utilize a lever-arm system to apply the tensile creep load. The majority of the short-term creep/creep recovery tests were conducted using an Applied Test Systems (ATS) creep machine

featuring an automatic loading system and load re-leveler. The lever arm for this frame is adjustable to either a 3:1 or 10:1 load ratio. The maximum applied load capacity at either ratio is 88,964 N (20,000 lb_f). The frame is equipped with an ATS series 2912 oven and series 230 temperature controller. Oven temperatures are maintained to within $\pm$1.1C ($\pm$2.0F).

A few short-term tests were conducted using a Budd creep frame, also equipped with a ATS series 2912 oven and series 230 temperature controller. The load ratio for this machine is fixed at 10:1. The maximum rated load for this frame is 26,690 N (6000 lb_f). This frame was used infrequently and only when the ATS machine was not available.

The long-term laminate creep tests were performed using a five-station creep frame. This frame was designed and built in-house during the present study, specifically for the long-term creep tests. The supporting structure of this frame is a channel- and I-beam weldment, produced in the VPI&SU University Machine Shop. Tool steel, surface treated to a hardness of R_c 58-60, was used for all knive edges and mating surfaces to reduce the effects of plastic deformation and friction. Each of the five lever arms has a fixed load ratio of 10:1, and were designed to apply a maximum load of 13,345 N (3000 lb_f) per arm. (Perhaps it should be noted for further reference that no loads greater than 4448 N were

applied during the present study.) Five individually controlled ovens were constructed using sheet steel and aluminum angles, and were insulated with a 2.5 cm (1.0 inch) thickness of Carborundum FIBERFAX ceramic insulation. The interior cavity of each oven is nominally 15.2 cm X 15.2 cm X 53.3 cm (6.0 in X 6.0 in X 21.0 in). Heat is introduced using Watlow resistance heating elements and controlled using Omega model D921 digital temperature controllers. Temperatures were maintained to within $\pm$1.1C ($\pm$2.0F) over the 10^5 minute creep period.

Strains were measured using either a Vishay series 2100 amplifier and strain gage conditioning unit with MTS model 408 voltmeter (used with either the ATS or Budd creep frames), or with a Vishay P-350A portable digital strain indicator with SB-1K ten-channel switch and balance unit (used with the five-station creep frame). Strain and time data pairs were logged by hand and subsequently entered into the IBM mainframe, housed at the VPI&SU Computing Center. All further data reduction was accomplished using the IBM mainframe and FORTRAN programs. Strain data were taken with an amplifier gage factor setting of 2.0, and were subsequently corrected for actual gage factor and (where appropriate) for transverse sensitivity effects.

Selection of Test Temperature

As previously noted, the Schapery theory can be considered to be a Time-Stress Superposition Principle. A viscoelastic material can therefore be characterized at a single temperature through a series of creep/creep recovery tests at several stress levels. This is in contrast to the Time-Temperature Superposition Principle, in which a material may be characterized at a single reference temperature through a series of creep tests at a common stress level but at several temperatures. Temperature-dependence was not considered in the present study, and all tests were conducted at a single test temperature.

Dramatic viscoelastic response was desired so as to provide a rigorous check of both the Schapery theory and of the laminate characterization scheme as a whole. Therefore, a test temperature approaching the T_g of the epoxy matrix was required. The T_g was determined through a series of 5 minute creep tests at temperatures ranging from 66C (150F) to 199C (390F). A 90-deg unidirectional specimen was used at the relatively low stress level of 11.4 MPa (1650 psi) to assure a linearly viscoelastic response. The creep strains at 1 and 5 minutes were recorded, and an "average creep rate" was defined as

$$\frac{\Delta\varepsilon}{\Delta t} = \frac{\varepsilon(t) - \varepsilon(1)}{4}$$

Both the 5 minute creep compliance and the average creep rate have been plotted as functions of temperature in Figure 6.2. As indicated, the 5 minute creep compliance measurements indicated gave a T_g of 178C (353F), while average creep rate measurements indicated a T_g of 180C (356F). This mild discrepancy was considered to be within experimental error bounds. These results are also in agreement with results presented elsewhere [11].

A test temperature of 149C (300F) was selected, based upon Figure 6.2. It was reasoned that adequate viscoelastic response would occur at this temperature, without severely reducing specimen strength or rigidity.

Tests of 0-deg Specimens

Two tensile tests were conducted using 0-deg specimens to determine the fiber-dominated properties E_{11} and ν_{12} (or equivalently, S_{11} and S_{12}). These properties were assumed equal in tension and compression. As expected from previous results [11,18-23], neither E_{11} nor ν_{12} exhibited appreciable time-dependent behaviour at a temperature of 149C, and were therefore treated as linear elastic properties during the laminate analysis. The results obtained and used in the analysis were

$$E_{11} = 132.2 \text{ GPa } (19.16 \times 10^6 \text{ psi})$$

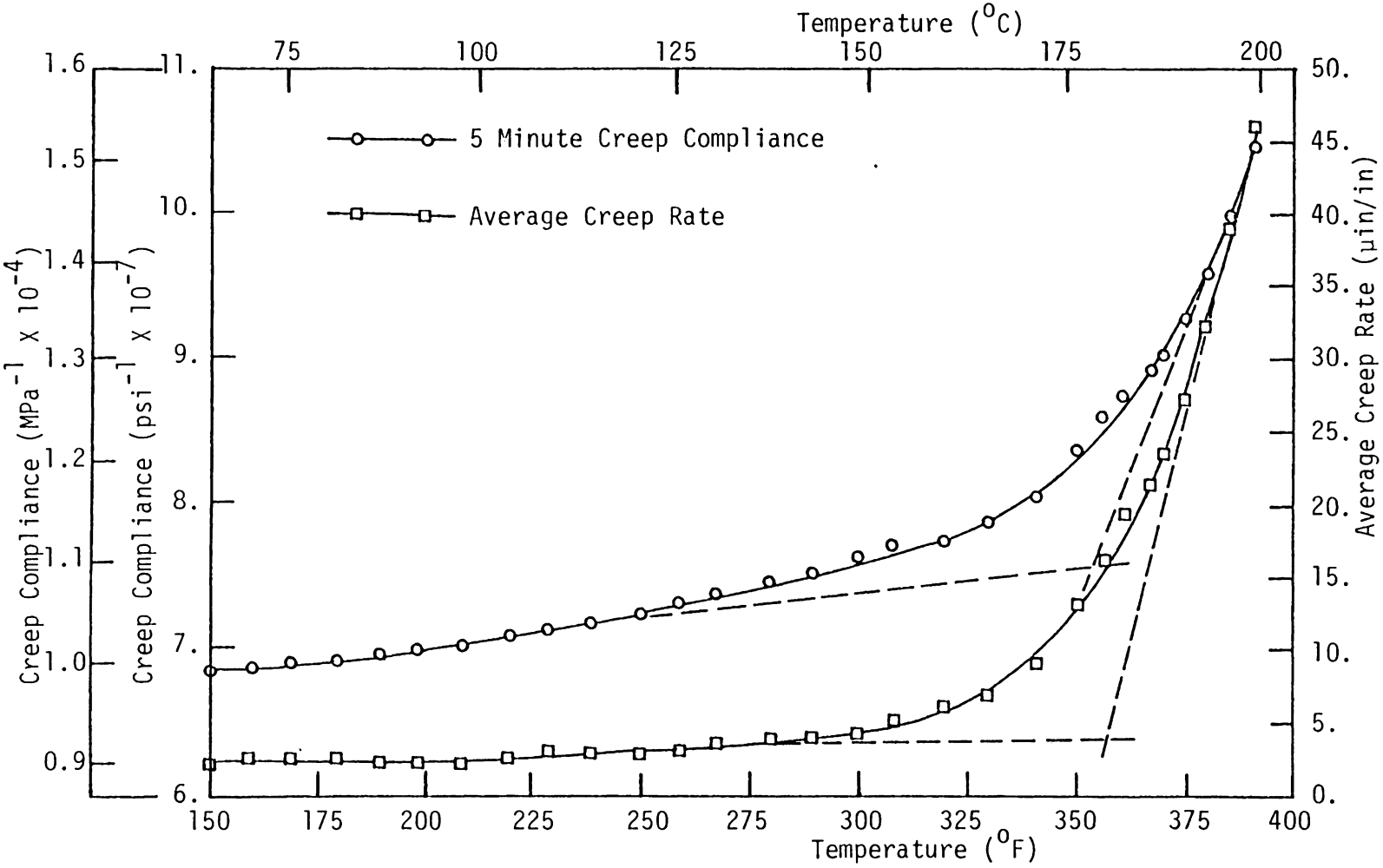

Figure 6.2: Five Minute Creep Compliance and Average Creep Rate for T300/5208; Stress = 11.4 MPa

$$\nu_{12} = 0.273$$

or,

$$S_{11} = \frac{1}{E_{11}} = 7.570 \times 10^{-12}\ \text{GPa}^{-1}\ (52.19 \times 10^{-9}\ \text{psi}^{-1})$$

$$S_{12} = \frac{-\nu_{12}}{E_{21}} = -\ 2.067 \times 10^{-12}\ \text{GPa}^{-1}\ (-14.25 \times 10^{-9}\ \text{psi}^{-1})$$

The tensile modulus value can be compared to the results of Kibler; E_{11} = 136 GPa [11].

Tests of 90-deg Specimens

The 90-deg tests were used to characterize the viscoelastic response of the matrix-dominated modulus E_{22}. The ultimate strength perpendicular to the fibers at 149C was inititally estimated to be 31.1 MPa (4500 psi), based upon a parallel study by Zhang [58]. This ultimate strength was somewhat lower than expected. Sendeckyj et al [59] report an ultimate strength of 49.6 MPa (7160 psi) at room temperatures for T300/5208. Therefore, an ultimate strength of perhaps 41.4 MPa (6000 psi) had been anticipated at a temperature of 149C. However, during the present study even the lower strength levels observed by Zhang were not attained, as all 90-deg specimens failed at stress levels greater than 20.7 MPa (3000 psi). This failure occurred for

a total of four specimens, two of which had been used in previous tests and two of which were virgin specimens. All failures occurred in the specimen grips rather than in the strain gage area. These specimens were rather delicate, and it is possible that they were damaged slightly during gaging and/or mounting in the grips, although care was taken to be gentle. Further tests with new specimens were not possible due to the material shortages mentioned above. It should be noted that in previous viscoelastic studies at VPI&SU 16-ply specimens were used rather than 8-ply specimens. Perhaps in future efforts 16-ply specimens should again be used, since the increased specimen thickness may help to improve durability.

Strain data for the entire 480 min/120 min creep/recovery test cycle were obtained at seven stress levels ranging from 10.5 to 20.7 MPa (1528 to 2997 psi). For each test, a minimum of 26 creep and 21 recovery data points were taken, at the nominal times listed in Table 6.1.

Following collection, the data were entered into the IBM mainframe computer and reduced using either the SCHAPERY or FINDLEY programs described in Chapter III. An interactive graphics routine was also written which allowed an immediate plot of the data and analytic fit. Sample plots are shown in Figures 6.3-6.5. The entire creep/recovery data set is shown in Figure 6.3. The solid line represents the analytic

Table 6.1: Nominal Measurement Times For The 480/120 Minute Creep/Creep Recovery Tests

Creep Measurement Time		Recovery Measurement Time	
Number	Time (minutes)	Number	Time (minutes)
1	0.5	1	0.25
2	1.0	2	0.50
3	1.5	3	0.75
4	2.0	4	1.0
5	3.0	5	1.5
6	4.0	6	2.0
7	5.0	7	3.0
8	7.0	8	4.0
9	10.	9	5.0
10	15.	10	7.0
11	20.	11	10.
12	25.	12	15.
13	30.	13	20.
14	40.	14	25.
15	50.	15	30.
16	60.	16	40.
17	90.	17	50.
18	120.	18	60.
19	150.	19	80.
20	180.	20	100.
21	210.	21	120.
22	240.		
23	300.		
24	360.		
25	420.		
26	480.		

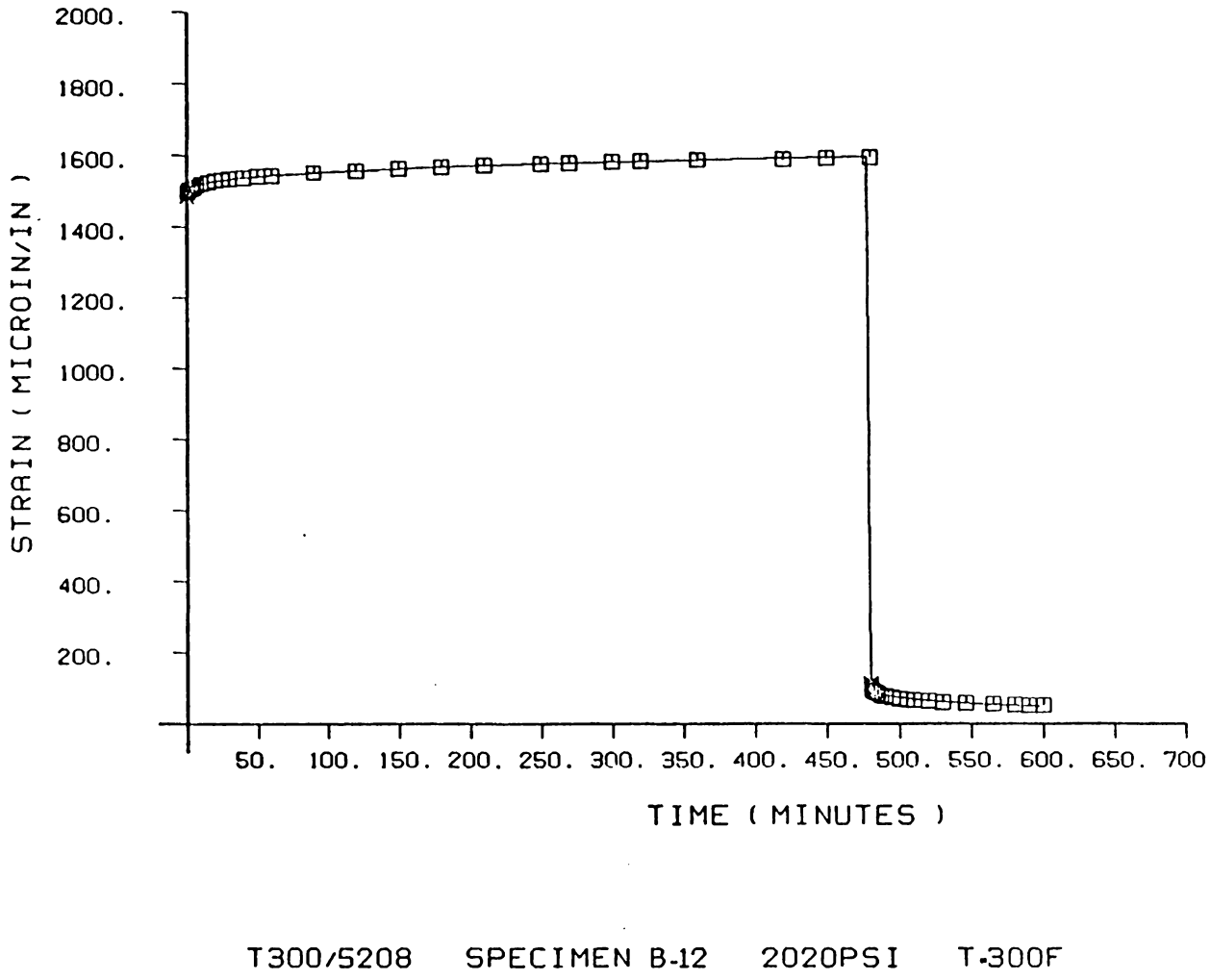

Figure 6.3: 480/120 Minute Creep/Creep Recovery Data Set and Analytic Fit, Plotted Using The Interactive Graphics Routine

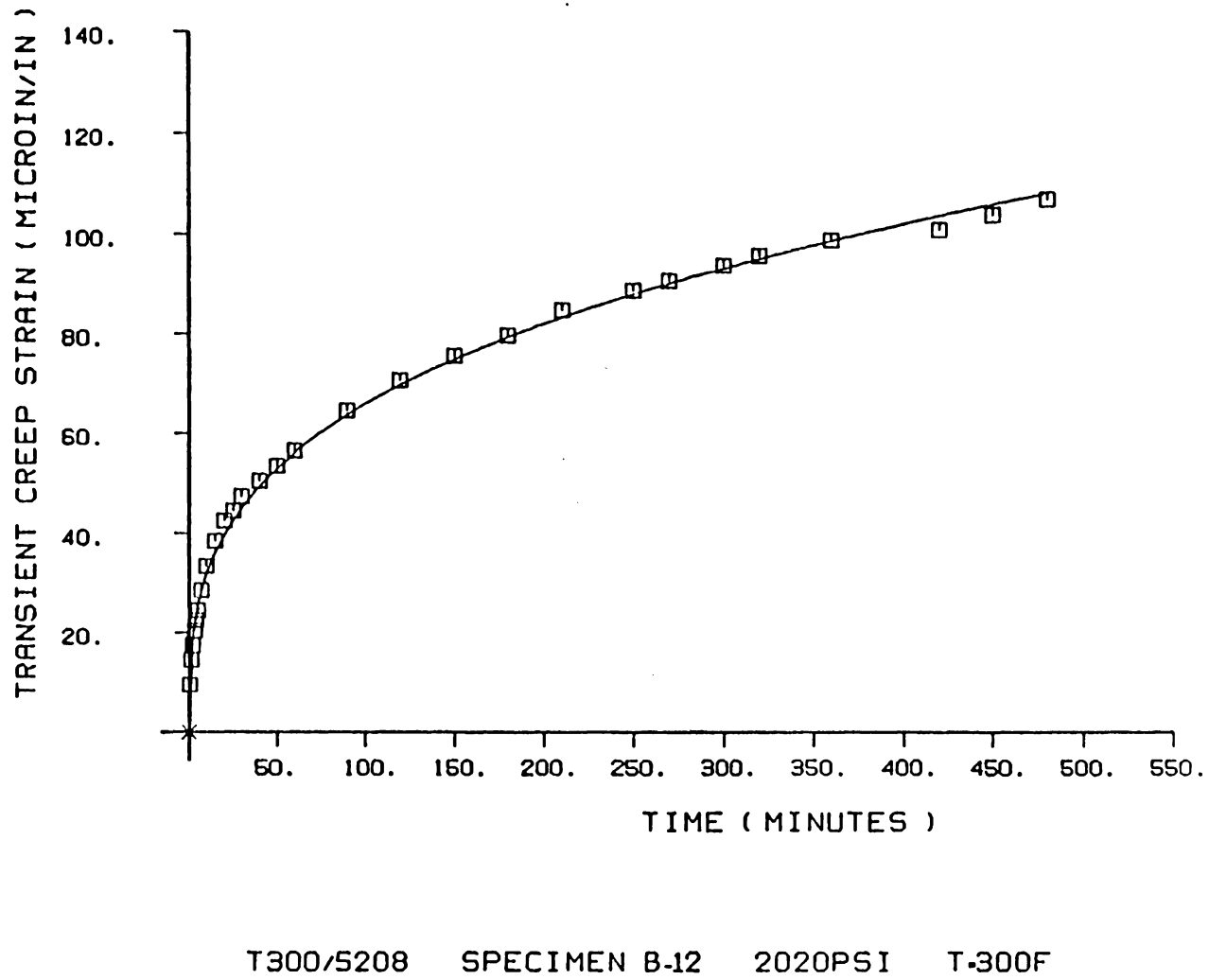

Figure 6.4: 480 Minute Transient Creep Data and Analytic Fit, Plotted Using the Interactive Graphics Routine

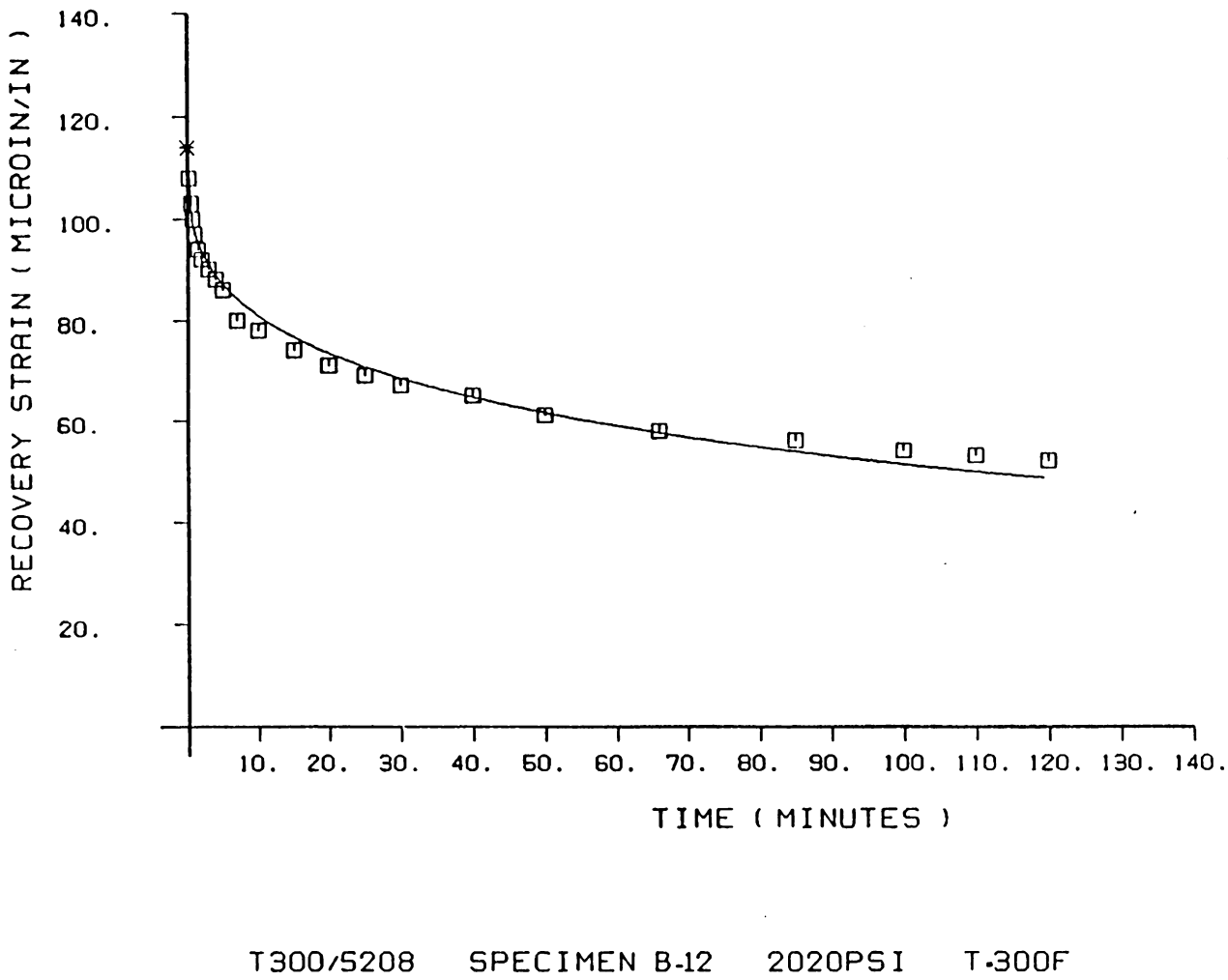

Figure 6.5: 120 Minute Recovery Data and Analytic Fit, Plotted Using the Interactive Graphics Routine

fit provided by the SCHAPERY program. The transient creep response is shown in Figure 6.4; i.e., the instantaneous response has been subtracted from the creep data and only the transient viscoelastic response is shown. Recovery data and analytic fit are shown in Figure 6.5. This plotting routine was used to detect any input errors and as a visual check of the analytic curve fit.

One difficulty associated with the relatively long 480 minute creep period used in this study was the resulting long time required for specimen recovery. At the lower stress levels, the recovery response was complete after a 1-2 day period, and a new test could be initiated. At the higher stress levels, a considerably longer recovery time was neccessary; at the highest stress levels a recovery period of 10 days was required. Also, at these higher stress levels, a permanent non-recoverable strain was recorded. The permanent strain following recovery will be further discussed below. In these cases, recovery was judged "complete" when the strain measurement did not change appreciably over a 24 hour period.

Stress-strain curves obtained at 0.5 and 480 minutes during the creep cycle are shown in Figure 6.6. Results indicate very slight nonlinear behaviour at stress levels greater than about 15.6 MPa (2250 psi). This result was not unexpected, since slight nonlinear behaviour for 90-deg

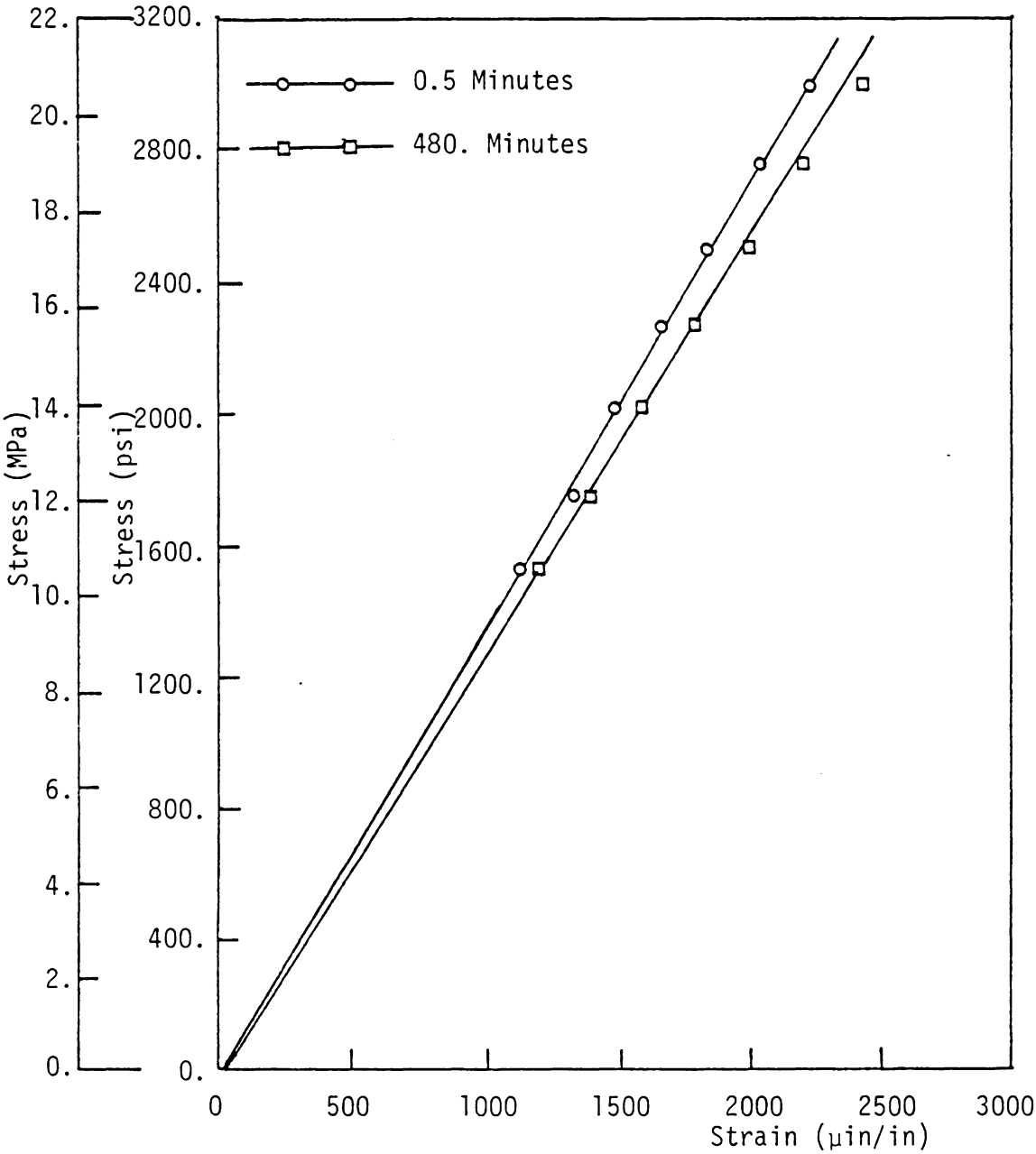

Figure 6.6: Stress-Strain Curves Obtained at 0.5 and 480 Minutes for 90-Deg T300/5208 Specimens

specimens of T300/934 had been suspected by Hiel [22], although the creep/creep recovery cycle he used was not long enough to distinguish nonlinear behaviour. The results presented in Figure 6.6 confirm this suspicion and also raise an interesting question regarding the concept of a linear/nonlinear distinction in stress level. That is, while the results obtained at 0.5 minutes indicate linear behaviour at any stress level, the results obtained at 480 minutes indicate nonlinear behaviour at stress levels greater than 15.6 MPa. It can be hypothesized that if creep data had been taken at times greater than 480 minutes nonlinear behaviour would have been evident at stresses lower than 15.6 MPa. Therefore, it may be that nonlinear behaviour occurs at any stress level for T300/5208, but is not apparent at short times for low stress levels.

From a practical viewpoint, if viscoelastic behaviour is to be predicted at time t = 0.5 minutes, then nonlinear effects can be neglected at any stress level. Conversely, if the prediction is to be made for 480 minutes, then nonlinear behaviour must be accounted for at stress levels greater than 15.6 MPa. Thus, the decision as to whether to include nonlinear effects in an analysis depends upon the desired length of prediction. This greatly complicates the process of accelerated characterization, since it implies that nonlinear effects important at long times cannot be sensed

with sufficient accuracy at short times. A possible solution would be to couple the TSSP (i.e., the Schapery model) with the TTSP, or in other words accelerate the time scale using both stress and temperature. This approach was not used in the present study, but is worthy of further consideration. For this study it was decided to treat data obtained at stress levels less than or equal to 15.6 MPa as linear data, and treat data obtained at the higher stress levels as nonlinear data.

Another factor which complicated the analysis was that complete recovery was not observed following each test, indicating an accumulation of damage within the test specimen. The permanent non-recoverable strains recorded for the 90-deg specimen are shown in Figure 6.7. As previously discussed this problem was also encountered by Hiel [22], and was treated as an offset error in the recovery data. In the present case the effects of permanent strain were investigated by comparing the results of five separate analyses. The linear viscoelastic parameters A_o, C, and n were first determined using the linear creep data and the FINDLEY program. Recall that the sensitivity analysis presented in Chapter IV indicates this to be the best approach for calculating the power law exponent n. Next, A_o, C, and n were determined using the SCHAPERY program and linear creep and uncorrected recovery data. That

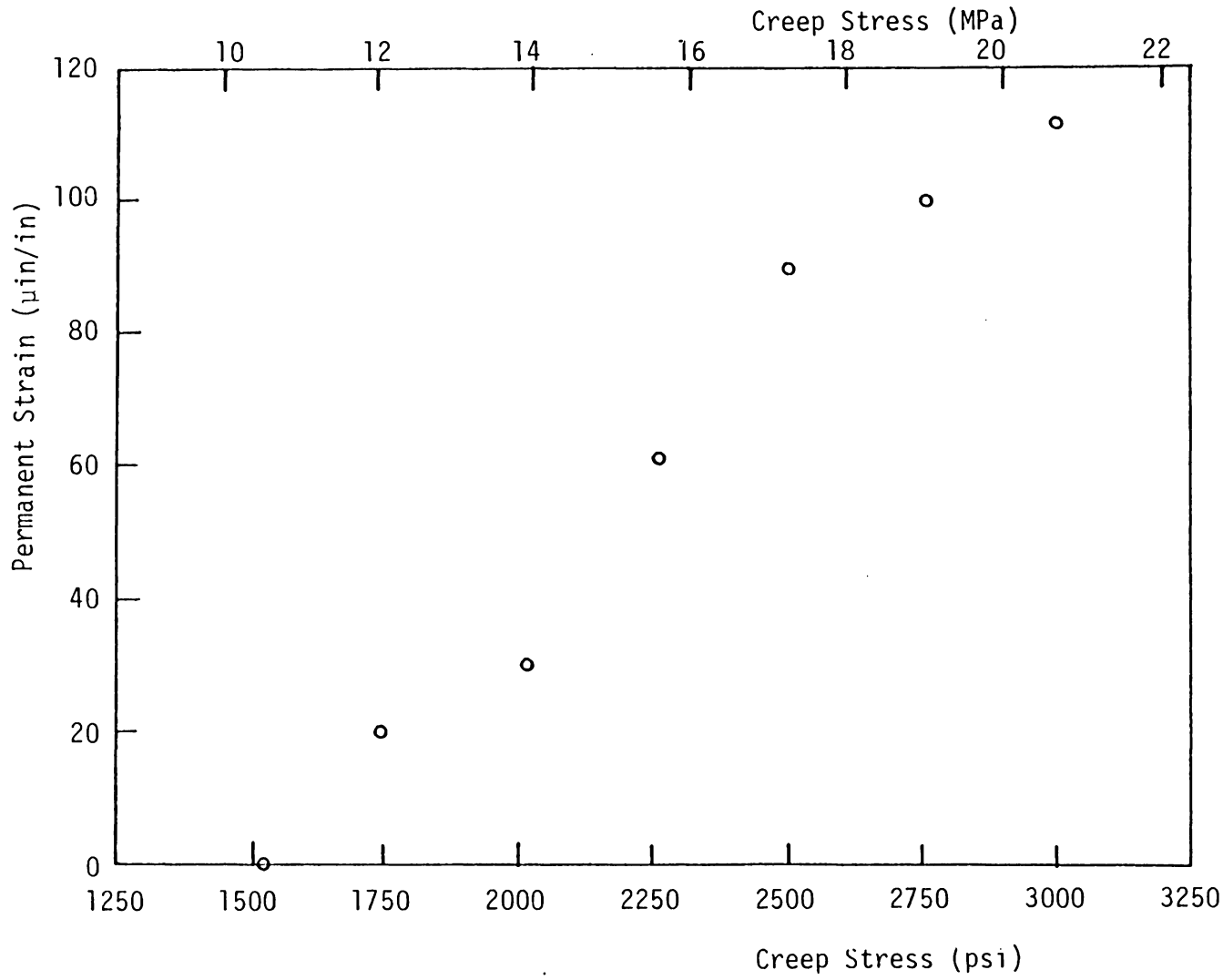

Figure 6.7: Permanent Strains Recorded Following the 480/120 Minute Creep/Creep Recovery Tests Using 90-Deg T300/5208 Specimens

is, the accumulated damage was not accounted for in this second analysis and the recovery data used contained an "offset error". This analysis is included to illustrate the detrimental effects of such errors on the viscoelastic analysis. In the third and fourth analyses attempts were made to account for the accumulated damage within the linear recovery data. Two approaches were used, which will be referred to as "Method 1" and "Method 2". Finally, the remaining nonlinear parameters g_0, g_1, g_2, and a_σ were determined using nonlinear data and the SCHAPERY program.

Analysis Using Creep Data

In this section, the results obtained using the program FINDLEY will be presented. The creep data used were obtained at stress levels of 10.5, 12.1, 13.9, and 15.6 MPa (1528, 1748, 2020, and 2263 psi). Note that the creep data was not corrected for any permanent strain error. The values obtained for A_o, C, and n are shown in Figure 6.8. The average value and standard deviation for each parameter were

$$A_o = 0.1.062 \pm 0.00037 \text{ (X 1/GPa)}$$
$$= 0.7321 \pm 0.00252 \text{ (X } 10^{-6}\text{/psi)}$$
$$C = 0.00136 \pm 0.00016 \text{ (X 1/GPa-min}^n\text{)}$$
$$= 0.009372 \pm 0.00111 \text{ (X } 10^{-6}\text{/psi-min}^n\text{)}$$
$$n = 0.289 \pm 0.0158$$

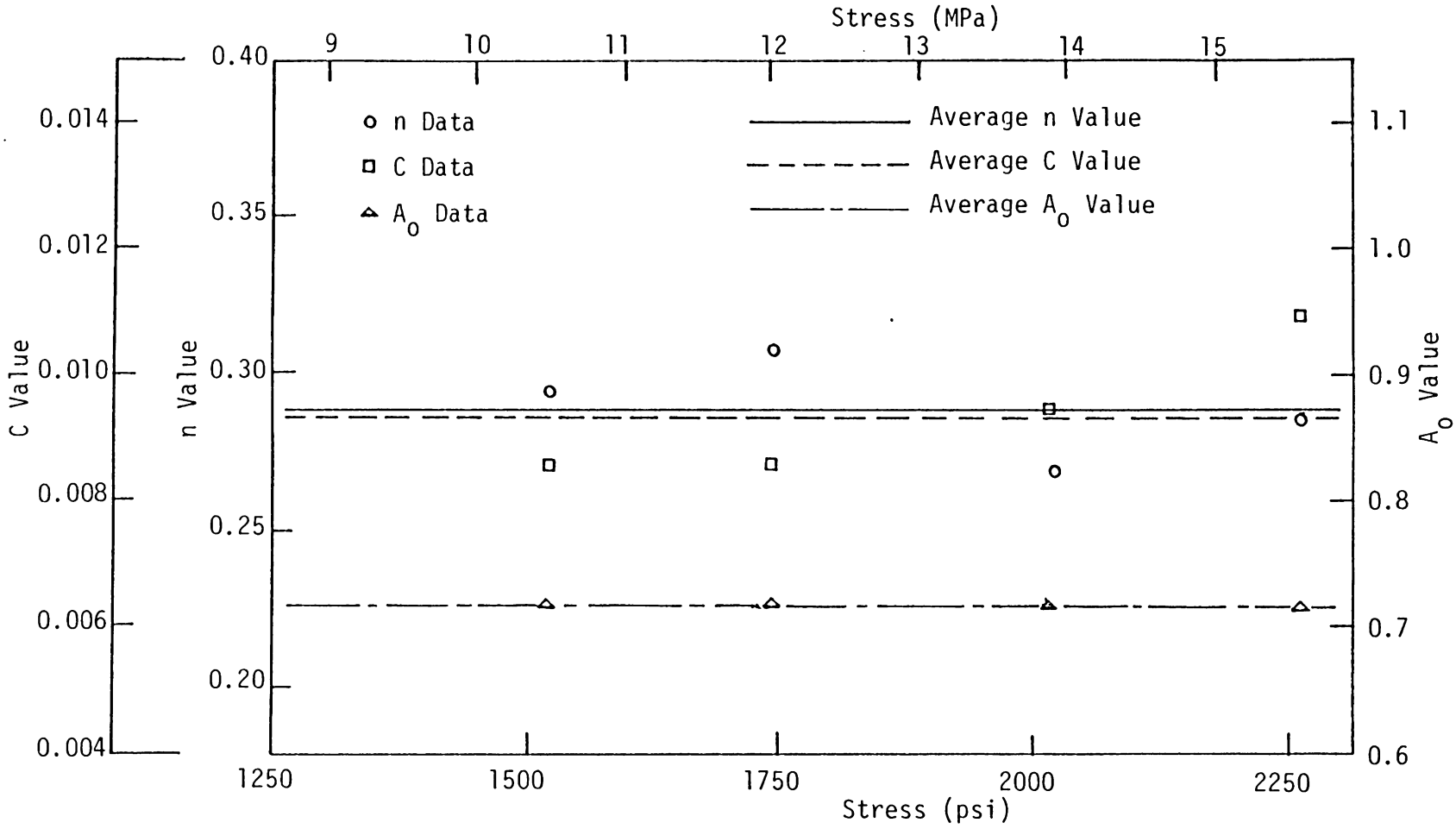

Figure 6.8: Values Obtained for the Linear Viscoelastic Parameters A_o, C, and n Using the Program FINDLEY

Recall that all three of these values are expected to remain constant with stress. Based upon the analysis presented in Chapter V, it was hoped that the test cycle selected would result in an accuracy in n ranging from -6.1% to +4.8% of the actual value. The standard deviation will be used as an indication of accuracy; thus possible experimental error in the value obtained for n is $\pm$5.5%. Therefore, the expected accuracy in n was not quite attained. Admittedly, neither the number of tests nor the number of stress levels used are of a statistically valid sample size. Nevertheless, these results exhibit considerably less scatter than those obtained using a different creep cycle [21]. The possible error in C (shown in Chapter IV to be less important than errors in n) is $\pm$11.8%, while the possible error in A_o is $\pm$0.3%.

Analysis With Uncorrected Recovery Data

The A_o, C, and n values obtained using the SCHAPERY program and uncorrected recovery data are shown in Figure 6.9. As indicated a very wide scatter in both C and n was encountered. This would be expected based upon the analysis described in Chapter IV, since the recovery data contains a large offset error due to accumulated damage. The average value and standard deviation for each parameter are

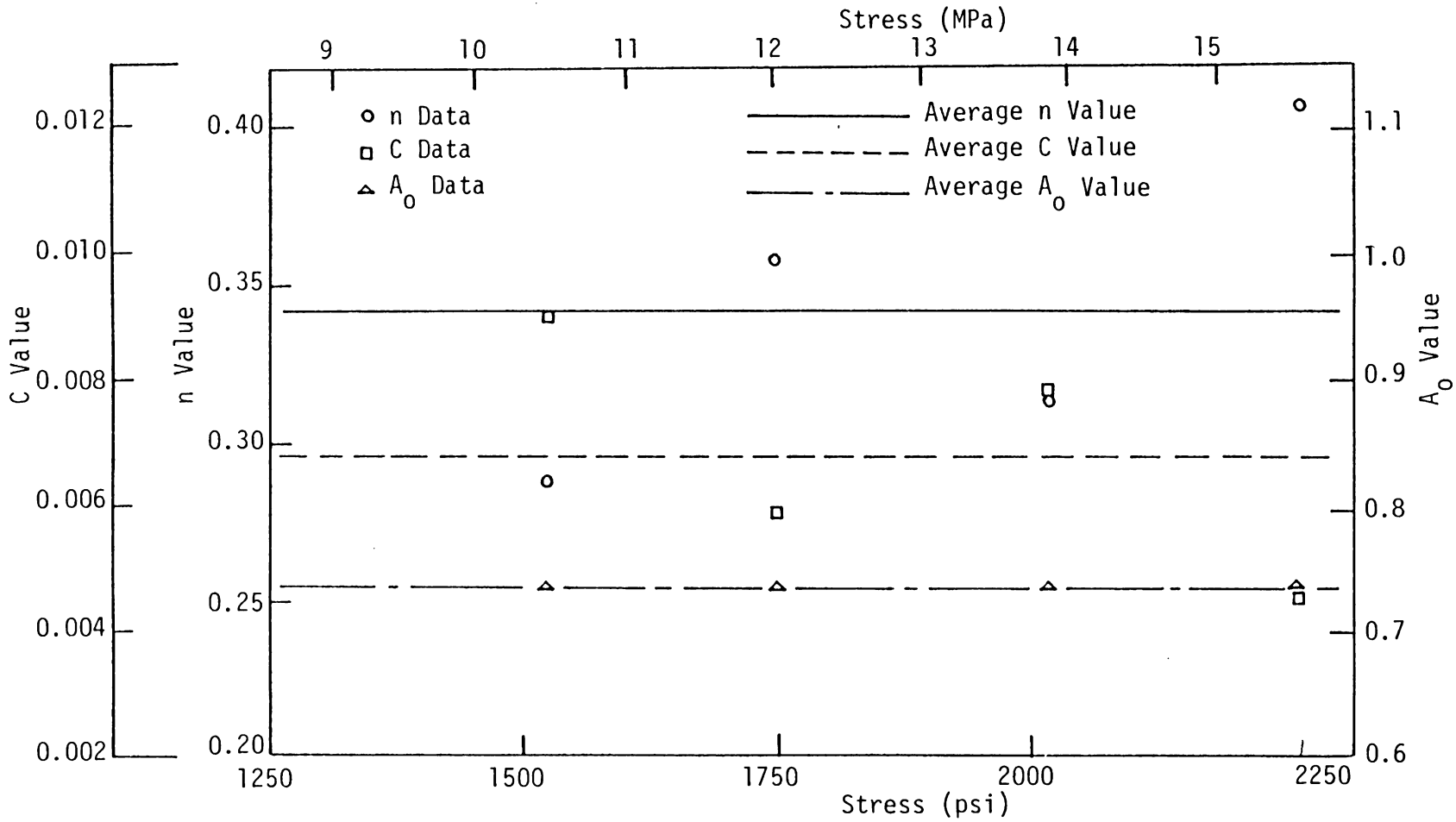

Figure 6.9: Values Obtained for the Linear Viscoelastic Parameters A_0, C, and n Using the Program SCHAPERY and Uncorrected Recovery Data

$$A_o = 0.1068 \pm 0.00048 \text{ (X 1/GPa)}$$
$$= 0.7363 \pm 0.00328 \text{ (X } 10^{-6}\text{/psi)}$$
$$C = 0.000986 \pm 0.000286 \text{ (X 1/GPa-min}^n\text{)}$$
$$= 0.006816 \pm 0.001970 \text{ (X } 10^{-6}\text{/psi-min}^n\text{)}$$
$$n = 0.342 \pm 0.0527$$

The possible error in n and C are therefore $\pm$15.4% and $\pm$28.9%, respectively. Note that the estimate for A_o obtained using either FINDLEY or SCHAPERY is essentially equivalent, since in both cases A_o is determined using the creep data.

Analysis With Recovery Data Corrected Using Method 1

In this analysis, the accumulated damage recorded following each test was subtracted from the recovery data. This approach was used by Hiel [22], and will be referred to as Method 1, to distinguish it from an alternate procedure described in the next paragraph. The A_o, C, and n values calculated using this approach are presented in Figure 6.10. The average values and standard deviations are

$$A_o = 0.1057 \pm 0.000398 \text{ (X 1/GPa)}$$
$$= 0.7288 \pm 0.002746 \text{ (X } 10^{-6}\text{/psi)}$$
$$C = 0.001813 \pm 0.0004186 \text{ (X 1/GPa-min}^n\text{)}$$
$$= 0.0125 \pm 0.002886 \text{ (X } 10^{-6}\text{/psi-min}^n\text{)}$$
$$n = 0.257 \pm 0.0258$$

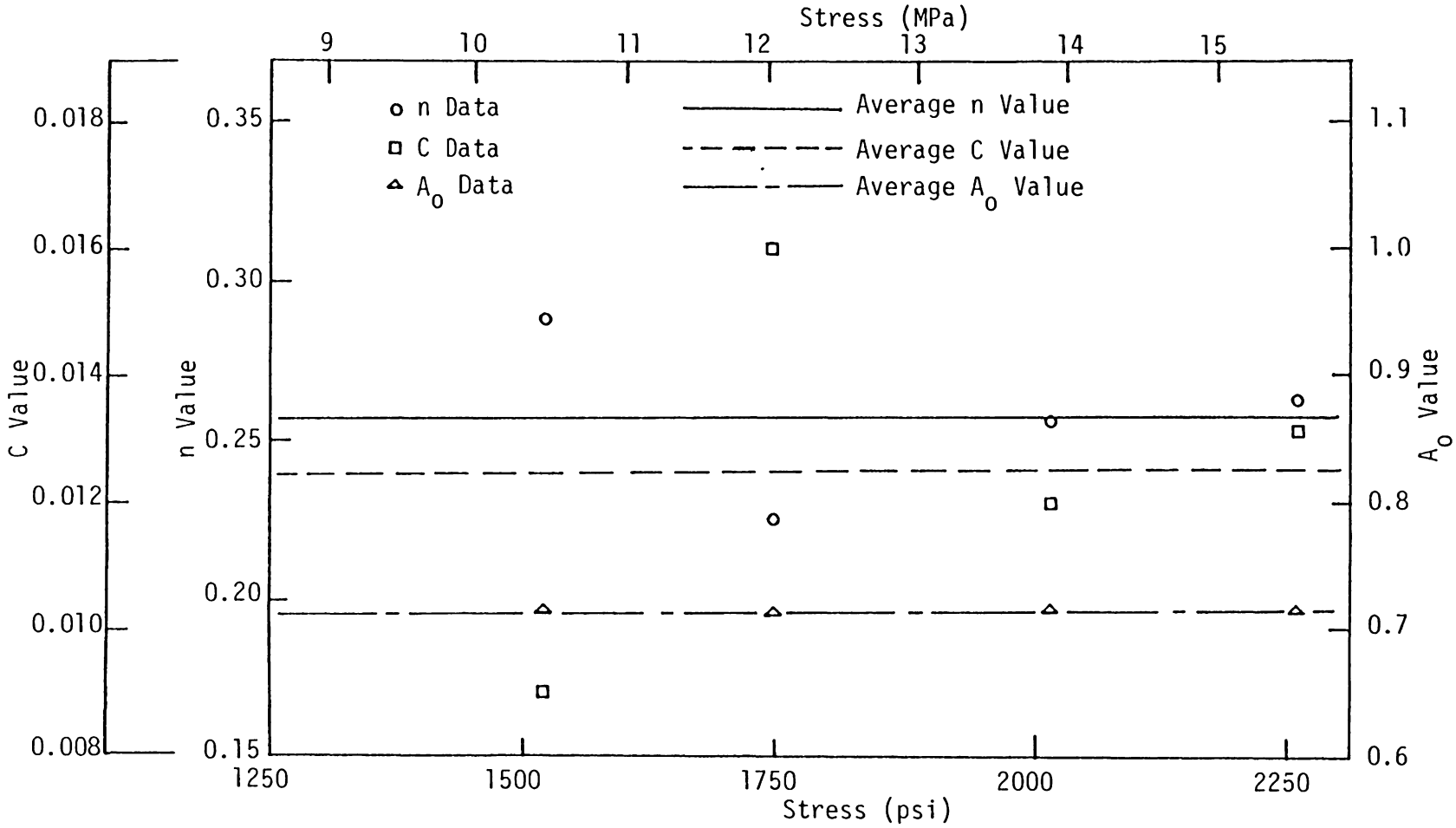

Figure 6.10: Values Obtained for the Linear Viscoelastic Parameters A_0, C and n Using the Program SCHAPERY and Recovery Data Corrected Using Method 1

The possible error in n and C for this case are ±10.0% and ±23.1%, respectively. Thus, correcting the recovery data by Method 1 reduced the scatter in n and C, but not to the levels obtained by using the creep data.

Analysis With Recovery Data Corrected Using Method 2

Note that since the response is assumed to be linear eq. 3.4 can be used to generate an analytic recovery curve based upon the creep response. That is, the C and n values obtained using the creep data (C = 0.009372; n = 0.289) can be substituted into eq. 3.4 to obtain an expression for the expected recovery strain at any time t. Based upon this approach, the recovery curve expected at a stress level of 15.6 MPa is compared with the uncorrected and corrected recovery data in Figure 6.11. It would appear from this figure that the difficulty lies in an inaccurate permanent strain measurement; i.e., the correction used to account for accumulated damage was too severe, causing the corrected recovery strains to "overshoot" the expected recovery curve. Similar calculations indicated an overshoot had occured at all stress levels. The discrepancy between expected recovery strains and corrected recovery strains was on the order of 5-15 μin/in in all cases. While this is a relatively small error, it has been demonstrated in Chapter

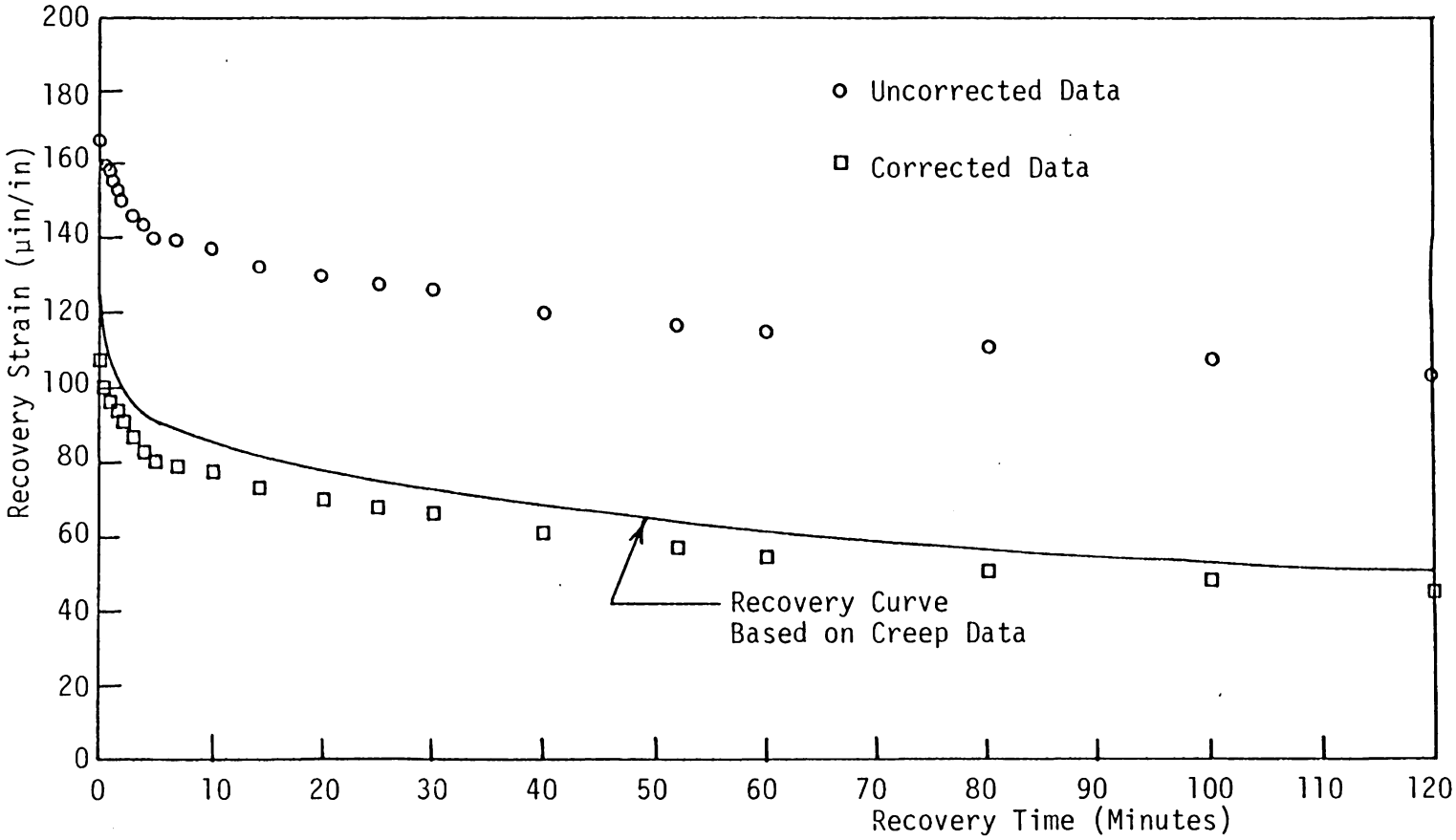

Figure 6.11: Comparison of Expected Recovery Curve at 15.6 MPa (2263 psi) Based on Creep Data and Measured Recovery Data Corrected Using Method 1

IV that errors of this magnitude severly distort the results obtained using recovery data.

These considerations gave rise to a second approach for correcting the recovery strain, which was to simply adjust the measured data so as to match with the expected recovery response as closely as possible. This is not proposed as a valid experimental technique, since it requires a priori knowledge of the recovery response. The intent is rather to determine whether the measured recovery data can be "forced" to agree with the results obtained from creep. This procedure will be referred to as Method 2. The optimum offset shift of the recovery data was determined as follows. The expected recovery response at each stress level was calculated and subtracted from the measured strain at each point in time. The difference was defined as an offset error for that point in time. The average offset error over the 120 minute recovery period was then calculated for each stress level and subtracted from the recovery data as before. The resulting fit between predicted and corrected recovery strains is illustrated in Figure 6.12 for a stress level of 15.6 MPa. Similar results were obtained at all stress levels. Casual inspection would suggest that a very good correlation between the C and n values calculated using creep and corrected recovery data would now be obtained. However, the correlation did not improve and in fact

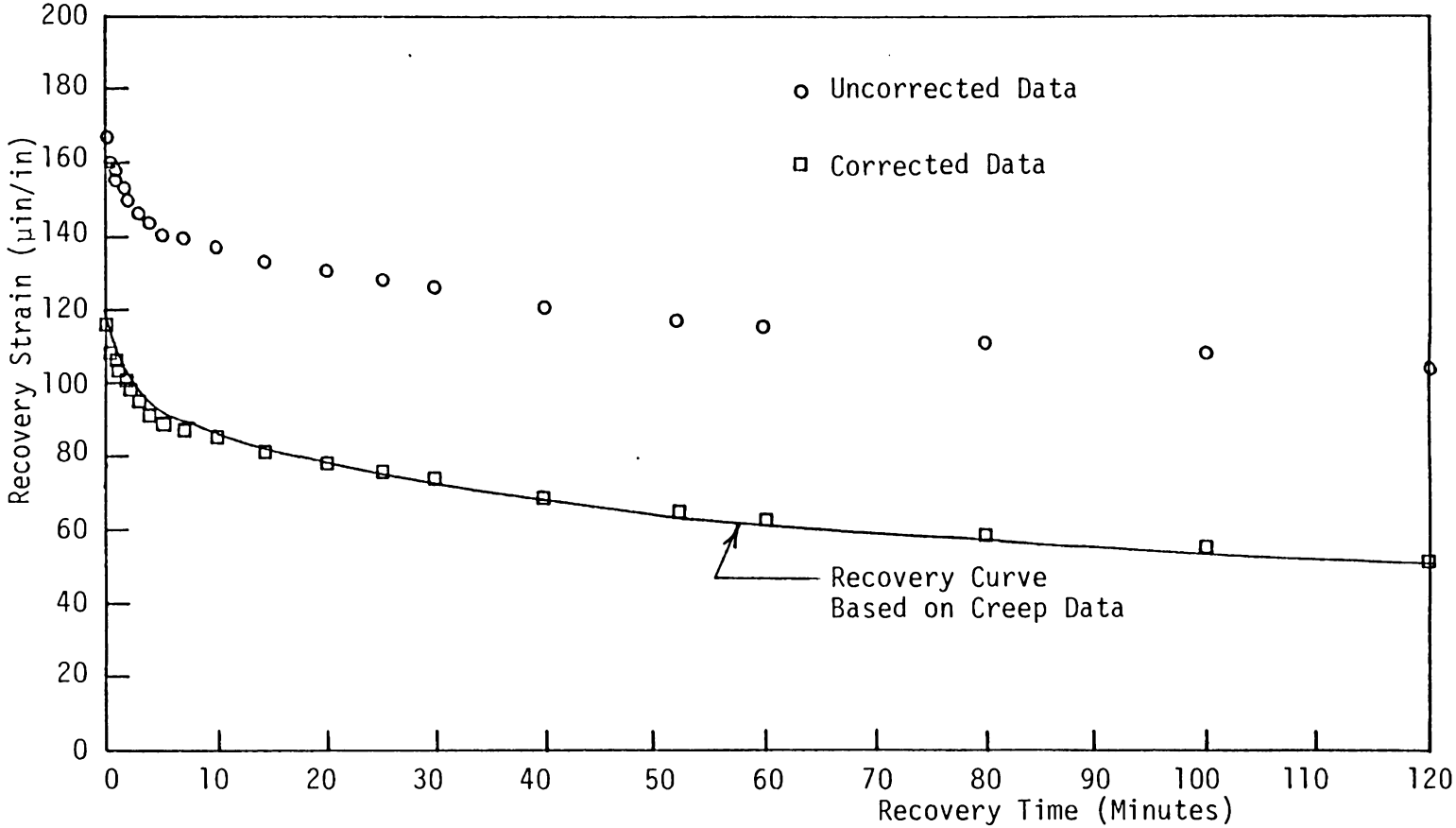

Figure 6.12: Comparison of Expected Recovery Curve at 15.6 MPa (2263 psi) Based on Creep Data and Measured Recovery Data Corrected Using Method 2

slightly worsened. The A_o, C, and n values obtained are presented in Figure 6.13. The average values and standard deviations are

$$A_o = 0.1062 \pm 0.000786 \text{ (X 1/GPa)}$$
$$= 0.7324 \pm 0.00542 \text{ (X } 10^{-6}\text{/psi)}$$
$$C = 0.001426 \pm 0.000472 \text{ (X 1/GPa-min}^n\text{)}$$
$$= 0.00983 \pm 0.00326 \text{ (X } 10^{-6}\text{/psi-min}^n\text{)}$$
$$n = 0.295 \pm 0.0401$$

The standard deviations indicate possible errors for n, C, and A_o of $\pm$13.5%, $\pm$33.2%, and $\pm$0.74%, respectively.

The reasons for this rather suprising result are not clear, although by careful inspection of Figure 6.12 a potential explanation is suggested. Note that for times less than about 10 minutes the corrected recovery data points lie slightly below the predicted recovery curve, while at longer times the data points lie slightly above the predicted curve. This same pattern existed at the other stress levels. Thus, the experimental data points describe a slightly "flatter" curve than predicted by linear viscoelastic theory. This indicates slightly nonlinear behaviour, which could perhaps explain the erratic results obtained. Specifically, a flatter recovery curve indicates that the g_1 parameter is greater than 1.0, as discussed in Chapter III. This reasoning also implies that the recovery

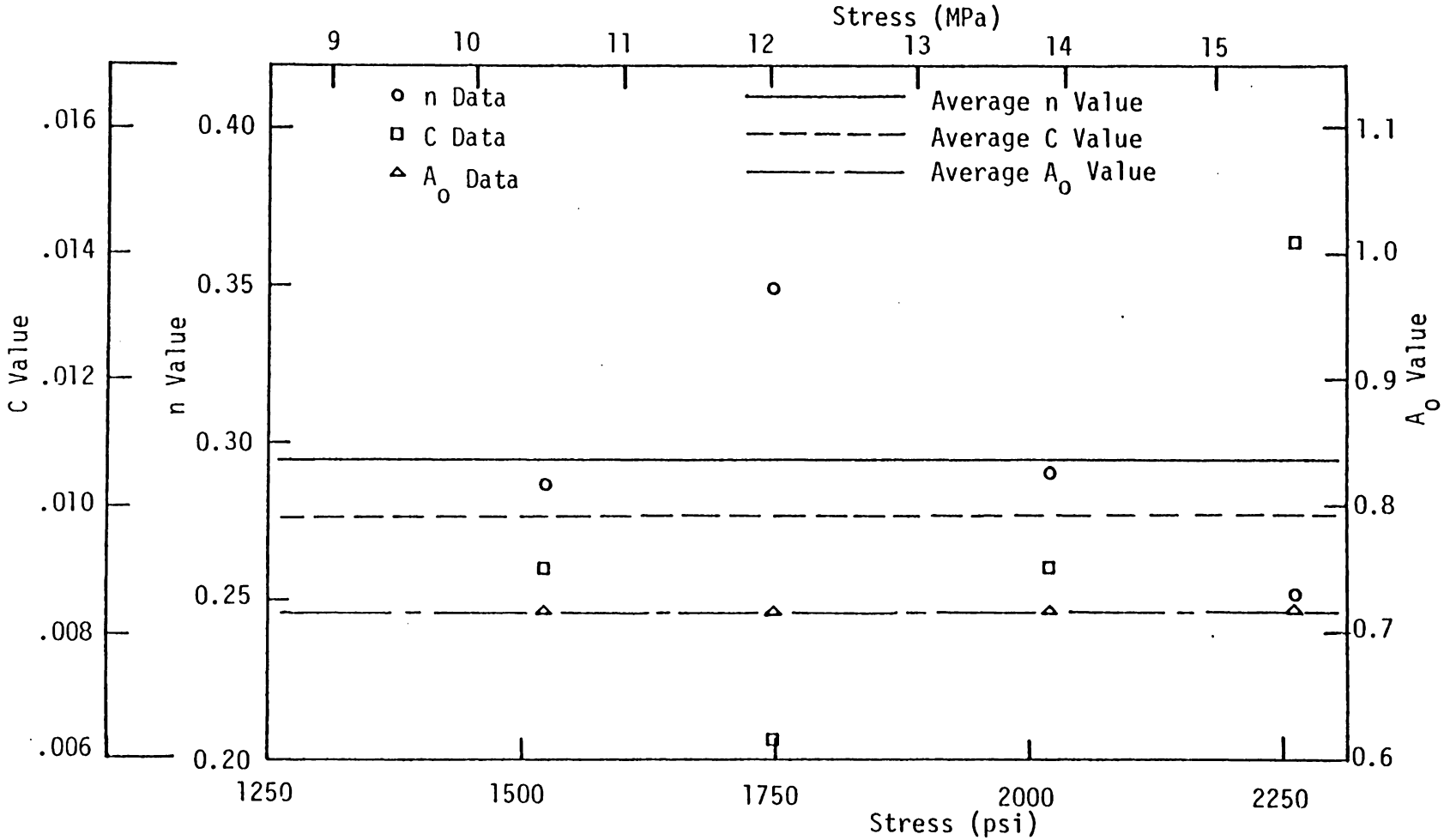

Figure 6.13: Values Obtained for the Linear Viscoelastic Parameters A_o, C, and n Using the Program SCHAPERY and Recovery Data Corrected Using Method 2

response is more sensitive to nonlinear effects than is the creep response, since satisfactory results were obtained using the creep data and linear theory. This greater sensitivity to nonlinear effects in the recovery data has also been observed by Lou and Schapery [35].

Another possible contributing factor would be that the effects of accumulated damage have not been properly accounted for. Damage is presumably accumulated through the formation of voids and/or microcracks which form during the creep cycle. Such imperfections may occur immediately upon loading, or may develop gradually during the creep cycle. In this second case the shape of the creep curve may be altered due to damage accumulation, ultimately affecting the calculated values of C and n. Upon unloading, these voids and microcracks would tend to close and perhaps modify the shape of the recovery curve as well. The creep/creep recovery response would therefore depend upon some combination of viscoelastic, plastic, and fracture mechanisms. Erratic results may have been obtained because the Schapery theory does not account for these hypothesized plastic or fracture mechanisms.

At the least, the above calculations indicate the extreme sensitivity of n and C to slight errors in the recovery strain data. This sensitivity tends to confirm the analysis presented in Chapter IV, where it was concluded

that stable values for A_o, C and n can best be obtained using creep rather than recovery data.

Calculation of the Nonlinear Parameters

The final step in the characterization process was to calculate the nonlinearizing parameters g_0, g_1, g_2, and a_σ at stress levels greater than 15.6 MPa. Specifically, these parameters were calculated at stress levels of 17.2, 19.0, and 20.7 MPa (2498, 2755, and 2997 psi). A permanent strain following recovery was also recorded at these stress levels, so it was neccessary to correct for accumulated damage by subtracting the permanent strain from the recovery data (Method 1). Note that since the response was nonlinear it was not possible to calculate an expected recovery response based solely upon the creep response, and hence it was not possible to use Method 2 of the previous section to analyze the data.

The SCHAPERY program was used to obtain best-fit values for each parameter. The results obtained for g_0 and g_1 are presented in Figure 6.14, as functions of both the applied normal stress and of the average matrix octahedral shear stress, τ_{oct}. (The average matrix octahedral shear stress was discussed in Chapter III.) The g_0 value was calculated as 1.0 at all stress levels. This implies that the elastic instantaneous response was linear at all stress levels and

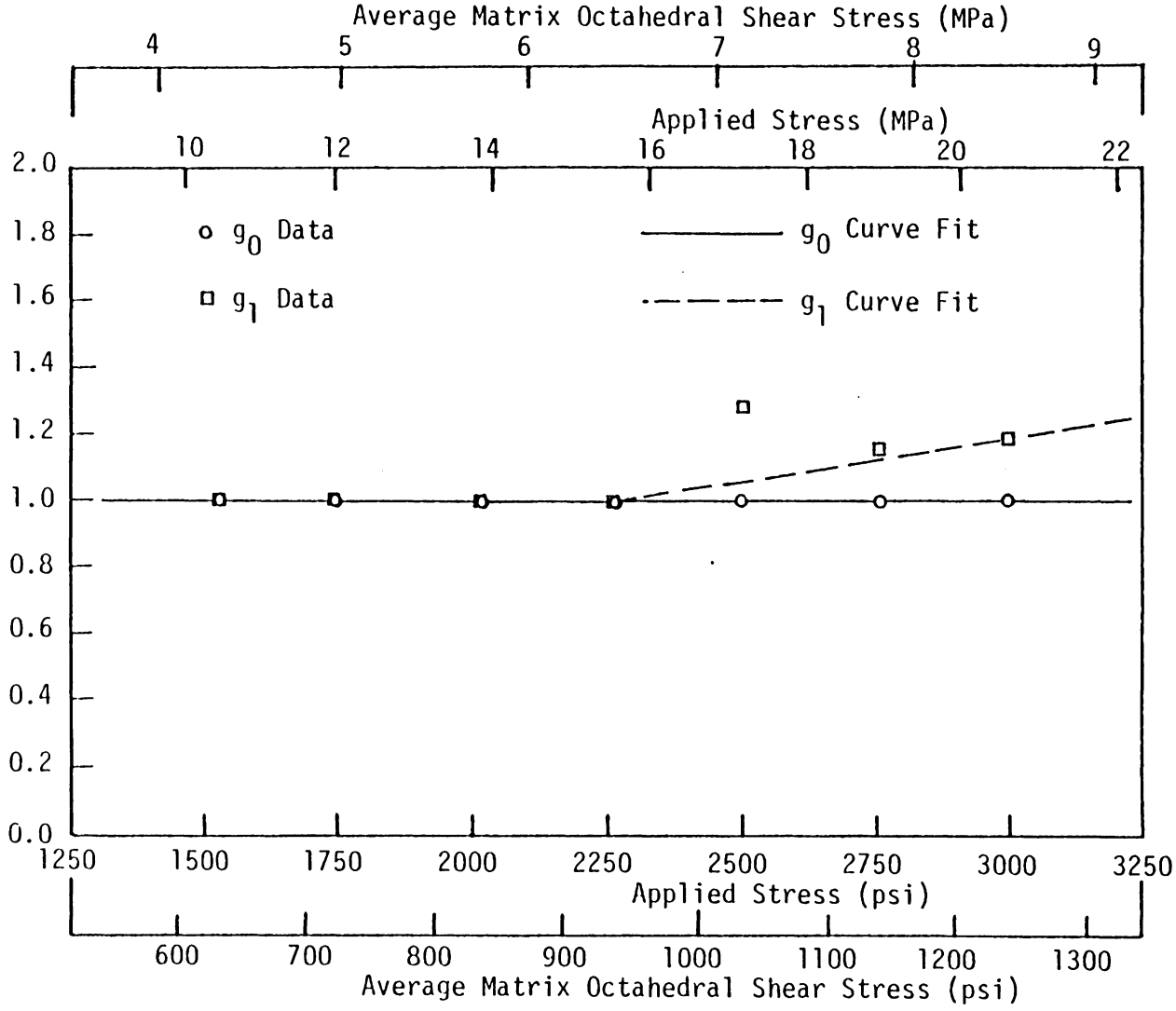

Figure 6.14: Values Obtained for g_0 and g_1 as Functions of Applied Stress and of the Average Octahedral Shear Stress

that the nonlinear behaviour previously noted in Figure 6.6 was due entirely to the viscoelastic response. The g_1 values were somewhat erratic; a value of 1.278 was obtained at an applied stress level of 17.2 MPa, while values of 1.14 and 1.17 were obtained at stress levels of 19.0 and 20.7 MPa, respectively. The results of Hiel for T300/934 indicate that g_1 is a gently increasing function of stress [22], so it was assumed that the g_1 value obtained at 17.2 MPa was in error and was not used in the analysis.

Recall that an expression for g_1 as a function of τ_{oct} was required in the lamination program VISLAP. Peretz and Weitzman [50] have characterized the g_1 parameter for the structural adhesive FM-73 using an expression of the form

$$g_1(\sigma) = 1.0 + S_1 \left(\frac{\sigma}{\sigma_0}\right)^{S_2}$$

where S_1, S_2, and σ_o are material constants determined experimentally. However, since FM-73 is a highly nonlinear material, the g_1 values obtained by Peretz and Weitzman span a much wider range than in the present case, and the above expression was not considered compatible with the mildly nonlinear behaviour observed for T300/5208. Therefore the following simple bilinear relation was used

$$g_1(\tau_{oct}) = \begin{cases} 1.0 \quad , \quad \text{for } \tau_{oct} \leq 6.43 \text{ MPa} \\ 1.0 + 0.0875\ (\tau_{oct} - 6.43), \text{ for } \tau_{oct} > 6.43 \text{ MPa} \end{cases} \tag{6.1}$$

Equation 6.1 is shown as a dashed line in Figure 6.14.

Values obtained for the g_2 and a_σ parameters are shown in Figure 6.15. No distinct pattern emerged for the g_2 parameter. Although a similar variation in g_2 with stress was observed by Hiel [22], it was not clear whether this deviation was due to some physical mechanism or due to experimental error. Therefore, g_2 was set equal to 1.0 at all stress levels. The a_σ value decreased dramatically after initiation of nonlinear behaviour. This distinctive pattern has also been observed by other researchers [22,35-37,50]. The a_σ parameter was related to τ_{oct} using the exponential function, following the approach used by Peretz and Weitzman [50]. The equation used in VISLAP was

$$a_\sigma(\tau_{oct}) = \begin{cases} 1.0 \quad , \quad \text{for } \tau_{oct} \leq 6.43 \text{ MPa} \\ e^{-0.247\ (\tau_{oct} - 6.43)}, \text{ for } \tau_{oct} > 6.43 \text{ MPa} \end{cases} \tag{6.2}$$

It might be noted that an exponential dependence of a_σ with stress has received some theoretical justification [35]. Equation 6.2 is shown as a dashed line in Figure 6.15.

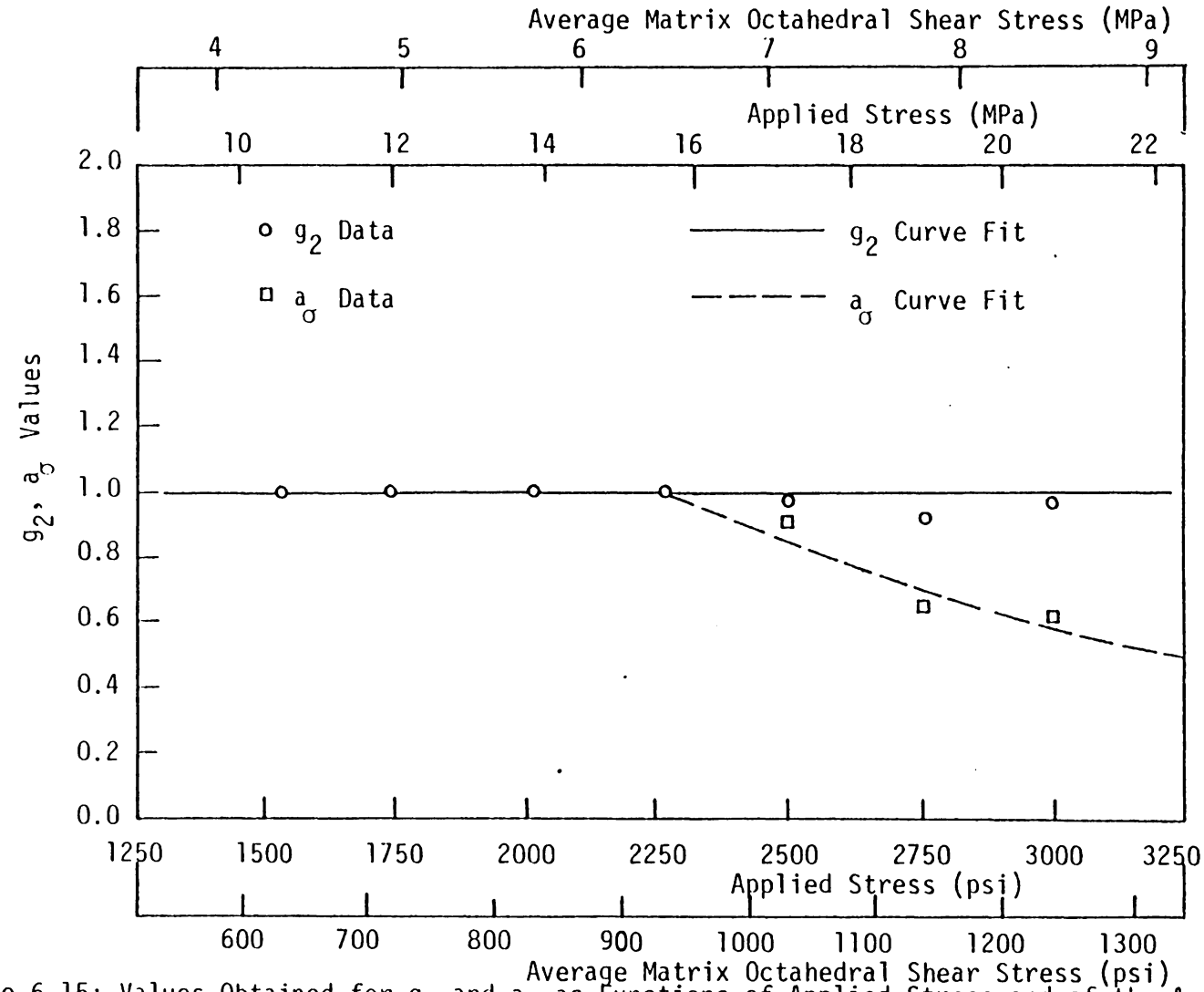

Figure 6.15: Values Obtained for g_2 and a_σ as Functions of Applied Stress and of the Average Matrix Octahedral Shear Stress

Tests of 10-deg Specimens

The 10-deg tests were performed to characterize the viscoelastic response of T300/5208 to shear stress. Creep/creep recovery tests were performed at eleven shear stress levels ranging from 2.9 to 32.5 MPa (426 to 4715 psi). It is well known that end constraints can severely distort the desired uniaxial stress field when testing off-axis tensile specimens, particularily near the specimen grips [60]. Therefore, the 10-deg specimens were 30 cm (12 inches) in length, resulting in a grip-to-grip distance of approximately 23 cm (9.0 inches). The effective length-to-width ratio was thus 18, which is considered adequate for tensile testing. The 480/120 minute creep/creep recovery test cycle was again utilized, and strain data were recorded at the nominal times previously listed in Table 6.1. A 3-element strain gage rosette was used to measure three independent normal strains. The rosette orientation has been noted in Figure 6.1. For the rosette/fiber orientation used, the shear strain γ_{12} along the 10-deg fiber direction can be calculated using the strains measured by gages a, b, and c as

$$\gamma_{12} = -0.598\ \varepsilon_a - 0.684\ \varepsilon_b + 1.282\ \varepsilon_c$$

Note that a different relationship is obtained if an alternate fiber angle or an alternate rosette/fiber orientation is used [22,47]. The shear stress τ_{12} along the fiber direction is related to the applied normal stress σ_x by

$$\tau_{12} = -0.171\ \sigma_x$$

It was found that for an applied tensile normal stress, gages a and b measured tensile (positive) strains, while gage c measured compressive (negative) strains. Thus, both γ_{12} and τ_{12} were negative; for simplicity the results obtained will be presented herein as positive values.

Stress-strain curves obtained at 0.5 and 480 minutes during the creep cycle are presented in Figure 6.16. A comparison of Figs. 6.6 and 6.16 indicates that nonlinear effects were much more significant in the case of shear stress than for the case of normal stress. Apparent linear behaviour with shear was exhibited at the lowest three stress levels of 2.9, 6.1, and 8.8 MPa (426, 878, and 1279 psi), while nonlinear behaviour was observed at higher stress levels. It can again be hypothesized that nonlinear behaviour would have been observed at stress levels less than 8.8 MPa if the creep response had been monitored for times greater than 480 minutes. Nevertheless, the data obtained at shear stress levels of 8.8 MPa or less were

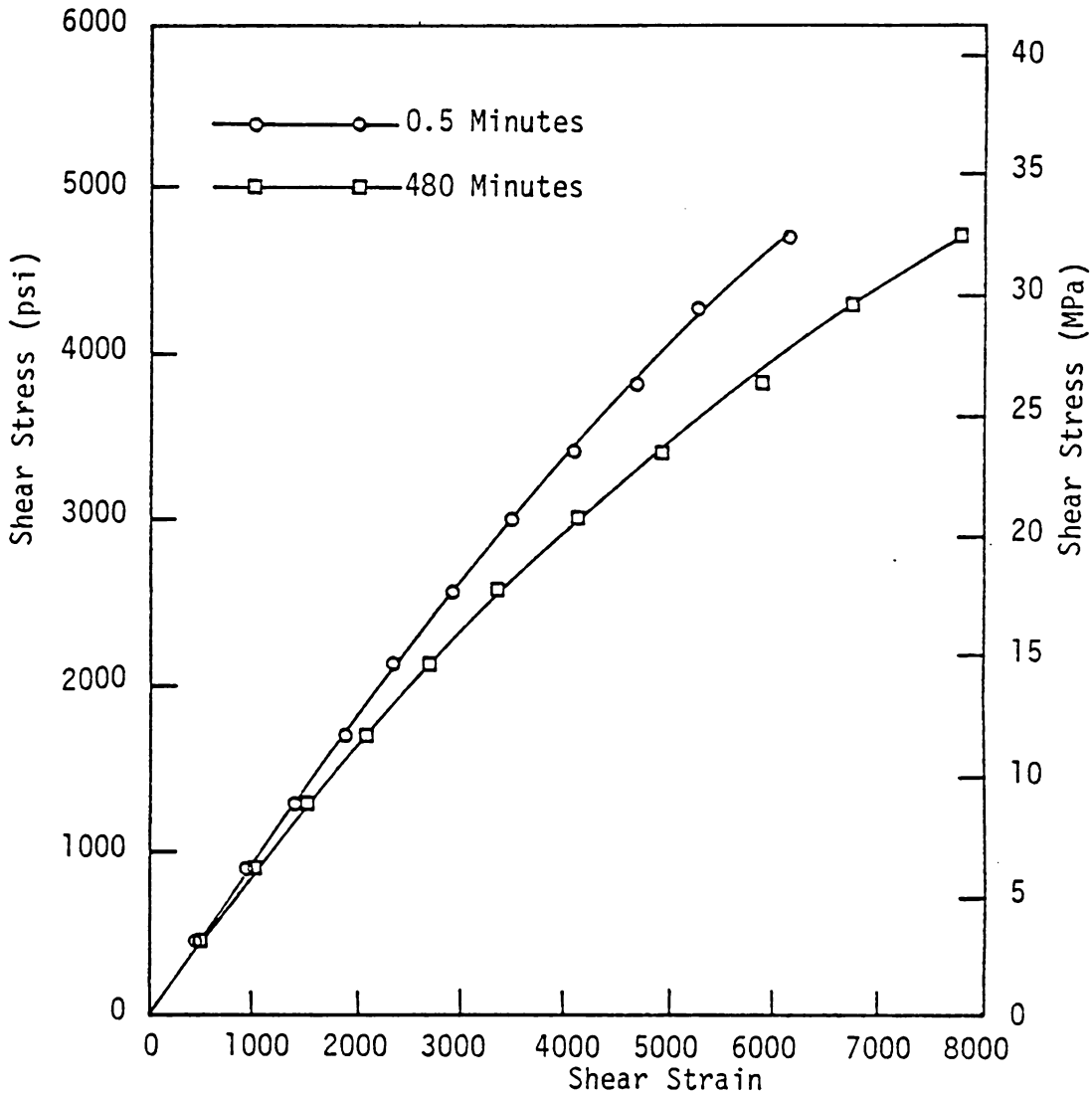

Figure 6.16: Stress-Strain Curves Obtained at 0.5 and 480 minutes for 10-deg T300/5208 Specimens

treated as linear data, while data obtained at higher stress levels were treated as nonlinear data.

Permanent strains apparently due to accumulated damage were again observed. The permanent strains recorded by each of the three gages are presented in Figure 6.17. As indicated a different permanent strain was recorded by each gage. The magnitude of permanent strain roughly reflects the magnitude of the transient response sensed by each gage. That is, gage c recorded both the largest transient response and the largest permanent strain, while gage b recorded both the smallest transient response and the smallest permanent strain. Note also that a large permanent strain was measured by gage c, even though this gage was subjected to compressive strains during the creep cycle. Since the formation of matrix voids and microcracks is not normally associated with compressive strain fields, the permanent strains observed cannot be attributed entirely to damage accumulation in the form of voids or microcracks. A permanent change in the matrix molecular structure must therefore have occurred during the creep cycle, as suggested by Hiel et al [22].

The shear data were analyzed using the conventional two-step process. First a linear analysis was performed using the data obtained at the lowest three stress levels, resulting in calculated values for the linear viscoelastic

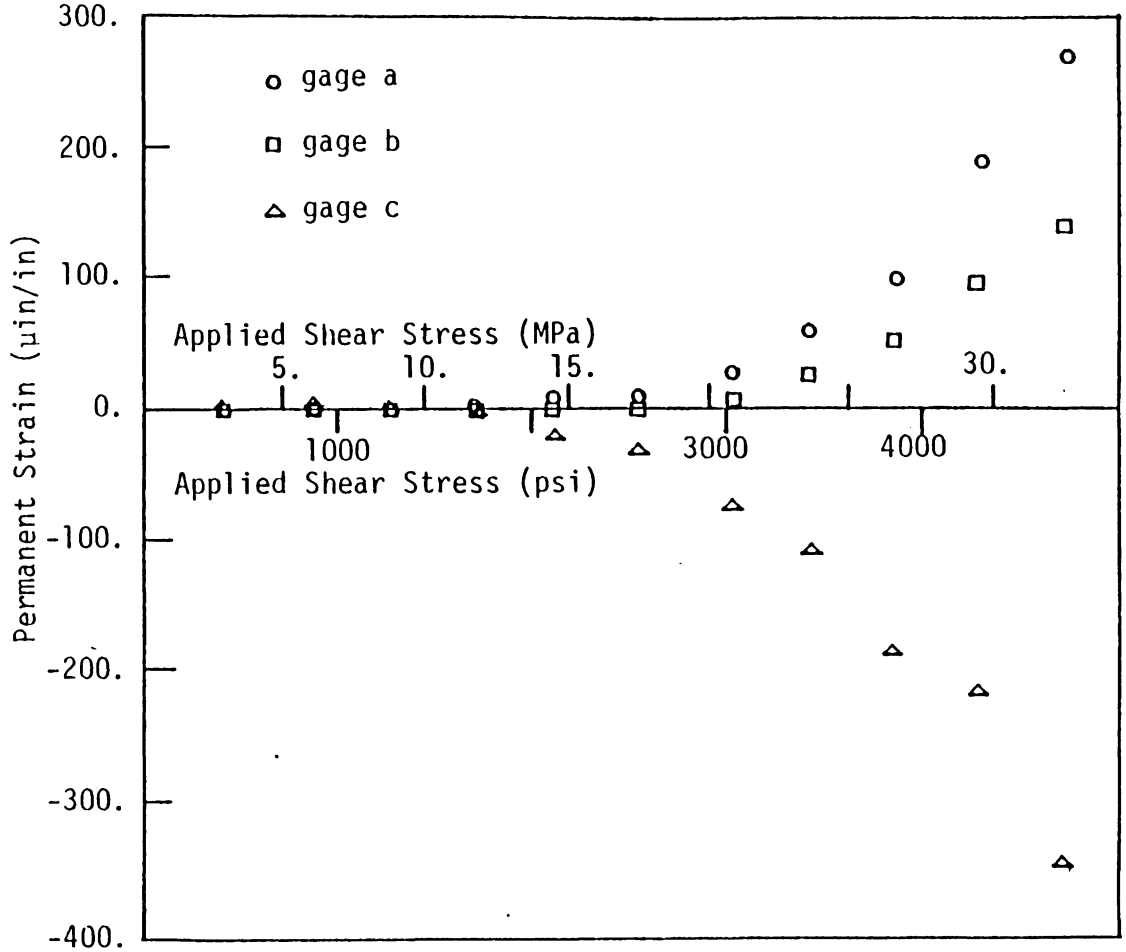

Figure 6.17: Permanent Strains Recorded by Gages a,b, and c Following the 480/120 Minute Creep/Creep Recovery Tests Using 10-Deg Off-Axis T300/5208 Specimens

parameters A_o, C, and n. The remaining nonlinear parameters were then calculated using the nonlinear data obtained at the higher stress levels.

Linear Analysis

A linear analysis was performed using the creep data obtained at shear stress levels of 2.9, 6.1, and 8.8 MPa. Unsatisfactory results were obtained for the lowest stress level of 2.9 MPa. The C and n values calculated using this data set were 0.01297 X 1/GPa-min^n and 0.083, respectively, which do not compare well with the results listed below, which were obtained at the other two stress levels. This discrepancy was probably due to the very low viscoelastic response, since the total transient shear strain measured over the 480 minute creep period was only 30 μin/in. Therefore, it was assumed that accurate measurement of C and n could not be obtained using this data set, and the above values were not used in the analysis.

The average values for A_o, C, and n calculated using the creep data obtained at 6.1 and 8.8 MPa were

$$A_o = 0.1561 \pm 0.001115 \text{ (X 1/GPa)}$$
$$= 1.0761 \pm 0.00769 \text{ (X } 10^{-6}\text{/psi)}$$
$$C = 0.00332 \pm 0.000140 \text{ (X 1/GPa-min}^n\text{)}$$
$$= 0.0229 \pm 0.000962 \text{ (X } 10^{-6}\text{/psi-min}^n\text{)}$$
$$n = 0.247 \pm 0.0214$$

Possible errors in the values for A_o, C, and n are therefore $\pm$0.71%, $\pm$4.20%, and $\pm$8.66%, respectively. Note that the desired error bound on n was not achieved. The reasons for the relatively high error bound are not clear, but may again be associated with the relatively low viscoelastic response at these stress levels. The data appear to be very uniform, and no permanent damage was recorded at these stress levels. In any case the nonlinear analysis presented below was successfully based upon these results.

Nonlinear Analysis

A nonlinear analysis was performed using data obtained at eight shear stress levels ranging from 11.8 to 32.5 MPa (1712 to 4715 psi). The recovery data were corrected by subtracting the permanent strains recorded at each stress level. The values obtained for the g_0 and g_1 parameters are presented in Figure 6.18, as functions of both the applied load and of the average matrix octahedral shear stress. The g_0 parameter was found to deviate from a value of 1.0 at all shear stress levels greater than 14.7 MPa (2132 psi). This indicates that the nonlinear behaviour observed is due to both a nonlinear elastic response and a nonlinear viscoelastic response in shear. This is in contrast to the results for normal stresses, where g_0 was found to be 1.0 at

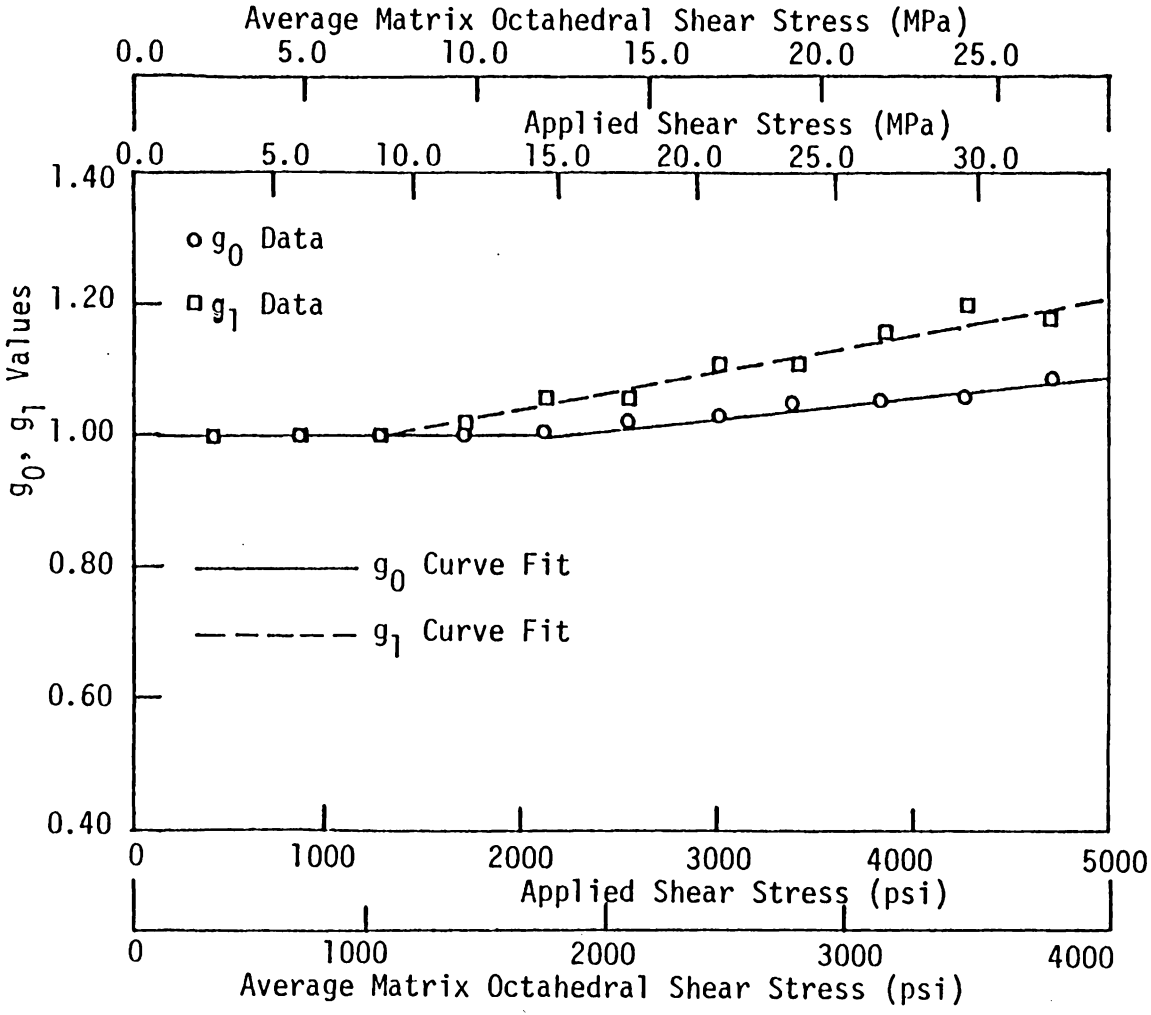

Figure 6.18: Values Obtained for g_0 and g_1 as Functions of Applied Shear Stress and of Average Matrix Octahedral Shear Stress

all normal stress levels, i.e., the elastic response was linear at all normal stress levels. A bilinear fit of the g_0 data for use with the VISLAP program resulted in

$$g_0(\tau_{oct}) = \begin{cases} 1.0 \quad , \quad \text{for } \tau_{oct} \leq 12.05 \text{ MPa} \\ 1.0 + 5.48 \times 10^{-3} \, (\tau_{oct} - 12.05), \text{ for } \tau_{oct} > 12.05 \text{ MPa} \end{cases}$$

The g_1 parameter was also found to be stress dependent. A bilinear fit of the g_1 data resulted in

$$g_1(\tau_{oct}) = \begin{cases} 1.0 \quad , \quad \text{for } \tau_{oct} \leq 7.23 \text{ MPa} \\ 1.0 + 9.79 \times 10^{-3} \, (\tau_{oct} - 7.23), \text{ for } \tau_{oct} > 7.23 \text{ MPa} \end{cases}$$

The bilinear curve fits of the g_0 and g_1 parameters are shown in Figure 6.18 as solid and dashed lines, respectively.

The results obtained for the g_2 parameter are presented in Figure 6.19. This parameter was found to be most sensitive to shear stress, ranging from a value of 1.0 at linear stress levels to about 3.6 at a shear stress of 32.5

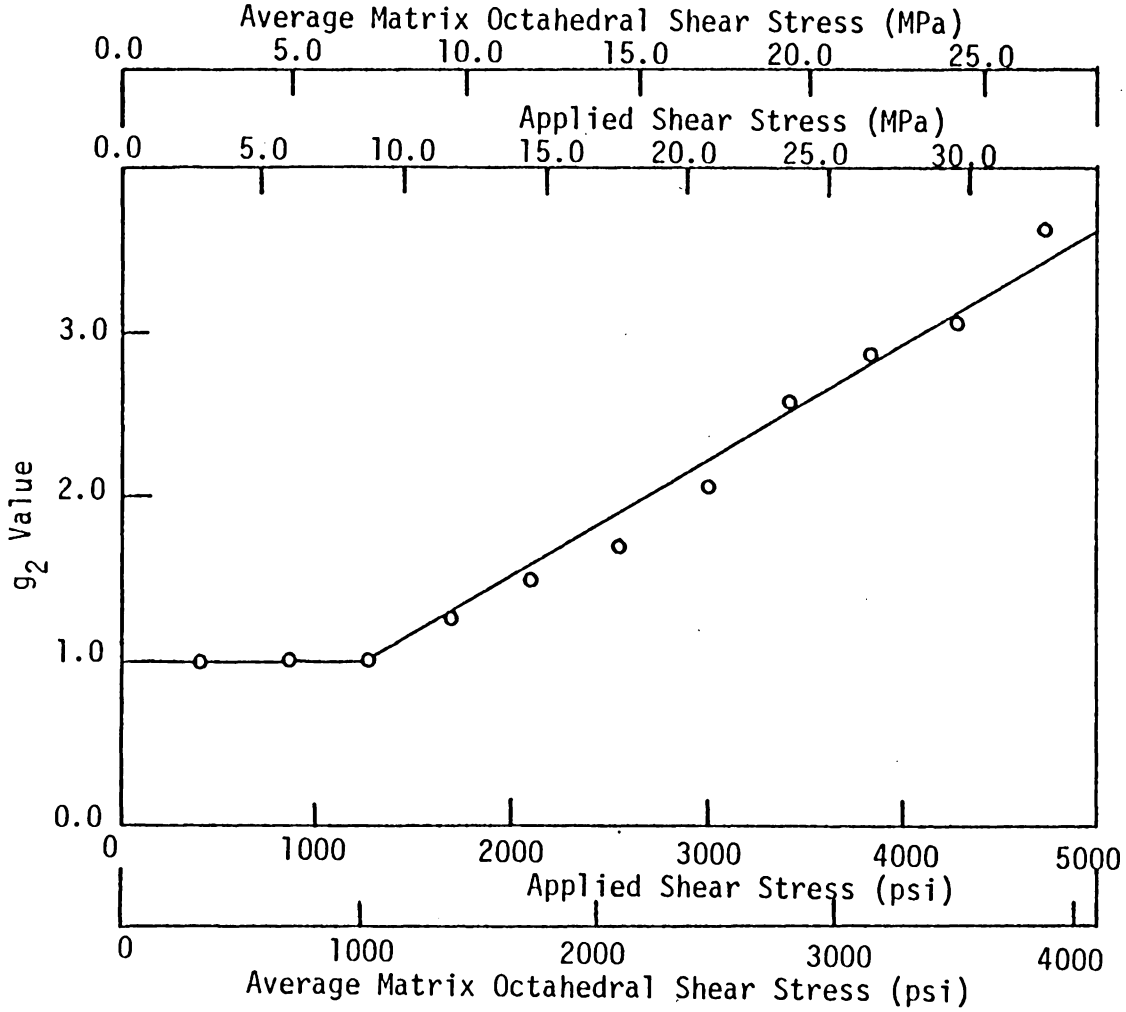

Figure 6.19: Values Obtained for g_2 as a Function of Applied Shear Stress and of the Average Matrix Octahedral Shear Stress

MPa (4715 psi). The g_2 data were also fit using a bilinear function, resulting in

$$g_2(\tau_{oct}) = \begin{cases} 1.0, \text{ for } \tau_{oct} \leq 7.23 \text{ MPa} \\ \\ 1.0 + 0.124\ (\tau_{oct} - 7.23), \text{ for } \tau_{oct} > 7.23 \text{ MPa} \end{cases}$$

This function is shown as a solid line in Figure 6.19.

The results obtained for a_σ are presented in Figure 6.20. The data for a_σ exhibited considerable scatter, and no truly distinctive pattern emerged. As previously noted the a_σ function was expected to exhibit an exponential dependence with stress. Therefore, the data were characterized using the following exponential function

$$a_\sigma(\tau_{oct}) = \begin{cases} 1.0, \text{ for } \tau_{oct} \leq 14.5 \text{ MPa} \\ \\ e^{-0.0340\ (\tau_{oct} - 14.5)}, \text{ for } \tau_{oct} > 14.5 \text{ MPa} \end{cases}$$

The above relation is shown as a solid line in Figure 6.20.

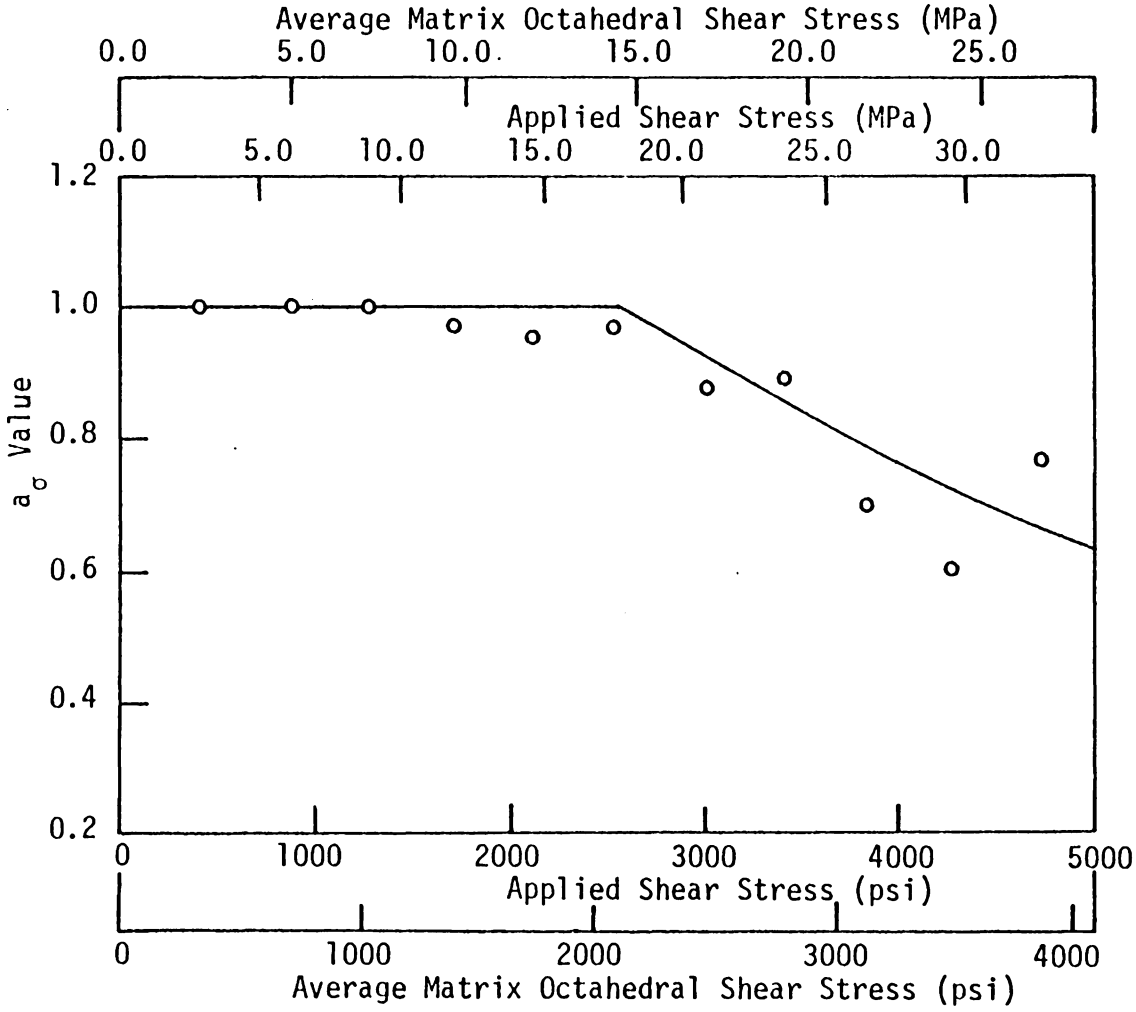

Figure 6.20: Values Obtained for a_g as a Function of Applied Shear Stress and of the Average Octahedral Shear Stress

VII. LONG TERM EXPERIMENTS

One of the major objectives of this study was to obtain experimental measurements of the long-term creep compliance of composite laminates. In previous studies at VPI&SU, compliance measurements were obtained for a maximum time of 10^4 minutes (6.9 days). It was felt that measurements at longer times were required so as to provide a more rigorous check of the long-term predictions obtained via the accelerated characterization scheme described in previous chapters. The efforts to obtain these long-term measurements will be described in this chapter.

Selection of the Laminate Layups

Two distinct laminate layups were to be tested during the long-term tests. The laminates were selected such that the stress state applied to the individual plies would differ significantly, so as to produce two distinct viscoelastic responses. A constraint on laminate selection was imposed by the material shortages previously mentioned. Due to these shortages, all long-term specimens had to be fabricated from a single $[0/30/-60/0]_s$ panel of T300/5208 graphite-epoxy. This panel was fabricated in the VPI&SU hot press facility, using the same NARMCO RIGIDITE 5208 prepreg tape and heat/pressure cycle used to fabricate the

unidirectional specimens. Different laminate layups could only be obtained by sawing specimens from the parent panel at various angles away from the 0-deg fiber directions. Thus, potential laminate layups for the tensile specimens were defined by an angle β ranging from 0 to 180 degrees, as depicted in Figure 7.1.

To aid in laminate selection, an analysis of the potential layups was performed using conventional (elastic) CLT. The results of this analysis are presented in Figure 7.2, where the transverse normal stress and shear stress induced in each ply as a function of the angle β are plotted. The laminate layups selected for testing are denoted by the dashed lines in Figure 7.2. The first was a $[100/-50/40/100]_s$ laminate, or equivalently, a $[-80/-50/40/-80]_s$ laminate. This laminate was selected because all plies were subjected to relatively high transverse normal and shear stresses, as indicated in Figure 7.2. The $[-80/-50/40/-80]_s$ laminate will be referred to as laminate "A". The second layup chosen was a $[20/50/-40/20]_s$ laminate. This layup results in relatively high shear stresses in all plies but relatively low transverse normal stresses. The $[20/50/-40/20]_s$ laminate will be referred to as laminate "B".

Static tensile tests to failure at a temperature of 149C (300F) were conducted for both laminates. Ultimate

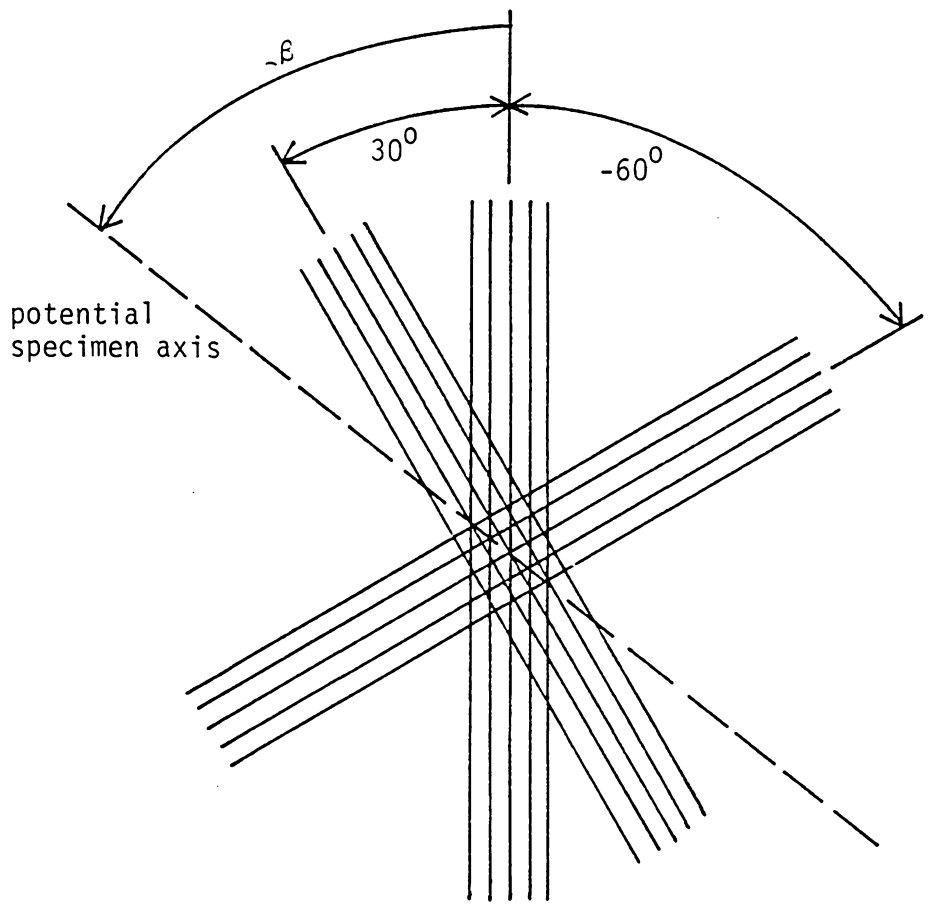

Figure 7.1: Layup of $[0/30/-60/0]_S$ Panel, Indicating Potential Tensile Specimen Axis Defined by Sawcut Angle β

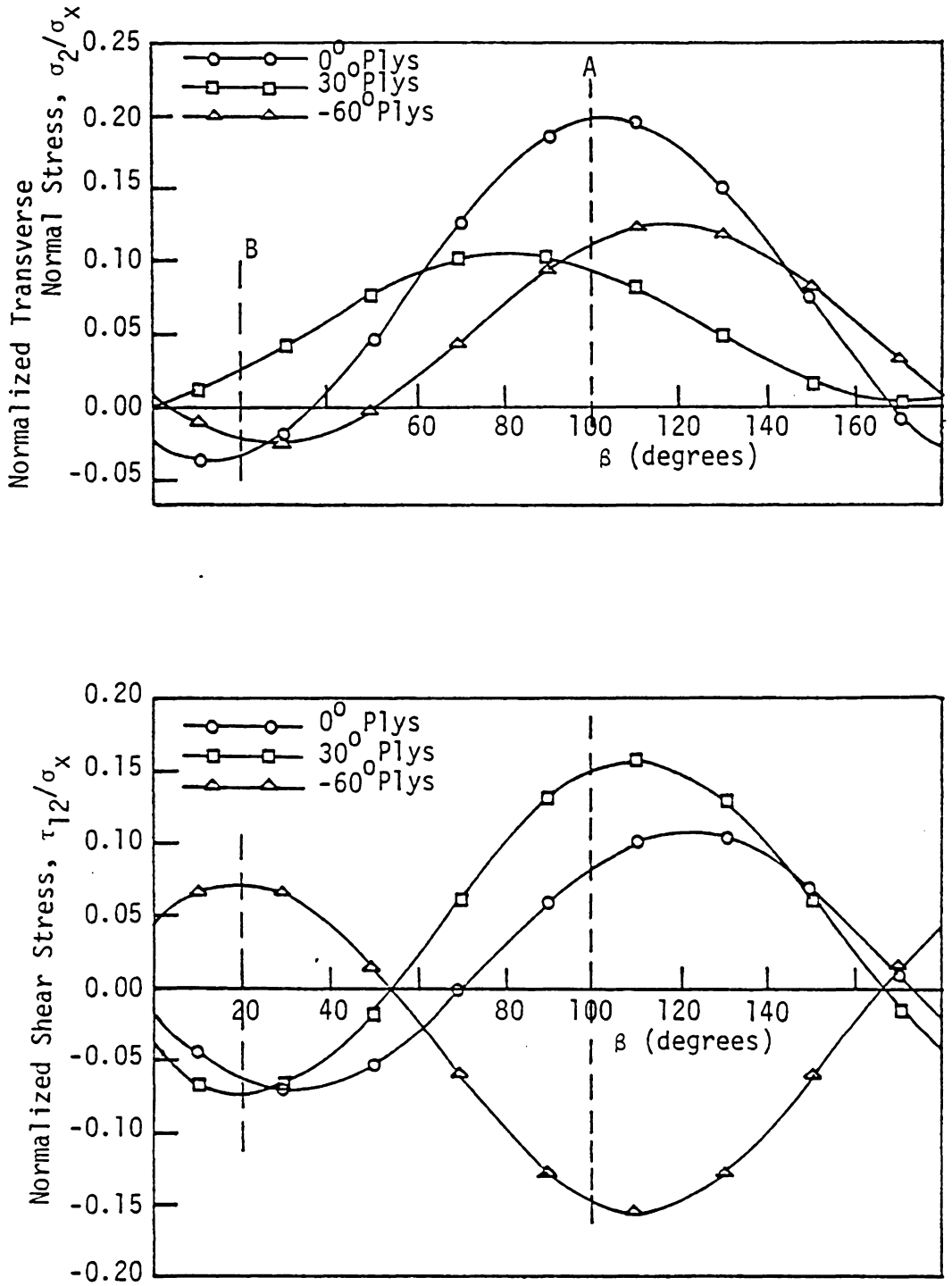

Figure 7.2: Transverse Normal and Shear Stresses Induced in Each Ply by an Applied Normal Stress σ_x as a Function of Sawcut Angle β

strengths of 136 and 271 MPa (19660 and 39320 psi) were measured for laminates A and B, respectively. Thus, the ultimate strength of laminate B was approximately twice as high as that of laminate A. The long-term creep tests were conducted at stress levels of 76 and 156 MPa (11000 and 23000 psi) for laminates A and B, respectively. These stress levels correspond to roughly 60% of the laminate static ultimate strengths.

As mentioned in Chapter VI, a five-station creep frame was used during the long-term study. Hence it was possible to test five specimens concurrently. Three specimens of laminate A and two specimens of laminate B were tested.

Drift Measurements

The long-term specimens were strain gaged with gages mounted back-to-back, as described for the unidirectional specimens in Chapter VI. Strains were measured using a Vishay P-350 portable digital strain indicator and a SB-1K ten channel switch and balance unit. An initial concern was that electronic "drift" of the gage signal might occur over the 10^5 minute test period. Drift can result from a variety of factors, including a change in strain gage or leadwire resistance, a change in strain gage gage factor, or amplifier instabilities. Since the laminate creep rate was expected to be rather low at long times, it was possible that drift could mask the actual viscoelastic response at

long times. The effective drift rate was therefore monitored during testing by placing separate Wheatstone bridge "drift" circuits within three test ovens, immediately adjacent to the mechanically-loaded tensile specimens. The drift specimens were gaged and wired exactly as the tensile specimens. At the start of the creep test, the drift circuits were balanced to zero, and the output of each circuit was monitored throughout the test.

Two of the three circuits indicated very low drift. After 10^5 minutes one had measured a total drift of 17 μin/in, while the second had measured 35 μin/in, indicating an average drift rate of 0.37 μin/in/day. The third drift circuit initially indicated a very low drift rate as well. However, after about 20000 minutes (5.5 days) substantially higher (and unreasonable) drift rates were observed. This third circuit finally failed after 57900 minutes (40 days). The final reading taken from this circuit was 734 μin/in, which was of the same magnitude as the total transient response measured until that time for the loaded specimens. Thus, it is concluded that the high drift rate indicated by this circuit was due to a faulty strain gage or solder joint, and the data obtained from this circuit were discarded.

The two drift circuits which did survive the total test period indicated that drift might account for perhaps 20-50

μin/in of the transient response recorded over the 10^5 minute period. On the other hand, the transient reponse was on the order of 1000 μin/in. The effects of drift were therefore estimated to be less than 5% of the transient response, and were neglected during the data reduction and analysis.

Specimen Performance

As described above, three specimens of layup A and two specimens of layup B were tested. After initiation of the long-term tests, two of the specimens of layup A apparently failed, the first after 14960 minutes (10.4 days) and the second after 46915 minutes (32.6 days). Since the ovens are not equipped with windows, it was not possible to view the specimens from outside of the test ovens. It was also undesirable to open the ovens for inspection since the other tests would likely be disturbed. Therefore, the "failed" specimens were left undisturbed for the entire 10^5 minute testing period. However, upon completion of the test it was discovered that these specimens had not failed but rather had merely slipped out of the upper specimen grips. In retrospect, it would have been advisable to use pins through the grips and specimens to prevent such slippage. Pins were used to prevent slippage of the B specimens, since these were tested at a much higher stress level. Short-term tests had been conducted at the specimen A stress level (76 MPa)

and no slipping had been observed. Therefore, slippage was not expected.

The third A specimen remained loaded for the entire 10^5 minute test period, but the strain gage circuit for this specimen failed after 34895 minutes (24.2 days). Reasonable strain measurements were obtained for this specimen until shortly before gage failure. Inspection following test completion revealed that the solder joint bonding the preattached leadwire ribbon to the gage tab had failed.

Due to these mechanical and electrical difficulties, results for the A laminate were obtained for a maximum time of 46915 minutes. While this was far short of the intended 10^5 minute test period, it was still a major increase in previous long-term test times.

Data for the two B laminates were obtained for the entire test period. Deformation of the B specimens occurred in a smooth and uniform manner, with no indication of any gage failures or excessive gage drift. The measured results for both the A and B laminates will be compared to the long-term response predicted by the program VISLAP in the following chapter.

VIII. COMPARISON BETWEEN PREDICTION AND MEASUREMENT

In previous chapters, the accelerated viscoelastic characterization of unidirectional specimens of T300/5208 graphite-epoxy was described. During characterization, a series of creep/recovery tests were performed at several stress levels and at a temperature of 149C (300F), using both 90-deg and 10-deg off-axis specimens. These short-term results may be used in conjunction with the lamination program VISLAP to provide predictions of the long-term viscoelastic response of T300/5208 composite laminates of arbitrary layup. To check the accuracy of these predictions, long-term creep tests were conducted using specimens with two distinct layups. Laminate A, consisting of a $[-80/-50/40/-80]_s$ layup, was selected because for this layup all plies are subjected to relatively high transverse normal and shear stresses. Laminate B, consisting of a $[20/50/-40/20]_s$ layup, was selected because for this layup all plies are subjected to relatively high shear stresses but relatively low transverse normal stresses. The ultimate strength of laminate B was slightly greater than twice that of laminate A. Both laminates A and B were tested at creep stress levels of approximately 60% of ultimate; laminate A was tested at 76 MPa (11,000 psi), while laminate B was tested at 156 MPa (23,000 psi). The viscoelastic response

of laminate A was expected to be significantly greater than that of laminate B.

The predicted and measured compliances for laminates A and B are presented in Figures 8.1 through 8.4. The comparison for laminate A is made in Figures 8.1 and 8.2, where the vertical compliance scale in Figure 8.2 is expanded relative to Figure 8.1, to provide a clear comparison between theory and experiment. The corresponding comparison for laminate B is presented in Figures 8.3 and 8.4. The comparison is similar for both laminates, in that a reasonably accurate prediction of the instantaneous (elastic) response was obtained, but at increased times the predicted response falls below the measured response. For laminate A the average measured compliance at 14960 minutes (the longest time at which all three A laminates were still functional) was approximately 10% higher than predicted. Figure 8.1 indicates that at longer times the differences between the average and predicted response would have been greater still. For laminate B, the average measured compliance at 10^5 minutes was approximately 12% higher than predicted.

Recall that a 480 minute creep time was used during the accelerated characterization tests using unidirectional specimens. The Schapery theory was applied to these data, and in each case the predicted and measured response

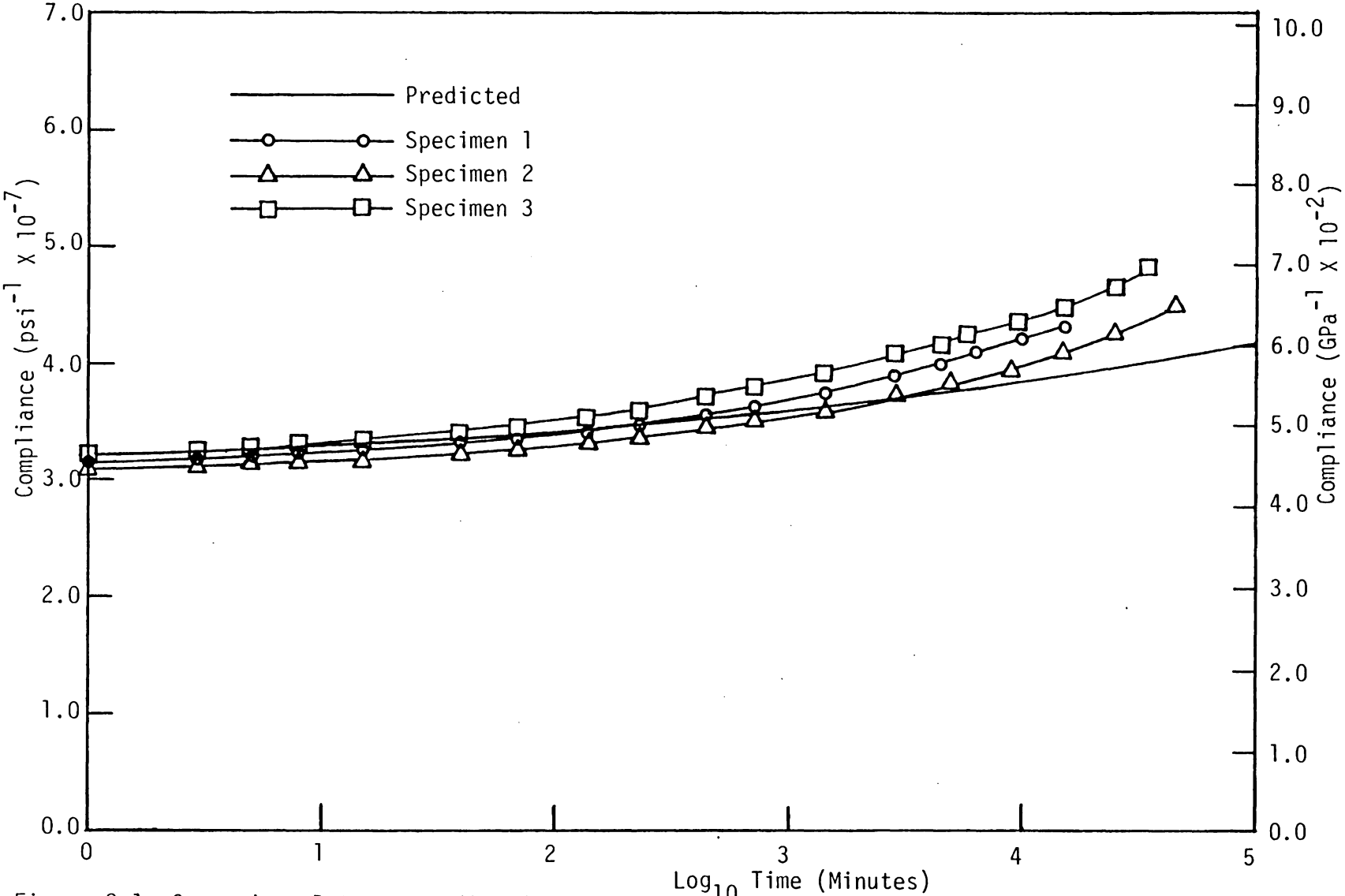

Figure 8.1: Comparison Between Predicted and Measured Compliances for $[-80/-50/40/-80]_S$ T300/5208 Laminate; Creep Stress = 76 MPa (11,000 psi), T = 149C (300F)

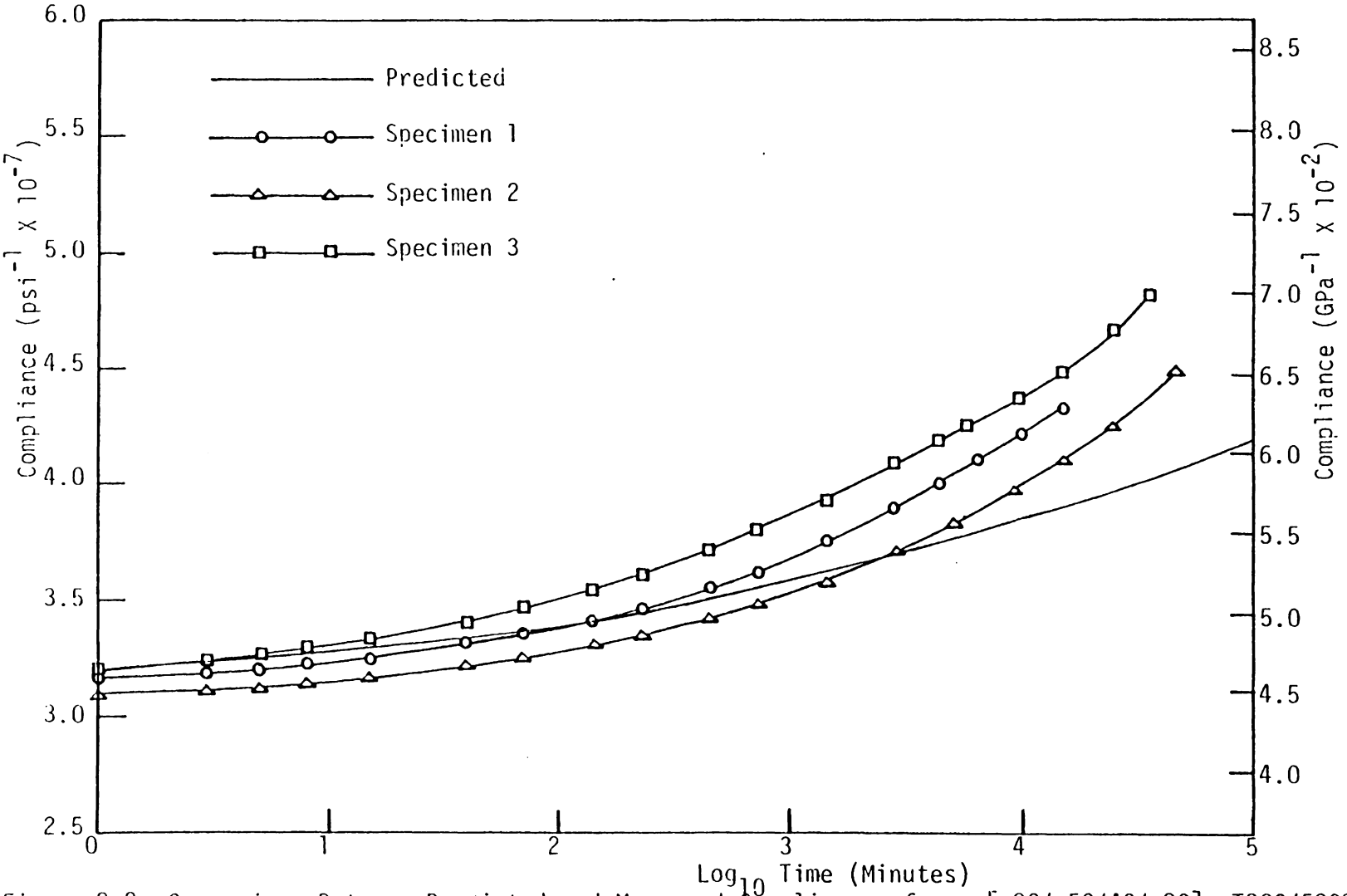

Figure 8.2: Comparison Between Predicted and Measured Compliances for a $[-80/-50/40/-80]_S$ T300/5208 Laminate; Creep Stress = 76 MPa (11,000 psi), T = 149C (300F); Expanded Scale

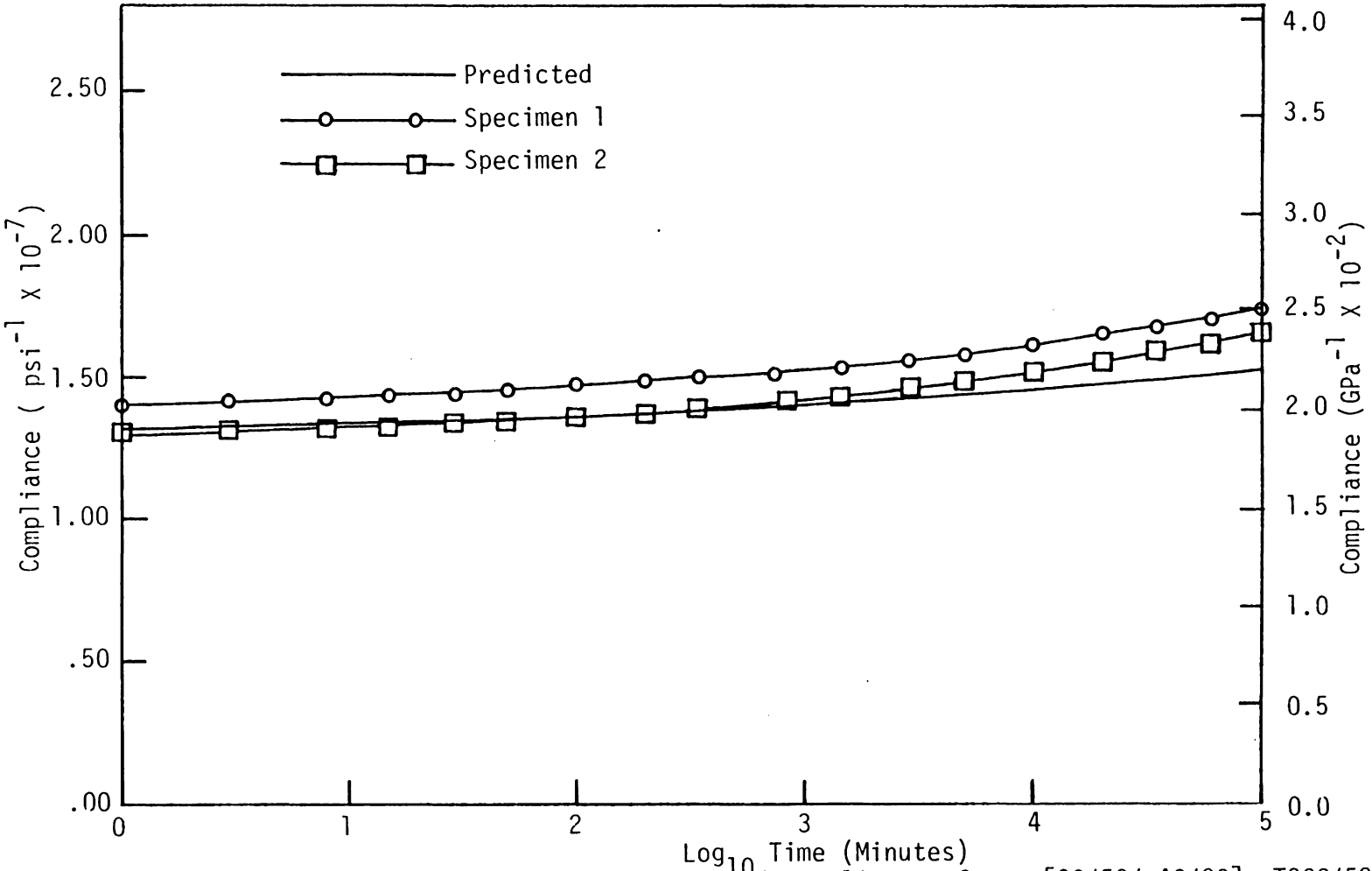

Figure 8.3: Comparison Between Predicted and Measured Compliances for a $[20/50/-40/20]_s$ T300/5208 Laminate; Creep Stress = 156 MPa (23,000 psi), T = 149C (300F)

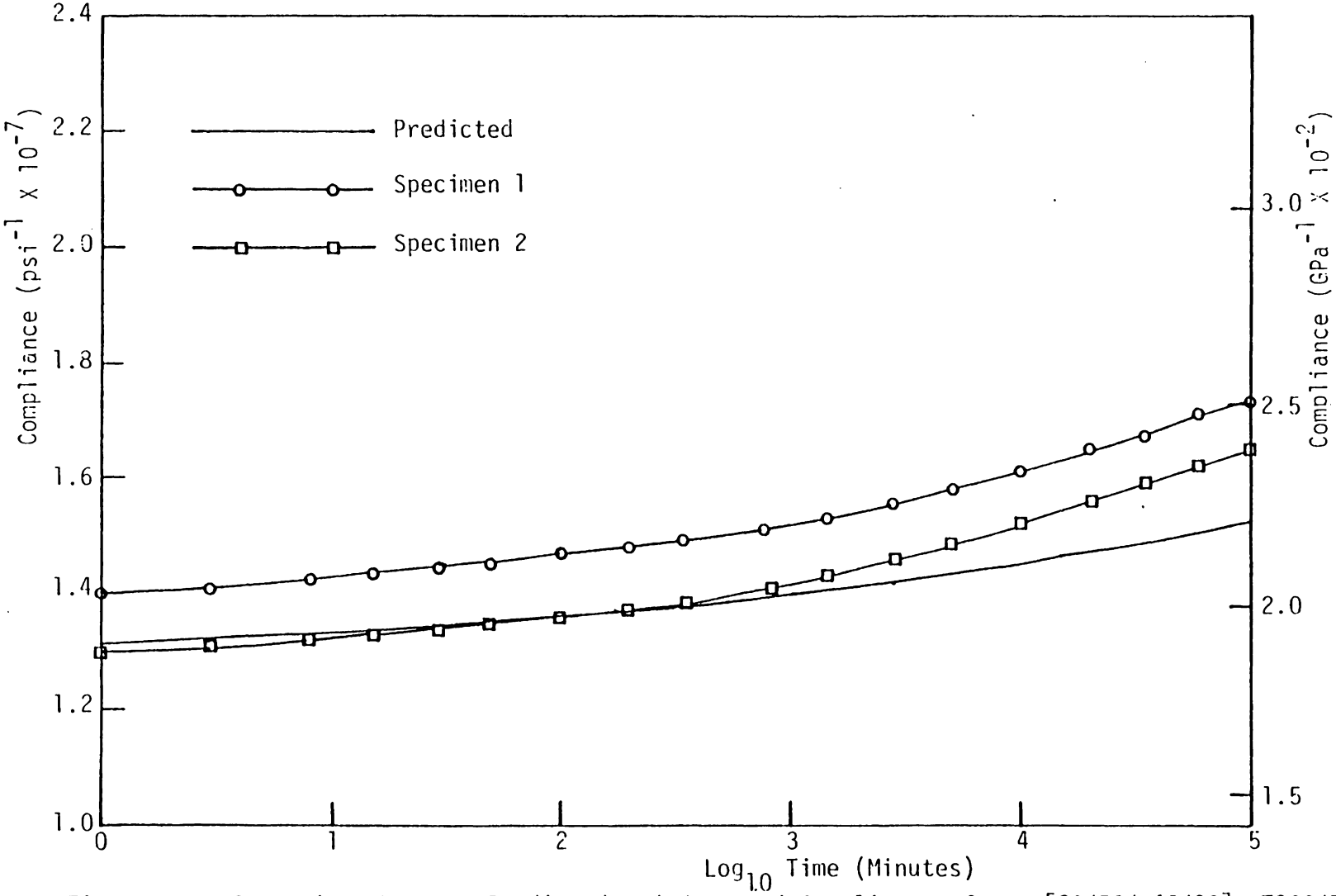

Figure 8.4: Comparison Between Predicted and Measured Compliances for a $[20/50/-40/20]_S$ T300/5208 Laminate; Creep Stress = 156 MPa (23,000 psi), T = 149C (300F); Expanded Scale

compared favorably. Typical results have been presented in Figures 6.3-6.5. It had therefore been anticipated that a good comparison for the laminates would be achieved over at least this shorter time period. Inspection of Figs. 8.2 and 8.4 indicates discrepancies between the slopes of the measured and predicted compliance curves even at short times, however. Although the magnitudes of the predicted and measured responses at short times are reasonably close, this simply reflects the accuracy of conventional (elastic) CLT. Thus, the error observed is mainly due to an inaccurate modeling of the laminate viscoelastic response.

The long-term laminate tests were conducted using a five station creep frame which had been fabricated in-house. The short-term tests on the other hand were conducted using a commercially available single station ATS creep frame. The test ovens used with the five station frame were known to produce relatively high thermal gradients, as compared to the ATS test oven. Therefore, it was suspected initially that the long-term specimens had been subjected to test temperatures higher than the intended test temperature of 149C, which could account for the discrepancies observed between predicted and measured response. However this is considered unlikely for two reasons. First, the oven control thermocouple was mounted to within about 0.64 cm (0.125 inch) of the strain gage site on each of the

mechanically loaded specimens. Even if significant thermal gradients existed along the length of the specimens, the material in the vicinity of the strain gage site was maintained at a temperature very near 149C. Also, nominal specimen thicknesses were 0.10 cm (0.04 inch), and so significant through-thickness thermal gradients were unlikely. Secondly, there was little discrepancy between predicted and measured results in initial elastic response. If the long-term test temperature had been appreciably higher than desired, a poor comparison between predicted and measured elastic response would have been observed.

Note that the measured viscoelastic response recorded for both laminates is very consistent and uniform from specimen to specimen. The experimental curves could be shifted up or down to form a distinct response curve for each laminate type. Discrepancies are due for the most part to small differences in the inital elastic response. This repeatable viscoelastic response from specimen to specimen as well as the very low strain gage drift rates previously noted tends to increase confidence in the measured results.

Based upon these observations, it must be concluded that some mechanism impacting the viscoelastic response of composite laminates has not been properly accounted for in the VISLAP analysis. It is possible that the viscoelastic parameters determined during the short-term tests were

calculated in error, causing discrepancies at long times. This would not explain the errors at short times, however.

One portion of the present analysis which may be suspect is the manner in which the effects of biaxial stress fields have been accounted for. Recall that the average matrix octahedral shear stress has been used to account for such stress interactions, using a mechanics of materials approach to determine the average matrix stresses. Perhaps this approach is too simple to characterize the effects of the complex three-dimensional stress state which exists at the micromechanics level at all fiber/matrix interfaces. The problem may be further accentuated at interfaces between alternating plies within the composite laminate.

Another area of concern is the accumulation of damage during the creep process, which has been observed during both the present study and in previous efforts [22]. Evidence suggests that this permanent damage is due to both the formation of voids and microcracks within the composite matrix material and permanent changes in the matrix molecular structure. It has not been possible to correct the unidirectional creep data for damage accumulation, although an attempt was made to correct the unidirectional recovery data by subtracting out any permanent strains recorded. A portion of the creep response is therefore due to viscoelastic mechanisms, while a portion is presumably

due to fracture mechanisms. This implies that the viscoelastic parameters calculated using the creep data may reflect to some extent the initial damage state of the specimen as well as the amount of damage accumulated during testing. This problem could be alleviated somewhat if the unidirectional specimens were mechanically conditioned prior to testing, but as previously noted this would not correspond to a practical situation. Furthermore, the damage which occurs in a unidirectional composite specimen is not necessarily representative of the damage which occurs in a composite laminate. Laminate damage may occur in various combinations of matrix cracking, fiber-matrix debonding, delamination between plies, or local fiber breakage. Many of these failure modes do not occur in unidirectional specimens. The type and extent of damage which occurs in a laminate depends upon stacking sequence, fabrication techniques, geometry, applied loads, and loading history [61,62]. Due to these effects, it may not be possible to characterize damage accumulation within a laminate based solely upon results obtained from unidirectional specimens.

Finally, note that the VISLAP analysis is based upon CLT, with slight modification to account for viscoelastic behaviour. If the analysis is to be valid, the principal assumptions associated with CLT must be satisfied. Namely,

the plane stress assumption and the Kirchoff hypothesis. Thus, interlaminar shear deformations are not considered in the VISLAP analysis. As a result, laminates with three or more fiber directions possess a theoretical upper bound on compliance, as pointed out by Dillard et al [22]. In practice, however, laminates may undergo significant viscoelastic interlaminar shear deformations and subsequently may have no upper bound on compliance. This shortcoming could be resolved if some method to integrate interlaminar shear deformations within lamination theory could be formulated. The only alternative would be to discard the present approach and utilize a more sophisticated (and more expensive) method such as the finite element technique.

IX. SUMMARY AND RECOMMENDATIONS

Summary of Results

In this study an accelerated characterization technique was applied to T300/5208 graphite-epoxy composites. The study utilized a characterization procedure previously developed at VPI&SU. The basic concept is to use short-term test data, obtained from unidirectional specimens, to predict the long-term behaviour of composite laminates of arbitrary layup. Previous efforts had focused exclusively on the T300/934 graphite-epoxy material system. Therefore, the T300/5208 material system was selected for use in the present study, to determine if the accelerated characterization scheme could be confidently applied to materials other than T300/934. Improvements in the characterization scheme were also implemented during this study, in the form of a more accurate viscoelastic compliance model and in improved short-term testing procedures.

Each of the six program objectives listed in Chapter I were achieved during the course of the study. First, the Schapery nonlinear viscoelastic theory was integrated with the accelerated characterization scheme. A recursive relationship was developed, based upon the Schapery theory.

This expression gives the nonlinear viscoelastic response at time t_j, following j-steps in stress. This allows calculation of the nonlinear viscoelastic response to a complex uniaxial load history. The complex load may be approximated to any degree of accuracy by using discrete steps in stress. The recursive relationship was integrated with an existing lamination computer program called VISLAP, allowing predictions of the long-term viscoelastic response of composite laminates.

The impact on long-term predictions induced by an error in one of the seven Schapery viscoelastic parameters was also investigated. The approach used was to calculate the predicted response using an "incorrect" value for the parameter of interest but the "correct" value for all other parameters. The prediction calculated using the erroneous parameter was then compared with the exact response. It was concluded that in the present case long-term predictions were most sensitive to error in the power law exponent n. It was noted however that this conclusion is contingent upon the length of prediction desired as well as the viscoelastic properties of the specific material being investigated. The above conclusion was based upon typical properties of T300/5208 and a maximum prediction time of 10^5 minutes. It is recommended that a similar analysis be performed if a different material is studied or if different prediction

times are required. However, as a general rule, long-term predictions are most sensitive to errors in n.

The data reduction techniques used to calculate the linear viscoelastic parameters A_o, C and n were also investigated. It was shown that in theory these parameters can be calculated using either linear creep or linear recovery data, i.e., the use of either creep or recovery data is theoretically equivalent. Consideration was then given to the type of experimental strain measurement errors likely to occur in practice. It was found that the power law exponent was sensitive to even small offset errors in recovery data, but insensitive to offset errors in creep data. Small offset errors in the recovery data were considered likely due to damage accumulation and slight strain gage zero drift during the creep cycle. Therefore, it was concluded that the linear viscoelastic parameters should be calculated using creep data.

A short-term creep/recovery testing cycle was selected which was keyed towards an accurate measure of the power law parameter n. The testing cycle was based upon strain gage accuracy and sensitivity, the expected viscoelastic response for T300/5208 at 149C, and a specified prediction accuracy of $\pm$10% at the maximum prediction time of 10^5 minutes. These considerations led to the selection of a 480/120 minute creep/recovery testing cycle. The concepts used in

selecting this cycle were also collected and listed as a proposed standard test selection procedure. This standard process should provide useful guidelines to the researcher studying a viscoelastic material which has not been previously investigated.

The 480/120 minute creep/recovery cycle was used to characterize the viscoelastic response of unidirectional specimens of T300/5208 graphite-epoxy. The viscoelastic response to transverse normal stress was characterized using 90-deg off-axis tensile specimens, while the response to shear stress was characterized using 10-deg off-axis tensile specimens. For the transverse case, nonlinear behaviour was observed at stress levels greater than about 15.6 MPa (2250 psi). However, it was also noted that nonlinear behaviour may occur at lower stress levels but may not become apparent for very long times. For the case of shear stress nonlinear behaviour was observed at stress levels greater than about 8.8 MPa (1279 psi). Nonlinear effects were much more significant in the case of shear stress than in the case of transverse normal stress.

Predictions obtained using the program VISLAP were compared to measured results for two distinct laminate layups. Comparisons were made for a maximum time of 10^5 minutes. It was found that although the predicted instantaneous response compared well with measured results,

the predicted viscoelastic response was significantly less than the measured viscoelastic response. Thus, the predicted response was non-conservative. The discrepancy between theory and experiment is believed to be due to an insufficient modeling of stress interaction effects within individual plies, to damage accumulation within individual plies, and/or to interlaminar shear deformations which develop during the viscoelastic creep process.

Although the comparison between theory and experiment obtained during this study is far from exact, it is believed that the fundamental approach used is valid. The accelerated characterization of composite laminates is a difficult problem, involving elements of lamination theory, nonlinear viscoelasticity, and fracture mechanics, among others. Accelerated characterization is an important research topic, however, due to the potential long-term viscoelastic response of composite laminates. A variety of load-bearing structural components fabricated from composites are being introduced into the marketplace. It is therefore important that the long-term viscoelastic response of composites be well understood and anticipated at the design stage.

Recommendations

A major question during application of the Schapery

theory in the present study was how to account for permanent damage. Damage has been attributed at least in part to the formation of voids and microcracks in the composite matrix material during creep. These voids and microcracks are in turn due in part to the highly heterogeneous nature of composites at the micromechanics level. Complex three dimensional stress states exist near fiber-matrix interfaces and near free edges, resulting in matrix cracks at applied stress levels far below the effective ultimate strength of the composite. It is believed that problems with damage accumulation could be minimized by using a "simpler" material, i.e., a homogeneous, initially isotropic, nonlinear viscoelastic material. Also note that in the present study the validity of the long-term predictions of the Schapery theory has been obscured since the Schapery results were not used directly but rather were combined using lamination theory to predict the long-term response of a laminate. Therefore, it is suggested that portions of this study be repeated with a "simple" material. Specifically, it is suggested that the Schapery analysis be applied as described herein to a homogeneous viscoelastic material, e.g., polycarbonate, and compared with long-term measurements. Such a study would indicate the level of accuracy possible using accelerated characterization techniques, and if successful would confirm that the

difficulties in long-term prediction encountered herein were due to the laminate analysis and not due to the short-term characterization process. Alternatively, the Schapery theory could be validated by predicting the response to a time-dependent loading history such as a ramp loading function or a low-frequency sinusoidal loading function. Response to such a load history could be approximated using the recursive relationship presented herein (eq. 3.10), or by integrating the Schapery single-integral expression (eq. 3.1) directly. If this latter approach were used a closed-form solution to eq. 3.1 may not be obtainable, requiring numerical integration. Peretz and Weitsman have used this approach in their studies on FM-73 [50].

In the present study the average matrix octahedral shear stress, τ_{oct}, has been used to account for the effects of biaxial stress states on the viscoelastic response, where τ_{oct} was calculated using a mechanics of materials model. Although this approach has been used in previous studies [21,35], to the author's knowledge the validity of this model has not been confirmed. It is suggested that creep tests be conducted using a biaxial loading state, e.g., static loads applied both parallel and perpendicular to the fiber direction. Although biaxial loading would be more difficult to apply than uniaxial loads, the test results would directly prove or disprove the average matrix

octahedral shear stress model. An alternate approach would be to use uniaxial test results for several different off-axis tensile specimens. In this case, the ratio of the loads applied parallel and perpendicular to the fibers is fixed by the specimen fiber angle. Although these tests would be much easier to perform than an externally applied biaxial load test, the selection of load ratios would be somewhat restricted.

A final recommendation involves possible interlaminar shear deformations which may occur during the viscoelastic creep process. A finite element analysis should be conducted for a few laminates to determine the contribution to creep due to interlaminar shear strains. If interlaminar effects are appreciable these must be incorporated into the CLT analysis. Otherwise, the relatively simple and inexpensive analysis possible using VISLAP must be replaced with a more complex and expensive procedure, probably based upon a finite element analysis of each laminate considered.

References

(1) Pipes, R.B., and Pagano, N.J.,"Interlaminar Stresses in Composite Laminates Under Uniform Axial Extension", J. Composite Materials , Vol. 4, 1970, pg 538.

(2) Wang, A.S.D., and Crossman, F.W.,"Some New Results on Edge Effect in Symmetric Composite Laminates", J. Composite Materials , Vol. 11, 1977, pg 92.

(3) Herakovich, C.T.,"On the Relationship Between Engineering Properties and Delamination of Composite Materials", J. Composite Materials , Vol. 15, 1981, pg 336.

(4) Quinn, W.J., and Matthews, F.L.,"The Effect of Stacking Sequence on the Pin-Bearing Strength in Glass-Fibre Reinforced Plastic", J. Composite Materials , Vol. 11, 1977, pg 139.

(5) Ford, J.L., Patel, H.P., and Turner, J.L.,"Interlaminar Shear Effects in Cord-Rubber Composites", Fibre Science and Technology , Vol 17, 1982, pg 255.

(6) Simitses, G.J., and Giri, J.,"Buckling of Rotationally Restrained Orthotropic Plates Under Uniaxial Compression", J. Composite Materials , Vol 11, 1977, pg 249.

(7) Hewson, P.,"Buckling of Pultruded Glass Fibre-Reinforced Channel Sections", Composites , Vol 9, 1978, pg 56.

(8) Hyer, M.W.,"Nonlinear Effects of Elastic Coupling in Unsymmetric Laminates",Presented at the IUTAM Symposium on Mechanics of Composite Materials, 1982, VPI&SU, Blacksburg, Virginia.

(9) Crawley, E.F.,"The Natural Modes of Graphite-Epoxy Cantilever Plates and Shells", J. Composite Materials , Vol 13, 1979, pg 195.

(10) Chao, C.C., and Lee, J.C.,"Vibration of Eccentrically Stiffened Laminates", J. Composite Materials , Vol 14, 1980, pg 233.

(11) Kibler, K.G.,"Effects of Temperature and Moisture on the Creep Compliance of Graphite-Epoxy Composites", AGARD Conf Proc No. 288, Effect of Service Environment on Composite Materials , AGARD-CP-288, 7 Rue Anuelle, 92200 Neuilly, Sur Seine, France.

(12) Shen, C.H., and Springer, G.S.,"Effects of Moisture and Temperature on the Tensile Strength of Composite Materials", J. Composite Materials , Vol 11, 1977, pg 2.

(13) Loos, A.C., and Springer, G.S.,"Effects of Thermal Spiking on Graphite-Epoxy Composites", J. Composite Materials , Vol 13, 1979, pg 17.

(14) Adamson, M.J.,"A Conceptual Model of the Thermal Spike Mechanism in Graphite-Epoxy Laminates", Presented at the ASTM Conference on Long-Term Behaviour of Composite Laminates, Williamsburg, Virginia, March 1981 (to appear in the Conference Proceedings).

(15) Rotem, A., and Nelson, H.G.,"Fatigue Behaviour of Graphite-Epoxy Laminates at Elevated Temperatures", NASA TM 81150, 1979.

(16) Sumison, H.T., and Williams, D.P.,"Effects of Environment on the Fatigue of Graphite-Epoxy Composites", ASTM STP 569, 1975.

(17) Sumison, H.T.,"Environmental Effects on Graphite-Epoxy Fatigue Properties", J. Spacecraft and Rockets , Vol 13, No 3, 1976.

(18) Yeow, Y.T., Morris, D.H., and Brinson, H.F.,"The Time-Temperature Behaviour of a Unidirectional Graphite-Epoxy Composite", ASTM STP 674, 1979 (see also VPI&SU Report, VPI-E-78-4, February, 1978).

(19) Griffith, W.I., Morris, D.H., and Brinson, H.F.,"The Accelerated Characterization of Viscoelastic Composite Materials", VPI&SU Report, VPI-E-80-15, April 1980.

(20) Griffith, W.I., Morris, D.H., and Brinson, H.F.,"Accelerated Characterization of Graphite-Epoxy Composites", VPI&SU Report VPI-E-80-27, September 1980.

(21) Dillard, D.A., Morris, D.H., and Brinson, H.F., "Creep and Creep Rupture of Laminated Graphite-Epoxy Composites", VPI&SU Report, VPI-E-81-3, March 1981.

(22) Hiel, C., Cardon, A.H., and Brinson, H.F.,"The Nonlinear Viscoelastic Response of Resin Matrix Composite Laminates", VPI&SU Report, VPI-E-83-6, March 1983.

(23) Brinson, H.F., Morris, D.H., and Yeow, Y.T.,"A New Experimental Method for the Accelerated Characterization of

Composite Materials", Proc 6th Int Conf on Experimental Stress Analysis, Munich, 1978, pg 395.

(24) Jones, Robert M., Mechanics of Composite Materials , McGraw-Hill, New York, 1975.

(25) Morris, D.H., Brinson, H.F., and Yeow, Y.T.,"The Viscoelastic Behaviour of the Principal Compliance Matrix of a Unidirectional Graphite-Epoxy Composite", Polymer Composites , Vol 1, No. 1, 1980, pg 32.

(26) Moehlenpah, A.E., Isha, O., DiBenedetto, A.T., "The Effect of Time and Temperature on the Mechanical Behaviour of Epoxy Composites", Polymer Engineering and Science , Vol 11, No 2, March 1971, pg 129.

(27) Miyano, Y., and Kansmitsu, M.,"Time and Temperature Dependence of Flexural Strength in Transversal Direction of Fibres in CFRP", Fibre Science and Technology , Vol 18, 1983, pg 65.

(28) Ferry, J.D., Viscoelastic Properties of Polymers , John Wiley and Sons, New York, 1970.

(29) Hahn, H.T.,"Nonlinear Behaviour of Laminated Composites", J. Composite Materials , Vol 7, 1973, pg 257.

(30) Findley, W.N., and Peterson, D.B.,"Prediction of Long-Time Creep With Ten-Year Creep Data on Four Plastic Laminates", ASTM Proc , Vol 58, 1958, pg 841.

(31) Findley, W.N.,"Prediction of Performance of Plastics Under Long-Term Static Loads", Trans Plastics Institute , Vol 30, 1962, pg 138.

(32) Findley, W.N., and Lai, J.S.Y.,"A Modified Superposition Principle Applied to Creep of Nonlinear Viscoelastic Material Under Abrupt Changes in State of Combined Stress", Trans Soc Rheology , Vol 11, No 3, 1967, pg 361.

(33) Schapery, R.A.,"A Theory of Non-Linear Thermoviscoelasticity Based on Irreversible Thermodynamics", Proc 5th U.S. National Congress Appl Mech, ASME (1966), pg 511.

(34) Schapery, R.A.,"Further Development of a Thermodynamic Constitutive Theory: Stress Formulation", Purdue University Report, AA&ES 69-2, Feb. 1969.

(35) Lou, Y.C., and Schapery, R.A.,"Viscoelastic Characterization of a Nonlinear Fiber-Reinforced Plastic", J. Composite Materials , Vol 5, 1971 (see also Tech. Report AFML-TR-70-113, Air Force Materials Laboratory, Wright-Patterson AFB, May 1970).

(36) Caplan, E.S., and Brinson, H.F.,"Nonlinear Viscoelastic Characterization of Polycarbonate", VPI&SU Report, VPI-E-82-7, March 1982.

(37) Rochefort, M.A., and Brinson, H.F.,"Nonlinear Viscoelastic Characterization of Structural Adhesives", VPI&SU Report, VPI-E-83-26, July 1983.

(38) Brinson, H.F., and Dillard, D.A.,"The Prediction of Long Term Viscoelastic Properties of Fiber Reinforced Plastics", Proc. of the Fourth International Conference on Composite Materials, Progress in Science and Engineering of Composites , Vol 1, T. Hayashi, K. Kawata, and S. Umekawa, editors, pg 795, 1982.

(39) Nielsen, L.E., Mechanical Properties of Polymers and Composites , Vol. 1, Marcel Dekker Inc., NY, 1974.

(40) Rosen, S.L., Fundamental Principles of Polymeric Materials for Practicing Engineers , Barnes and Noble Inc., NY, 1971.

(41) Green, A.E., and Rivlin, R.S., "The Mechanics of Non-Linear Materials with Memory, Part I", Arch Rational Mech Anal , Vol 1, No 1, pg 1, 1957.

(42) Green, A.E., Rivlin, R.S., and Spencer, A.J.M.,"The Mechanics of Non-Linear Materials with Memory, Part II", Arch Rational Mech Anal , Vol 3, No 1, pg 82, 1959.

(43) Green, A.E., and Rivlin ,R.S.,"The Mechanics of Non-Linear Materials with Memory, Part III", Arch Rational Mech Anal , Vol 4, No 5, pg 387, 1960.

(44) Onaran, K., and Findley, W.N.,"Combined Stress-Creep Experiments on a Nonlinear Viscoelastic Material to Determine the Kernel Functions for a Multiple Representation of Creep", Trans Soc Rheol , Vol 9, No 2, pg 299, 1965 (see also Lawrence Rad. Lab., Univ of California, P.O. Number 5396205, Tech. Report No. 1, June 1964).

(45) Findley, W.N., and Khosla, G.,"Application of the Superposition Principle and Theories of Mechanical Equation of State, Strain, and Time Hardening to Creep of Plastics

Under Changing Loads", Jrnl Appl Physics , Vol 26, No 7, pg 821, 1955.

(46) Yen, S.C.,"The Creep and Creep Rupture of SMC-R50 Under Different Thermomechanical Conditions", Ph.D Dissertation, Department of Engineering Science and Mechanics, VPI&SU, Blacksburg, VA, March 1984.

(47) Chamis , C.C., and Sinclair, J.H.,"Ten-deg Off-axis Test for Shear Properties in Fiber Composites", Experimental Mechanics , Vol 17, No 9, pg 339, 1977.

(48) Yeow, Y.T., and Brinson, H.F.,"A Comparison of Simple Shear Characterization Methods for Composite Laminates", Composites , January 1978.

(49) Schapery, R.A.,"On the Characterization of Nonlinear Viscoelastic Materials", Polymer Engineering and Science , Vol 9, No 4, pg 295, 1969.

(50) Peretz, D., and Weitzman, Y.,"Nonlinear Viscoelastic Characterization of FM-73 Adhesive", Jrnl of Rheology , Vol 26, No 3, pg 245, 1982.

(51) Peretz, D., and Weitzman,Y.,"The Nonlinear Thermoviscoelastic Characterization of FM-73 Adhesives", Jrnl of Rheology , Vol 27, No 2, pg 97, 1983.

(52) Bertolotti, A., Hiel, C.C., and Brinson, H.F., Unpublished research, Experimental Mechanics and Non-Metallic Characterization of Materials Lab, VPI&SU, 1982.

(53) Tougi, A., Gambi, D., Lagarde, A., and Brinson, H.F.,"Nonlinear Photoviscoelasticity: Theory and Measurement", Experimental Mechanics , Vol 23, No 3, pg 314, Sept. 1983.

(54) M-M Catalog 200 Gage Listing Section , available from Micro-Measurements, Measurements Group, PO Box 27777, Raleigh, NC 27611.

(55) Product information provided with the M-Bond 600 adhesive kit, Micro-Measurements, Measurements Group, PO Box 27777, Raleigh, NC 27611.

(56) Tuttle, M.E., and Brinson, H.F.,"Resistance Foil Strain Gage Technology as Applied to Orthotropic Composite Materials", accepted for publication in Experimental Mechanics , Dec. 1983.

(57) Dally, J.W., and Riley, W.F., Experimental Stress Analysis , McGraw-Hill Book Co., New York, N.Y., 1965.

(58) Zhang, Mao-jiong, Unpublished research, Experimental Mechanics and Non-Metallic Characterization of Materials Lab, VPI&SU, 1983.

(59) Sendeckyj, G.P., Richardson, M.D., and Pappas, J.E.,"Fracture Behaviour of Thornel 300/5208 Graphite-Epoxy Laminates- Part I: Unnotched Laminates", Composites Reliability , ASTM STP 500, pg 528, 1974.

(60) Pagano, N.J., and Halpin, J.C.,"Influence of End Constraint in the Testing of Anisotropic Bodies", Jrnl Comp Matl's , Vol 2, No 1, pg 18, 1968.

(61) Jamison, R.P.,"Advanced Fatigue Damage Development in Graphite Epoxy Laminates", Ph.D Dissertation, Department of Engineering Science and Mechanics, VPI&SU, Blacksburg, VA 24061, August 1982.

(62) O'Brien, T.K., and Reifsnider, K.L.,"Fatigue Damage Evaluation Through Stiffness Measurements in Boron-Epoxy Laminates", Jrnl Comp Matls , Vol 15, No 1, January 1981, pg 55.

The vita has been removed from the scanned document